AN ABSTRACT OF THE THESIS OF

DONALD ROBERTSON CONANT, JR. for the Doctor of Philosophy
(Name) (degree)

in Chemistry
(Major)

Date thesis is presented May 15, 1963

Title I. INFRARED SPECTRA OF SOLID SOLUTIONS IN ALKALI HALIDE CRYSTALS. II. METHOD FOR OBTAINING MINIMAL KINEMATICALLY COMPLETE SETS OF INTERNAL COORDINATES.

Abstract approved [redacted]
(Major Professor)

A study was made of the infrared absorption spectrum for cyanate ion in KCl and KBr host lattices containing small amounts of calcium or barium ion. Both pellets and single crystals were scanned during the course of this study. The spectra of the barium or calcium doped crystals contained many new peaks which do not appear in the spectra of cyanate doped KCl or KBr crystals having no divalent cations present. The proposal was made that new absorptions arise from calcium ion-cyanate ion pairs in which the strong field of the calcium ion reorients the longitudinal axis of the cyanate ion along the cell edge from the more usual body diagonal orientation of unpaired cyanate ion. This configuration increases the repulsive forces acting on the end atoms of cyanate causing an increase

in the vibrational frequencies. The observed frequency shifts in the spectra for crystals with barium ion present indicated, however, that cyanate ion remains in the body diagonal orientation when barium ion is a near neighbor. An additional effect examined was the change of charge distribution within the cyanate ion caused by the presence of calcium or barium ions as near neighbors. The magnitudes of force constant changes, caused by the action of the surrounding lattice upon the cyanate ion and caused by the shift in the cyanate ion charge distribution, were estimated from theoretical calculations.

A method for obtaining a minimal kinematically complete set of internal coordinates was proposed. According to this method, once such a set is obtained for a molecule, any additional internal coordinates added to the set to obtain symmetrical completeness are declared redundant, thus facilitating the removal of redundancies from the symmetry G matrix after factorization of the secular equation. A procedure was given for choosing the internal coordinates used in the kinematically complete set which leads to a reduction in redundancies when the set is expanded to obtain symmetric completeness. Several examples illustrating this method were given.

I. INFRARED SPECTRA OF SOLID SOLUTIONS IN ALKALI HALIDE CRYSTALS
II. METHOD FOR OBTAINING MINIMAL KINEMATICALLY COMPLETE SETS OF INTERNAL COORDINATES

by

DONALD ROBERTSON CONANT, JR.

A THESIS

submitted to

OREGON STATE UNIVERSITY

in partial fulfillment of
the requirements for the
degree of

DOCTOR OF PHILOSOPHY

June 1963

APPROVED:

Professor of Chemistry

In Charge of Major

Chairman of Department of Chemistry

Dean of Graduate School

Date thesis is presented May 15, 1963

Typed by Nancy Kerley

ACKNOWLEDGMENT

I would especially like to thank Dr. J. C. Decius for his stimulating interest and untiring assistance during my years of graduate work. It has been a privilege to know him and to have studied under him.

My deep appreciation goes to Mr. Robert Holmes for his extensive contributions to the design of the crystal-growing apparatus and for his friendship. Mr. Woods has also been most helpful with his careful construction of the apparatus.

For the help, diversion, and funds which she provided, I thank my wife, Janet.

I am grateful to Dr. Wayne Woodmansee, Dr. Latif Khidir, Dr. Roy Caton, Mr. Jerome Blank, Mr. Ralph Bain, and other colleagues for their friendship and discussion.

To the organizations which provided the funds that made this work possible, I am indebted.

TABLE OF CONTENTS

LIST OF FIGURES

LIST OF FIGURES (continued)

LIST OF TABLES

PART I. INFRARED SPECTRA OF SOLID SOLUTIONS IN ALKALI HALIDE CRYSTALS

I. INTRODUCTION

The study of infrared spectra has become one of the most important methods for investigating molecular structure. Information obtained from these spectra may be used to determine the symmetry of any given molecule and the character of its valence bonds. The infrared absorption spectrum arises from the rotational and vibrational motion of a molecule. Since the vibrational frequencies are governed by the kinetic and potential energies of the atoms of a molecule, they must consequently be related to the forces between molecules as well as to the forces between atoms of the molecule. Thus, the environment of a molecule affects its frequencies of vibration, and therefore affects the absorption spectrum, with the result that the spectra of polyatomic molecules or ions may be used to obtain some information about their environment.

Coker, Decius, and Scott (8, p. 38-77; 9) have studied the infrared spectrum of sulfate ion in order to obtain knowledge about the association of sulfate ion with divalent cations in a potassium chloride host lattice. They found that divalent metal sulfates would dissolve in potassium chloride to form isolated MSO_4 ion pairs. The sulfate ion replaces a chloride ion in the potassium chloride lattice

with each oxygen directed toward a corner of the unit cell containing the sulfate ion, and the divalent metal ion replaces one of the nearest neighbor potassium ions.

The success of the above investigation has encouraged further study in this laboratory of the spectra arising from polyatomic ions dissolved in alkali halide crystals containing divalent cation impurities. Part I of this thesis deals primarily with the infrared absorption spectra of cyanate ion incorporated in alkali halide crystals containing divalent cation impurities. The purpose of this section is to propose several models which would give rise to spectral shifts of the same order of magnitude as those observed for cyanate ion that has been perturbed by divalent cation, with the hope that additional knowledge may be gained regarding the effect of the environment on infrared absorption.

Previous investigations of the structure of cyanate ion have been carried out using x-ray diffraction and Raman and infrared spectroscopy. Hendricks and Pauling (15, p. 2912-2916) in their study of potassium cyanate with x-ray diffraction found that cyanate ion is linear and that the interatomic distances were about 1.16 Å. Raman spectra of cyanate ion in aqueous solution were studied by Pal and Sen Gupta (31, p. 30), J. Goubeau (14, p. 912-919), and Forrest Cleveland (7, p. 622-623). A major problem that arose in this work was the hydrolysis of cyanate to potassium carbonate, potassium

bicarbonate, ammonium hydroxide, and ammonium carbonate giving rise to numerous absorption bands caused by the ammonium and carbonate ions. D. Williams (43, p. 2442-2444) made the first examination of the infrared spectrum of cyanate ion. His study was carried out in aqueous solution with equipment of rather low resolution and consequently was somewhat limited. Rao, Ramachandran, and Shankar (36) have investigated the infrared spectra of inorganic cyanates in nujol mulls and concluded that of the three resonance structures

$$\bar{O} - C \equiv N \qquad (A)$$

$$O = C = \bar{N} \qquad (B)$$

$$\overset{+}{O} \equiv C - \bar{\bar{N}} \qquad (C)$$

the first (A) probably predominates.

The most extensive study of infrared spectra of cyanate ion in potassium chloride, potassium bromide, and potassium iodide host lattices has been carried out by Maki and Decius (25; 26, p. 772-782; 24, p. 1-151). Table 1 summarizes their assignments for cyanate ion in potassium chloride and in potassium bromide host lattices.

Finally, the investigation of the infrared spectra of cyanate ion incorporated in all of the alkali halide lattices ranging from sodium chloride to cesium iodide has been carried out by Price, Sherman, and Wilkinson (34, p. 15-17; 34, p. 668-671). Their method for

Table 1. Assigned vibrational frequencies for cyanate ion in single crystals.

Assignment						Isotopic species	Observed frequency in cm^{-1} for	
Lower			Upper					
ν_1	ν_2^l	ν_3	ν_1	ν_2^l	ν_3		KCl	KBr
0	0^0	0	0	1^1	0	C^{13}	613.2	612.0
0	0^0	0	0	1^1	0	...	631.0	629.4
0	0^0	0	1	0^0	0	O^{18}	...	1175.8
0	0^0	0	0	2^0	0	O^{18}	...	...
0	0^0	0	1	0^0	0	N^{15}	...	1188.9
0	0^0	0	0	2^0	0	N^{15}	...	1282.3
0	0^0	0	1	0^0	0	C^{13}	...	1191.0
0	0^0	0	0	2^0	0	C^{13}	1277.4	1272.5
0	0^0	0	1	0^0	0	...	1210.7	1205.5
0	0^0	0	0	2^0	0	...	1297.3	1292.6
0	0^0	0	0	0^0	1	$N^{15}C^{13}$	...	2094.6
0	0^0	0	0	0^0	1	$C^{13}O^{18}$	...	2104.8
0	0^0	0	0	0^0	1	C^{13}	2124.7	2112.8
0	0^0	0	0	0^0	1	N^{15}	...	2152.5
0	0^0	0	0	0^0	1	O^{18}	...	2161.5
0	0^0	0	0	0^0	1	...	2181.8	2169.6
0	0^0	0	2	0^0	0	C^{13}	...	2360.3
0	0^0	0	1	2^0	0	C^{13}	...	2462.6
0	0^0	0	0	4^0	0	C^{13}	...	2554.2
0	0^0	0	2	0^0	0	...	2402.8	2392.9
0	0^0	0	1	2^0	0	...	2498.8	2487.3
0	0^0	0	0	4^0	0	...	2612.8	2602.5
0	0^0	0	0	1^1	1	C^{13}	...	2714.0

Table 1 (continued).

Assignment						Isotopic species	Observed frequency in cm^{-1} for	
Lower			Upper					
ν_1	ν_2^{ℓ}	ν_3	ν_1	ν_2^{ℓ}	ν_3		KCl	KBr
0	0^0	0	0	1^1	1	...	2801.9	2788.1
0	0^0	0	1	0^0	1	C^{13}	...	3284.1
0	0^0	0	0	2^0	1	C^{13}	...	3366.0
0	0^0	0	1	0^0	1	N^{15}	...	3322.0
0	0^0	0	0	2^0	1	N^{15}	...	3414.7
0	0^0	0	1	0^0	1	...	3372.6	3355.0
0	0^0	0	0	2^0	1	...	3458.8	3442.2
0	0^0	0	2	0^0	1	...	...	4524.7
0	0^0	0	1	2^0	1	...	...	4623.0
0	0^0	0	0	4^0	1	...	...	4737.5
0	1^1	0	1	0^0	0	...	...	574.4
0	1^1	0	0	2^0	0	...	...	663.2
0	1^1	0	1	1^1	0	C^{13}	...	1174.4
0	1^1	0	0	3^1	0	C^{13}	...	1285.7
0	1^1	0	1	1^1	0	...	1193.0	1188.1
0	1^1	0	0	3^1	0	...	1314.4	1309.1
0	1^1	0	0	1^1	1	C^{13}	...	2102.2
0	1^1	0	0	1^1	1	...	2170.7	2158.6
0	1^1	0	2	1^1	0	...	...	...
0	1^1	0	1	3^1	0	...	...	...
0	1^1	0	0	5^1	0	...	...	2628.3
0	1^1	0	1	0^0	1	...	...	2725.0
0	1^1	0	0	2^0	1	...	...	2813.0
0	1^1	0	0	2^2	1	...	...	2776.6

Table 1 (continued).

Assignment						Isotopic species	Observed frequency in cm^{-1} for	
Lower			Upper					
v_1	v_2^{ℓ}	v_3	v_1	v_2^{ℓ}	v_3		KCl	KBr
0	1^1	0	1	1^1	1	C^{13}	...	3257.2
0	1^1	0	0	3^1	1	C^{13}	...	...
0	1^1	0	1	1^1	1	...	3342.1	3325.7
0	1^1	0	0	3^1	1	...	...	...
0	2^2	0	1	2^2	0	...	...	1175.5
0	2^2	0	0	4^2	0	...	...	1320.4
0	2^2	0	0	2^2	1	...	2160.4	2147.9

incorporating the cyanate ion into the alkali halide lattices was to powder either NCS^-, NO_3^-, or CN^- with the alkali halide and then to press the mixture to form a disk. The impurity ions were dispersed in the lattice and converted to NCO^- by heating. The spectra were obtained over a temperature range from 5° K to 500° K. They determined that the relation

$$\Delta(l\nu_i + m\nu_j + n\nu_k) = l\,\Delta\nu_i + m\,\Delta\nu_j + n\,\Delta\nu_k$$

is valid where $\Delta\nu_i$ is the shift produced in the fundamental ν_i by the environment, and l, m, n are the vibrational quantum numbers associated with the modes ν_i, ν_j, ν_k.

II. THEORY

1. Molecular Vibrations and the Absorption of Light

The wavelength of infrared radiation is large with respect to the dimensions of molecules and atoms. Under these conditions perturbation theory shows that the probability for absorption of a quantum in unit time with unit radiation density by a molecule is given by the equation

$$B_{n \leftarrow m} = \frac{8\pi^3}{3h^2} \left[(\mu_x)^2_{nm} + (\mu_y)^2_{nm} + (\mu_z)^2_{nm} \right]$$

where μ_x, μ_y, and μ_z are the x, y, and z components of the dipole moment, $(\mu_x)_{nm} = \int \psi_n^* \mu_x \psi_m d\tau$, and ψ_n is the wave function for the nth quantum state. If $|(\mu)_{nm}|$ is zero for a given transition m→n, then no radiation will be absorbed due to that transition. Calculation of the above integral for diatomic and triatomic molecules leads to the general principle that a vibration must cause a change in the dipole moment to be active in the absorption spectra. In addition, a molecule may absorb infrared radiation by increasing its rotational energy provided that the molecule has a permanent dipole moment. In the solid state, rotation of molecules is restricted, consequently the following discussion will treat only the vibrational problem.

Absorption of radiation by a molecule takes place during its oscillatory motion, with the frequencies of vibration for the fundamental bands being the same as those for the vibrating molecule. The frequencies of vibration for a molecule are functions of the strengths of its chemical bonds, of its structure, and of the atomic masses. The solution to the vibrational problem is complicated and extremely tedious in the case of large polyatomic molecules. In order to simplify the problem, various coordinate systems have been used to describe the molecule. Best known are the cartesian displacement coordinates. For theoretical purposes, however, mass-weighted cartesian displacement coordinates are more useful because of the simple form they give to the kinetic energy.

A molecule consisting of N atoms has 3N degrees of freedom. 3N-6 (or 3N-5 for linear molecules) internal coordinates are required to describe the vibrations of the molecule, and 6 (or 5 for linear molecules) more coordinates are necessary to describe translation and rotation. If the cartesian displacement coordinates x_1, x_2, - - -, x_{3N} give the displacement of the atoms from their equilibrium position, then 3N-6 internal coordinates can be expressed in terms of the cartesian coordinates by equations of the form

$$S_t = \sum_{i=1}^{3N} B_{ti} X_i \quad , \qquad t = 1, 2, \cdots, 3N-6$$

or in matrix notation

$$\underline{S} = \underline{B}\,\underline{X} .$$

The kinetic energy of vibration of the molecule may be written as:

$$2T = \dot{\underline{X}}^{\dagger}\underline{M}\dot{\underline{X}} = \underline{p}^{\dagger}\underline{M}^{-1}\underline{p}$$

where $\underline{M}$ is a diagonal matrix containing the masses of the atoms as the non-zero components, and $\underline{p}$ is a column matrix of the momenta, p_i, conjugate to the coordinates x_i.

If we define $\underline{P}$ as a column matrix of the momenta, P_t, conjugate to the coordinates S_t, then

$$\underline{P} = \frac{\partial T}{\partial \dot{\underline{S}}} .$$

Also

$$\frac{\partial \dot{\underline{S}}^{\dagger}}{\partial \dot{\underline{X}}} = \frac{\partial \underline{S}^{\dagger}}{\partial \underline{X}} = \underline{B}^{\dagger} .$$

Thus, using the rules of partial differentiation

$$\underline{p} = \frac{\partial T}{\partial \dot{\underline{X}}} = \frac{\partial \dot{\underline{S}}^{\dagger}}{\partial \dot{\underline{X}}}\frac{\partial T}{\partial \dot{\underline{S}}} = \underline{B}^{\dagger}\underline{P} .$$

Substituting for $\underline{p}$ in the kinetic energy expression

$$2T = \underline{p}^{\dagger}\underline{M}^{-1}\underline{p} = \underline{P}^{\dagger}\underline{B}\,\underline{M}^{-1}\underline{B}\,\underline{P}$$

$$= \underline{P}^{\dagger}\underline{G}\,\underline{P} , \quad \text{where} \quad \underline{G} = \underline{B}\underline{M}^{-1}\underline{B}^{\dagger} .$$

If G is not singular, then by the Hamilton equation

$$\dot{\underset{\sim}{S}} = \frac{\partial T}{\partial \underset{\sim}{P}} ,$$

$$\dot{\underset{\sim}{S}} = \underset{\sim}{G}\,\underset{\sim}{P}$$

or

$$\underset{\sim}{P} = \underset{\sim}{G}^{-1}\dot{\underset{\sim}{S}} .$$

Thus

$$2T = \underset{\sim}{P}^{\dagger}\underset{\sim}{G}\,\underset{\sim}{P} = \dot{\underset{\sim}{S}}^{\dagger}(\underset{\sim}{G}^{-1})^{\dagger}\underset{\sim}{G}\,\underset{\sim}{G}^{-1}\dot{\underset{\sim}{S}}$$

$$= \dot{\underset{\sim}{S}}^{\dagger}(\underset{\sim}{G}^{\dagger})^{-1}\dot{\underset{\sim}{S}} = \dot{\underset{\sim}{S}}^{\dagger}\underset{\sim}{G}^{-1}\dot{\underset{\sim}{S}} .$$

The potential energy may be expanded about the equilibrium position of the molecule in a Taylor series for small displacements giving

$$2V = V_0 + 2\left[\frac{\partial V}{\partial \underset{\sim}{S}^{\dagger}}\right]_0 \underset{\sim}{S} + \underset{\sim}{S}^{\dagger}\left[\frac{\partial^2 V}{\partial \underset{\sim}{S}\,\partial \underset{\sim}{S}^{\dagger}}\right]_0 \underset{\sim}{S}$$

$$+ \text{higher terms} .$$

If the equilibrium position is chosen as the zero of potential energy, then $V_0 = 0$. Furthermore, the energy at the equilibrium position is at a minimum so that $\left(\frac{\partial V}{\partial \underset{\sim}{S}^{\dagger}}\right)_0 = \underset{\sim}{0}$. Therefore, if cubic and higher terms are neglected

$$2V = \underset{\sim}{S}^{\dagger}\left[\frac{\partial^2 V}{\partial \underset{\sim}{S}\,\partial \underset{\sim}{S}^{\dagger}}\right]_0 \underset{\sim}{S} = \underset{\sim}{S}^{\dagger}\,\underset{\sim}{F}\,\underset{\sim}{S} .$$

In order to carry out the quantum mechanical treatment of molecular vibrations, a set of normal coordinates Q_k are introduced together with the defining equations

$$\underset{\sim}{Q} = \underset{\sim}{L}^{-1} \underset{\sim}{S}$$

$$2V = \underset{\sim}{Q}^{\dagger} \underset{\sim}{\Lambda} \underset{\sim}{Q}$$

and

$$2T = \dot{\underset{\sim}{Q}}^{\dagger} \dot{\underset{\sim}{Q}}$$

where $\underset{\sim}{\Lambda}$ is a diagonal matrix. From the equations

$$2V = \underset{\sim}{Q}^{\dagger} \underset{\sim}{\Lambda} \underset{\sim}{Q} = \underset{\sim}{S}^{\dagger} \underset{\sim}{F} \underset{\sim}{S} = \underset{\sim}{Q}^{\dagger} \underset{\sim}{L}^{\dagger} \underset{\sim}{F} \underset{\sim}{L} \underset{\sim}{Q}$$

and

$$2T = \dot{\underset{\sim}{Q}}^{\dagger} \underset{\sim}{E} \dot{\underset{\sim}{Q}} = \dot{\underset{\sim}{S}}^{\dagger} \underset{\sim}{G}^{-1} \dot{\underset{\sim}{S}} = \dot{\underset{\sim}{Q}}^{\dagger} \underset{\sim}{L}^{\dagger} \underset{\sim}{G}^{-1} \underset{\sim}{L} \dot{\underset{\sim}{Q}}$$

the equations

$$\underset{\sim}{L}^{\dagger} \underset{\sim}{F} \underset{\sim}{L} = \underset{\sim}{\Lambda} \qquad \text{and} \qquad \underset{\sim}{L}^{\dagger} \underset{\sim}{G}^{-1} \underset{\sim}{L} = \underset{\sim}{E}$$

are obtained by virtue of the properties of quadratic forms. From the last equation it follows that $\underset{\sim}{L}^{\dagger} = \underset{\sim}{L}^{-1} \underset{\sim}{G}$. Substituting for $\underset{\sim}{L}^{\dagger}$ gives

$$\underset{\sim}{L}^{-1} \underset{\sim}{G} \underset{\sim}{F} \underset{\sim}{L} = \underset{\sim}{\Lambda}$$

or

$$\underset{\sim}{G} \underset{\sim}{F} \underset{\sim}{L} = \underset{\sim}{L} \underset{\sim}{\Lambda} .$$

If the $\underset{\sim}{L}$ matrix is partitioned into columns and multiplication is expressed in terms of these columns, then

$$\underset{\sim}{G}\,\underset{\sim}{F}\,\underset{\sim}{L_k} = \underset{\sim}{L_k}\,\lambda_k$$

or

$$(\underset{\sim}{G}\,\underset{\sim}{F} - \lambda_k \underset{\sim}{E})\,\underset{\sim}{L_k} = 0$$

where $\underset{\sim}{L_k}$ is the kth column of the $\underset{\sim}{L}$ matrix and $\underset{\sim}{O}$ is a zero matrix of 3N-6 rows and one column. If a trivial solution of no vibration is to be avoided, then

$$\left|(\underset{\sim}{G}\,\underset{\sim}{F} - \lambda_k \underset{\sim}{E})\right| = 0$$

The physical meaning of λ_k can be determined by applying the Lagrangian equation to the kinetic and potential energy with respect to normal coordinates giving

$$\frac{d}{dt}\,\frac{\partial T}{\partial \dot{\underset{\sim}{Q}}} + \frac{\partial V}{\partial \underset{\sim}{Q}} = 0$$

Recalling the equations

$$2T = \dot{\underset{\sim}{Q}}^{\dagger}\,\dot{\underset{\sim}{Q}}$$

and

$$2V = \underset{\sim}{Q}^{\dagger}\,\underset{\sim}{\Lambda}\,\underset{\sim}{Q}$$

the result is

$$\ddot{\underset{\sim}{Q}} + \underset{\sim}{\Lambda}\,\underset{\sim}{Q} = \underset{\sim}{O}\ .$$

Solutions to the component second order differential equations of the above matrix equation must have the form

$$Q_k = A_k \cos(\lambda_k^{1/2} t + \epsilon_k)$$

$$= A_k \cos(2\pi \nu_k t + \epsilon_k)$$

where ν_k is the frequency of vibration associated with the kth normal coordinate. Thus

$$\lambda_k = 4\pi^2 \nu_k^2 \quad .$$

The matrix $\underset{\sim}{G}$ can be determined from the geometry of the molecule and the masses of the atoms. λ_k's can be determined from spectroscopic measurements. Referring to the secular equation

$$\left|(\underset{\sim}{G}\underset{\sim}{F} - \lambda_k \underset{\sim}{E})\right| = \underset{\sim}{0}$$

the $\underset{\sim}{F}$ matrix may be determined if sufficient experimental data can be obtained. For insufficient data, the problem is often solved by assuming some of the off-diagonal $\underset{\sim}{F}$ matrix elements to be zero.

From the above information $\underset{\sim}{L}_k$ and $\underset{\sim}{L}$ may be determined, except for a normalization constant; i.e.,

$$\underset{\sim}{L} = \underset{\sim}{S}^{\circ} \underset{\sim}{N}$$

where $\underset{\sim}{N}$ is a diagonal matrix and $\underset{\sim}{S}^{\circ}$ is obtained from above. Substituting for $\underset{\sim}{L}$

$$\underset{\sim}{\Lambda} = \underset{\sim}{L}^{\dagger} \underset{\sim}{F} \underset{\sim}{L} = \underset{\sim}{N}^{\dagger} \underset{\sim}{S}^{\circ\dagger} \underset{\sim}{F} \underset{\sim}{S}^{\circ} \underset{\sim}{N}$$

and the component equations are

$$N_k^2 \sum_{t,t'=1}^{3N-6} F_{tt'} S^{\circ}_{tk} S^{\circ}_{t'k} = \lambda_k .$$

The solution for N_k is

$$N_k = \left[\frac{\lambda_k}{\sum_{t,t'=1}^{3N-6} S^{\circ}_{tk} S^{\circ}_{t'k}} \right]^{\frac{1}{2}} .$$

Knowing $\underset{\sim}{S}^{\circ}$ and $\underset{\sim}{N}$, $\underset{\sim}{L}^{-1}$ can be found by the equation

$$\underset{\sim}{L}^{-1} = \underset{\sim}{N}^{-1} \underset{\sim}{S}^{\circ -1} ,$$

and $\underset{\sim}{Q}$ is then given from one of the defining equations

$$\underset{\sim}{Q} = \underset{\sim}{L}^{-1} \underset{\sim}{S} .$$

The sets of internal coordinates generally used represent changes in bond lengths and angles. They are particularly important because they provide the most physically significant set for use in describing the potential energy of the molecule. Their force constants denote the stiffness of the bonds; consequently, they provide a measure of the difference between bonds.

The solution of the secular equation is difficult for any but the smallest molecules. However, application of group theory to molecules with some symmetry can lead to a set of symmetry coordinates which will factor the secular equation. Theoretical considerations give the relationships between symmetry coordinates and internal

coordinates so that the symmetry $\underset{\sim}{G}$ matrix can be determined from knowledge of the internal $\underset{\sim}{G}$ matrix. A solution for the factored symmetry secular equation

$$\left|\left(\underset{\sim}{G}\,\underset{\sim}{F} - \lambda\,\underset{\sim}{E}\right)\right| = \underset{\sim}{0}$$

is obtained, and the internal coordinate $\underset{\sim}{F}$ matrix is determined from the symmetry $\underset{\sim}{F}$ matrix.

It was stated previously that normal coordinates are used for the quantum mechanical treatment of molecular vibrations. From the equations

$$2T = \dot{\underset{\sim}{Q}}^{\dagger}\,\dot{\underset{\sim}{Q}}$$

and

$$2V = \underset{\sim}{Q}^{\dagger}\,\underset{\sim}{\Lambda}\,\underset{\sim}{Q}$$

the vibrational wave equation for the molecule is given as

$$-\frac{\hbar^2}{8\pi^2}\,\frac{\partial^2\psi_v}{\partial\underset{\sim}{Q}^{\dagger}\,\partial\underset{\sim}{Q}} + \frac{1}{2}\,\underset{\sim}{Q}^{\dagger}\,\underset{\sim}{\Lambda}\,\underset{\sim}{Q}\,\psi_v = W_v\,\psi_v\,.$$

If

$$\psi_v = \psi(Q_1)\,\psi(Q_2)\cdots\psi(Q_{3N-6})$$

and

$$W_v = W(Q_1) + W(Q_2) + \text{----} + W(Q_{3N-6})$$

then

$$-\frac{h^2}{8\pi^2}\frac{d^2\psi(Q_k)}{dQ_k^2} + \frac{1}{2}\lambda_k Q_k^2 \psi(Q_k) = W(Q_k)\,\psi(Q_k).$$

This is the differential equation for a harmonic oscillator for which the energy levels are

$$W_k = h\nu_k\left(n+\tfrac{1}{2}\right), \quad \begin{matrix} k = 1, 2, ----, 3N-6 \\ n = 0, 1, 2, ---- \end{matrix}.$$

Here, as in previous discussions, $\lambda_k = 4\pi^2\nu_k^2$. The energy of a normal mode of vibration is therefore directly related to its frequency by a factor h known as Plank's constant.

So far, the potential energy has been expressed as a function containing only quadratic terms and all higher terms were neglected. This is known as the "harmonic oscillator approximation." The difference between the potential function of the actual molecule and that given by this approximation is known as "anharmonicity" and arises because the cubic and quartic terms may not be entirely neglected.

In order to determine a potential energy that includes anharmonicity, perturbation theory is used, since the solution of the wave equation using a potential function for an anharmonic oscillator is extremely difficult.

First order perturbation theory gives rise to energies of the

form $W'_k = H'_{kk}$, and second order yields energies of the form

$$W'_k = \sum_{l}{}' \frac{H'_{kl} H'_{lk}}{W^\circ_k - W^\circ_l}$$

where the prime on the summation symbol denotes exclusion of l = k, $H'_{nm} = \int \psi_n V_{anh.} \psi_m d\tau$, and W°_n refers to the energy of a harmonic oscillator in its nth quantum state; i.e., $W^\circ_n = h\nu\,(n + \frac{1}{2})$.

Maki (24, p. 29-40) has carried out these computations for the cyanate ion and has concluded that the energy can be represented to a high degree of approximation by an equation of the type

$$\frac{W}{k} = \sum_{k=1}^{3N-5}{}' \nu_k \left(n_k + \frac{g_k}{2}\right) + \sum_{k=1}^{l} \sum_{l=1}^{3N-5} x_{kl} \left(n_k + \frac{g_k}{2}\right)\left(n_l + \frac{g_l}{2}\right)$$

where g_k is the degeneracy of the k'th vibration and the x_{kl}'s are the anharmonicity constants.

In the denominator of the second order perturbation term given previously, the difference between the unperturbed energies of the two levels may approach zero for a case of accidental degeneracy. This causes the perturbation term to be large, and the validity of the method breaks down. Under these conditions, the two energy levels perturb each other and two new energy levels are created. The actual transition observed will be from the ground state to these two new levels. This type of resonance was first proposed by Fermi

(13, p. 250-259) and is commonly known as Fermi Resonance.

Because of the breakdown of perturbation theory, this problem is treated by the linear variation method. If W_1^o and W_2^o are the energies of the unperturbed levels and

$$W_{12} = W_{21} = \int \psi_1 V_{anh.} \psi_2 \, d\tau ,$$

then the usual secular equation

$$\begin{vmatrix} W_1^o - W & W_{12} \\ W_{21} & W_2^o - W \end{vmatrix} = 0$$

may be solved for the energies W_+ and W_- of the two perturbed levels. The solution yields

$$W_+ = \frac{1}{2} \left(W_1^o + W_2^o + \sqrt{(W_1^o - W_2^o) + 4 W_{12}^2} \right)$$

and

$$W_- = \frac{1}{2} \left(W_1^o + W_2^o - \sqrt{(W_1^o - W_2^o) + 4 W_{12}^2} \right).$$

Thus, the difference between perturbed levels is just

$$\sqrt{(W_1^o - W_2^o) + 4 W_{12}^2} .$$

Previous discussion indicated that the intensity of absorption was related to integrals of the type

$$(\mu_x)_{nm} = \int \psi_n^* \mu_x \psi_m \, d\tau$$

where μ_x was the x component of the dipole moment, or $\mu_x = \sum_a e_a x_a$. The sum is taken over all atoms in the molecule and e_a is the effective charge on each atom. Not very much

is actually known about the function $\mu(r)$, but it may be presumed to approach zero for both very small and very large values of r and to vary between in some manner, where r is the internuclear distance.

In terms of normal coordinates the moment can be represented by the expansion

$$\mu_x = \mu_x^\circ + \left[\frac{\partial \mu_x}{\partial Q^T}\right]_0 Q + Q \left[\frac{\partial^2 \mu_x}{\partial Q \partial Q^T}\right]_0 Q + \text{higher terms.}$$

Therefore

$$(\mu_x)_{mn} = \mu_x^\circ \int \psi_m^* \psi_n \, d\tau + \sum_{k=1}^{3N-6} \left[\frac{\partial \mu_x}{\partial Q_k}\right]_0 \int \psi_m^* Q_k \psi_n \, d\tau + \sum_{i,j=1}^{3N-6} \left[\frac{\partial^2 \mu_x}{\partial Q_i \partial Q_j}\right]_0 \int \psi_m^* Q_i Q_j \psi_n \, d\tau .$$

If the vibrational portion of the wave function is assumed to be a product of harmonic oscillator functions, then the first term on the right hand side of the above equation is zero unless m = n by the orthogonality of the harmonic oscillator wave functions. If m = n then no absorption of light can occur so that this term contributes nothing to the absorption. The second term is zero unless $m = n \pm 1$, and the third term is zero unless $m = n$, $m = n \pm 2$, or $m_i = n_i \pm 1$ and $m_j = n_j \pm 1$. Since higher derivatives of the electric moment rapidly

diminish in magnitude, and since the intensities of fundamentals depend upon the coefficient of the second integral while those for overtone and combination bands depend upon the coefficients of the third and higher integrals, the intensities of the latter are generally weak compared to the fundamental intensities. The intensities of higher overtones diminish rapidly.

2. Lattice Effects

When small amounts of impurity ions form a solid solution by replacing ions in the lattice of some other crystalline substance, the impurity ions are subjected to the electrostatic fields and the repulsive forces arising from the host lattice. These effects upon the vibrational frequencies of the impurity ions are related to the second derivative of the energy for the host lattice taken in the direction of the vibration.

Calculations of the cohesive energy for ionic crystals were first made by Born (4, p. 704-727) and Madelung (23). Born's theory of the lattice energy is based on the assumption that the crystals under consideration are built up of positive and negative ions and that the charge distribution in these ions is spherically symmetric. Thus, the force between two such ions depends only on their distance apart.

In order to account for the stability of these crystals, repulsive forces between the ions must be introduced, otherwise the

crystal would collapse under the influence of the attractive forces. Born in his early work made the simple assumption that the repulsive energy between two ions could be expressed by a power law of the type B'/r^n, where B' and n are constants and r is the distance between the ions. Through quantum mechanical calculations Pauling (33, p. 379-382) has shown that the power law cannot be rigorous. This law is replaced by an exponential one of the form

$$\epsilon_{rep}(r) = b\, e^{-\frac{r}{\rho}}$$

where b and ρ are constants.

The potential of a system consisting of two ions at a distance r apart is

$$\phi_T = \frac{-Z_1 Z_2 e^2}{r} + b\, e^{-\frac{r}{\rho}}$$

or the energy per stoichiometric molecule in a crystal is

$$\epsilon_T = -\frac{\alpha^2 e^2}{r} \sum_i \sum_j{}' \left(\frac{z_i}{\alpha} \frac{z_i}{\alpha} \frac{r}{r_{ij}} \right) + \sum_i \sum_j{}' b_{ij}\, e^{-\frac{r_{ij}}{\rho}}$$

where T refers to the absolute temperature, α is the largest common factor in the valences of all the ions, r is the shortest interionic distance, e is the charge of one electron, z_k is the valence of the kth ion, r_{ij} is the distance between the ith and jth ions, b_{ij} is a repulsive constant determined by the type of ion pair involved, ρ is a constant, the summation with respect to the index i extends over

the ions in a stoichiometric molecule, the summation with respect to the index j extends over all ions in the crystal except for the term with i = j.

If the repulsions are only between nearest neighbors, then

$$\epsilon_T = -\frac{\alpha^2 e^2 A}{r} + B e^{-\frac{r}{\rho}} .$$

The constant A is a pure number and is called the Madelung constant. It has been calculated by Madelung (22), Ewald (12, p. 253-287), and Evjen (11, p. 678-686) for various crystal structures.

The volume of a crystal containing a mole of ions is given in terms of the nearest neighbor distance by the equation

$$V = C N r^3$$

where N is Avogadro's constant and C is a constant determined from the structure of the crystal under consideration. Hence

$$\frac{\partial \epsilon_T}{\partial r} = \frac{1}{N} \frac{\partial (N\epsilon_T)}{\partial r} = \frac{1}{N} \frac{\partial E}{\partial r} = \frac{1}{N} \left(\frac{\partial E}{\partial V}\right)_T \frac{\partial V}{\partial r}$$

$$= \frac{1}{N} \left(\frac{\partial E}{\partial V}\right)_T (3CNr^2) = \frac{3V}{Nr} \left(\frac{\partial E}{\partial V}\right)_T$$

where E is the internal energy of a crystal containing one mole of material. The derivative $\left(\frac{\partial E}{\partial V}\right)_T$ may be expressed in terms of the coefficient of expansion γ_T, the coefficient of compressibility β_T, and the pressure on the crystal p, by the equation

$$\left(\frac{\partial E}{\partial V}\right)_T = T\frac{\gamma_T}{\beta_T} - p .$$

Therefore at equilibrium

$$a_T \left(\frac{\partial \epsilon_T}{\partial r}\right)_{r=a_T} = 3\left(\frac{V}{N}\right)\left(\frac{T\gamma_T}{\beta_T} - p\right)$$

where a_T is the equilibrium nearest neighbor distance at temperature T and V/N is the molecular volume. At zero pressure and temperature

$$\left(\frac{\partial \epsilon_0}{\partial r}\right)_{r=a_0} = \frac{\alpha^2 e^2 A}{a_0^2} - \frac{B}{\rho} e^{-\frac{a_0}{\rho}} = 0 .$$

Solving for B yields

$$B = \frac{\alpha^2 e^2 A}{a_0^2} \rho e^{\frac{a_0}{\rho}} .$$

Therefore

$$\epsilon_T = -\alpha^2 e^2 A \left[\frac{1}{r} - \frac{\rho}{a_0^2} e^{\frac{a_0 - r}{\rho}}\right] .$$

The constant ρ may be determined from compressibility data extrapolated to zero degrees Kelvin. The relationship is obtained by taking the second derivative of the energy with respect to r. Thus

$$\frac{\partial^2 \epsilon_T}{\partial r^2} = \frac{\partial}{\partial r}\left[\frac{3V}{Nr}\left(\frac{\partial E}{\partial V}\right)_T\right] = \frac{3V}{N}\left[-\frac{1}{r^2}\left(\frac{\partial E}{\partial V}\right)_T + \frac{1}{r}\left(\frac{\partial^2 E}{\partial V^2}\right)_T \left(\frac{\partial V}{\partial r}\right)\right]$$

$$= \frac{3V}{Nr^2}\left[-\left(\frac{\partial E}{\partial V}\right)_T + 3V\left(\frac{\partial^2 E}{\partial V^2}\right)\right] .$$

At zero temperature and pressure then

$$a_0^2\left(\frac{\partial^2 \epsilon_0}{\partial r^2}\right)_{r=a_0} = \frac{9V_0}{N}\left[-V_0\left(\frac{\partial P}{\partial V}\right)_T\right] = \frac{9V_0}{N\beta_0} = -\alpha^2 e^2 A\left[\frac{2}{a_0} - \frac{1}{\rho}\right] .$$

The compressibility is related to the exponent n of the repulsive term in Born's original equation by the expression

$$\beta_0 = \frac{9 C a_0^4}{\alpha^2 e^2 A (n-1)} .$$

Substituting for β_0 and solving for ρ yields

$$\rho = \frac{a_0}{n+1} ,$$

and the final form of the energy equation is

$$\epsilon_T(r) = -\alpha^2 e^2 A \left[\frac{1}{r} - \frac{1}{(n+1) a_0} e^{(n+1)\left(1 - \frac{r}{a_0}\right)} \right] .$$

At temperatures above zero degrees Kelvin, a_T, the equilibrium value of r at temperature T, is larger than a_o. This occurs because the vibrating ions exert a force upon nearest neighbors averaged over time which is similar to the force exerted upon the walls of a container by a gas. This force increases with temperature and causes the ions to increase their equilibrium distances of separation. The first derivative of the potential energy with r is nonzero at other than absolute zero temperature because the attractive coulombic force is greater than the repulsive force for a separation r greater than a_o.

Thermal vibrations of the ions about their mean position causes a statistical number of the ions to be in a potential field which is not well defined but which covers the range of the potential field over the region of space within which the ion moves. Since infrared

absorptions depend upon molecular vibrational frequencies, they must depend upon the potential field in which the ion finds itself. The more clearly defined the field is for the ions, the more exactly will the vibrational frequencies be defined. As the temperature of a crystal is lowered, the amplitude of thermal vibration decreases, and the absorption lines become sharper. Also as the temperature is decreased, thus decreasing the lattice dimensions, the ions will be subjected to greater forces arising from the potential energy causing the frequencies of vibration to increase.

A third effect related to temperature is that the equilibrium population of excited states will vary with change of temperature according to the Boltzmann distribution law

$$\frac{n_i}{n_j} = \frac{g_i}{g_j} e^{\frac{-(\epsilon_i - \epsilon_j)}{kT}}$$

where n_i is the number of molecules with energy ϵ_i , g_i is the degeneracy of the ith energy state, T is the absolute temperature, and k is the Boltzmann constant. At very low temperatures the intensity of absorption for excited vibrational states may decrease to zero due to this effect.

In the solid state, the rotational and translational degrees of freedom associated with the gaseous state become fixed into librational and vibrational motions due to intermolecular forces which limit the motion of the molecules. These frequencies still are lower

than the vibrational frequencies due to polyatomic ions and molecules and therefore do not mask out any of the vibrational spectrum. Nevertheless, coupling can take place between lattice vibrations and molecular vibrations giving rise to various combination bands which appear in the vicinity of absorption bands due to molecular vibrations.

III. EXPERIMENTAL METHODS

1. Pressed Pellets

The pressed pellet technique (39, p. 1805) is advantageous for holding a measured and controlled amount of sample in the light path of a spectrometer with a minimal amount of light scattering. In addition, several investigators (24, p. 58; 6; 19) have reported that the formation of solid solutions in alkali halides can be accomplished with this technique. Usually before formation of the pellet a high degree of intermixing of the sample and the alkali halide is brought about by coprecipitation techniques in order for solid solution to occur.

In the present work the following procedure was used for preparing pressed pellets. A small amount of the sample was mixed with alkali halide using a mortar and pestle, then reduced to a fine powder in a ball mill. The powder was placed in an evacuable die and subjected to a pressure of approximately 100,000 psi. With dilute concentrations of the sample, a clear disk was formed. Higher concentrations caused brown or black pellets to be formed.

Several requirements must be met in order to prepare a good disk. The alkali halide and the sample should both be dry and evenly distributed in the die. The sample is more evenly distributed if the

plunger is rotated while in contact with the salt. The die must be evacuated before and during the application of pressure. Applying the pressure slowly and removing the pressure slowly also seems to help.

2. Crystal-Growing Apparatus

Alakli halide crystals were grown from the melt using the Kyropoulos Method (21). Due to the decomposition of the doping agent in the air at temperatures of the molten alkali halides, an apparatus for growth of uniformly doped crystals in an argon atmosphere was constructed by Robert E. Holmes and the author. Illustrations of the apparatus appear in Figures 1 and 2.

The seed crystal was mounted on the end of a rotating cold finger cooled with flowing water. Growth proceeded as the furnace, and consequently the level of the molten salt was lowered on a table at a rate which could be varied from a few tenths of an inch to several inches per hour. The rate of rotation of the cold finger could be varied from 80-120 rpm by setting a governor. A rotation rate of 90 rpm is sufficient for uniform doping of crystals (8, p. 18). In order to remove oxides and hydroxides from the molten salt before introduction of the doping agent, provision was made for introducing hydrogen bromide gas or chlorine gas, depending upon the halide present, over the melt. The doping agent was held in a Pyrex glass

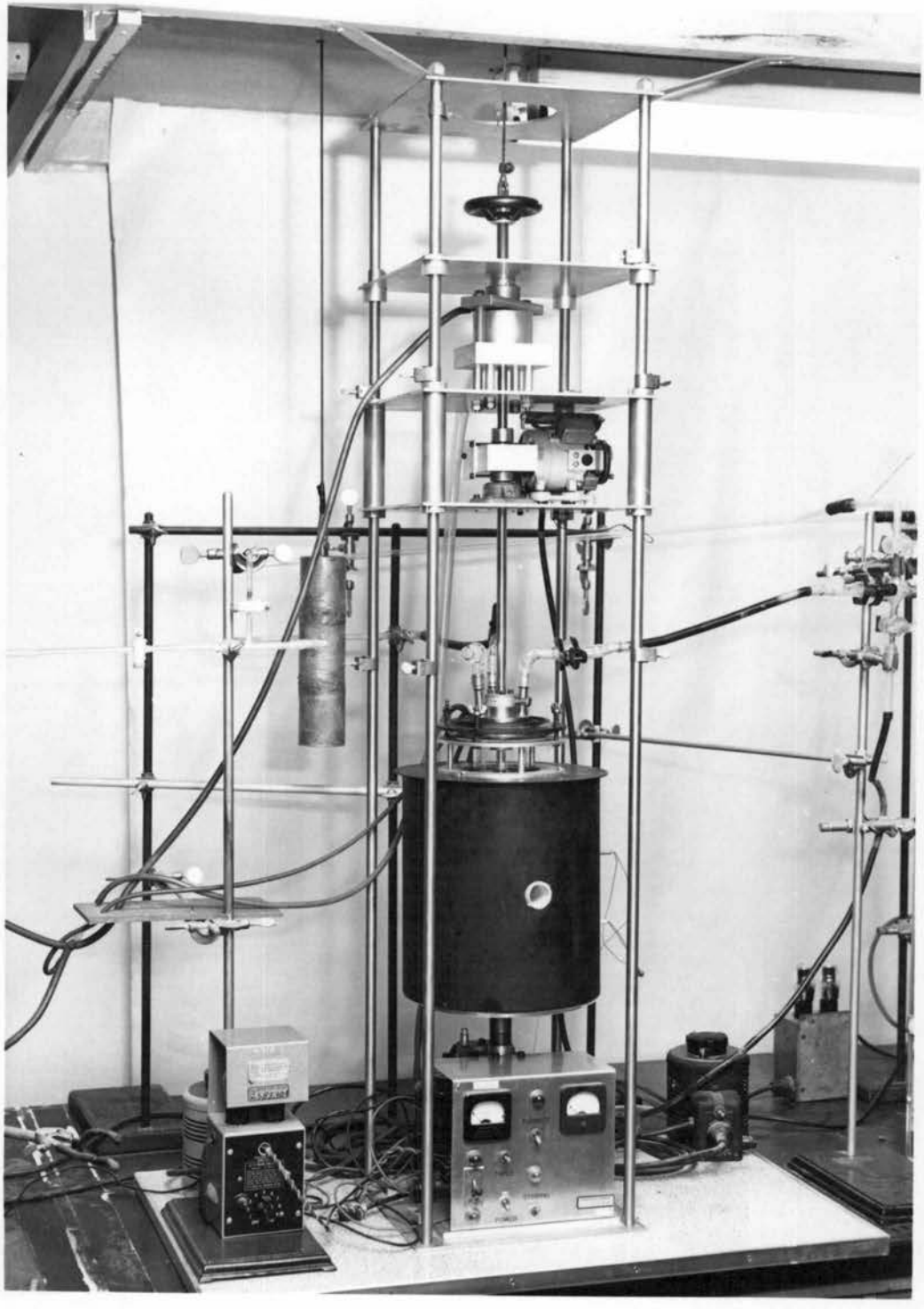

Figure 1. Photograph of the crystal-growing apparatus.

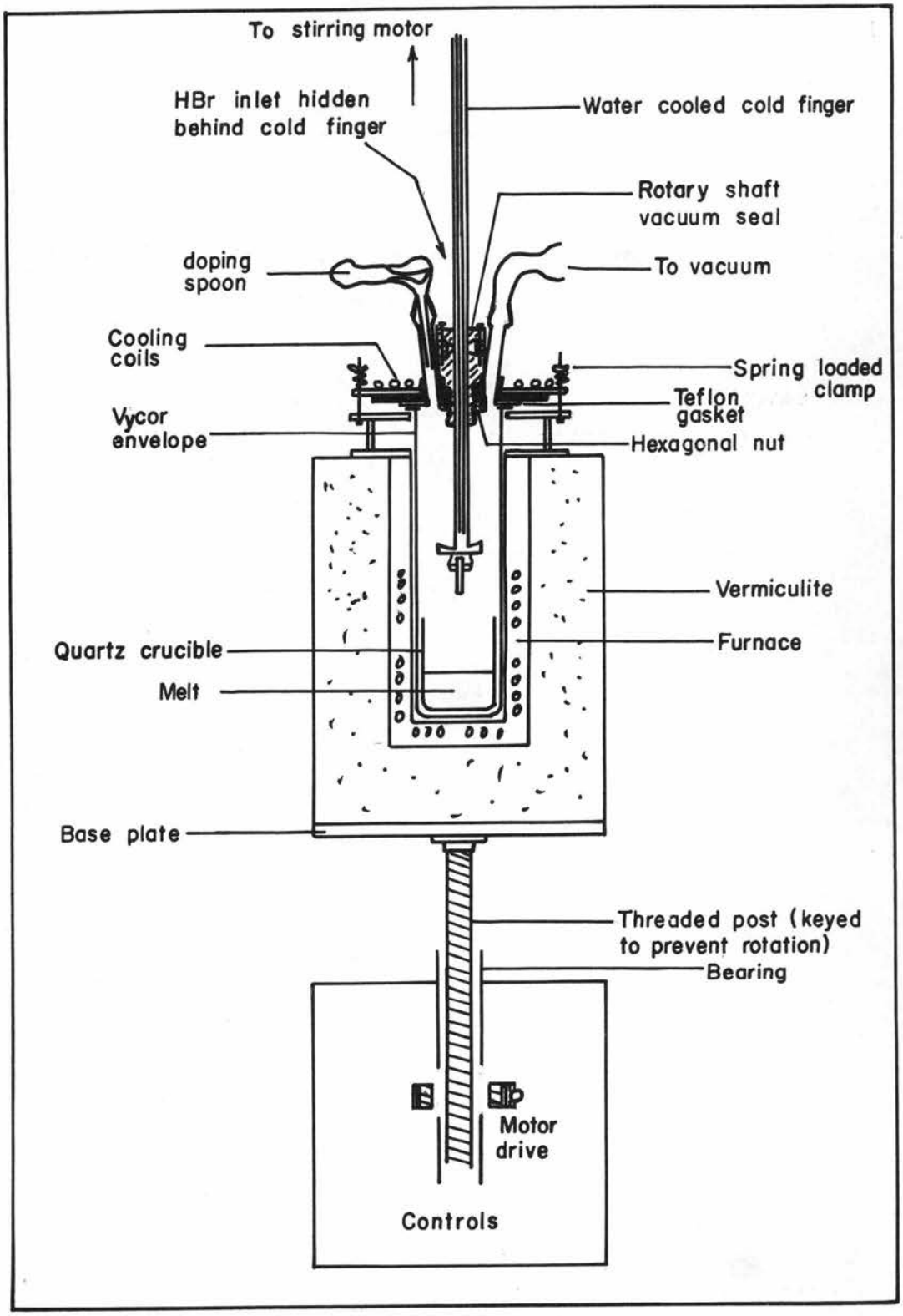

Figure 2. Schematic diagram of the crystal growing apparatus.

spoon which could be rotated upside down to drop the sample into the melt below.

The apparatus was constructed primarily from aluminum, brass, and stainless steel. The four support rods for the apparatus were of stainless steel. The three horizontal square plates were free to slide up or down the rods, but were counter-weighted so that they did not tend to move unless pushed by hand. All three plates were locked together and were moved as a unit along the rods in order to bring the seed crystal near the surface of the melt. The top plate could then be locked to the rods, and the lower two plates moved downward relative to the top plate by means of a wheel attached to a threaded shaft so that a fine adjustment of the seed near the surface of the melt could be accomplished. All parts exposed to the corrosive gases were plated with electrolous nickel, then with rhodium. The outside of the furnace was constructed from black iron. The furnace was made by coiling nichrome wire on an alundum core and covering the windings with alundum cement. Vermiculite was used for insulation. A chromel-alumel thermocouple placed at the inner surface of the core next to the envelope was used for temperature measurements. A view of the melt and the growing crystal from the side was obtained by looking through a hole one inch in diameter through the side of the furnace. The envelope containing the crucible and melt was made of Vicor glass and the crucible was of

quartz so that one could view the melt through them quite well.

3. Growth Procedures

The apparatus was cleaned and the rotary shaft vacuum seal repacked before every run. The Vicor envelope and quartz crucible were inserted into the furnace and the seed crystal was affixed to the cold finger. All connections were greased. Those exposed to the corrosive gases were greased with Kel-F. The doping agent was weighed and placed in the spoon next, because only a small amount of doping agent was used, and it did not tend to acquire moisture rapidly. The final step before closing the apparatus was to unseal a bottle of specially prepared alkali halide, weigh out rapidly approximately one hundred grams, and deposit the salt in the crucible with the aid of a funnel. The apparatus was then sealed as rapidly as possible and evacuated. A typical pressure of about two to eight microns resulted. The system was backfilled with argon, heated by the furnace until the salt was molten, flushed with hydrogen bromide or chlorine, flushed with argon, evacuated, and backfilled with argon once more. Corrosive gases were used only when the doping agent was calcium cyanamide, since traces of oxide or hydroxide present will rapidly oxidize the cyanamide to cyanate. Cyanate, on the other hand, is much more resistant to oxidation and does not require such complete removal of oxides and hydroxides from the

melt before doping.

When the galvanometer attached to the chromel-alumel thermocouple indicated that the temperature of the melt was just slightly above the melting point of the alkali halide, the rotation of the cold finger was begun. The seed crystal was brought into contact with the melt, and the furnace current was regulated so that the tip of the seed was melted on contact with the molten salt to improve the chances for the crystal to grow single. Lowering of the melt was begun, and the furnace current was lowered in small increments until the crystal began to expand at the proper rate. When the crystal had grown to proper cross section, the speed of lowering the furnace was increased until further expansion of the crystal ceased. Only slight adjustments were required for the duration of crystal growth. When the major part of the melt had been used in growing the crystal, the system was unsealed and the crystal removed. The remaining melt in the crucible was sucked out by means of a quartz tube into a metal container, then the crucible was removed and the furnace turned off.

4. Preparation and Purification of Reagents

Barium and magnesium bromides were prepared from their oxides by treatment in aqueous solution with hydrogen bromide. The solutions were evaporated, and the salts that crystallized out were dried in a vacuum oven. The magnesium bromide hexahydrate which

crystallizes from solution will lose four molecules of water of crystallization as its temperature is raised, then will lose hydrogen bromide gas, leaving the oxide in preference to removing the last two water molecules. Therefore, it was necessary to heat the magnesium bromide slowly under a flowing atmosphere of hydrogen bromide to 500 degrees centigrade in order to remove the water of crystallization.

Reagent grade potassium bromide and potassium chloride were triply recrystallized in order to remove impurity ions and organic material. The salts were then heated to approximately 500° C for 36 hours under an appropriate flowing atmosphere (chlorine over potassium chloride, hydrogen bromide over potassium bromide) to remove water, oxides, and hydroxides from the salt. If the alkali halide had been recrystallized only twice before being heated to temperature under the corrosive atmosphere, traces of organic material still remaining would color the salt grey. The water and hydroxides had to be removed in order not to etch the quartz crucible and the Vycor glass envelope as the salt was heated in the crystal-growing apparatus. Etching would prevent a sufficient view of the melt from being obtained during crystal growth.

Other reagents used were analyzed reagent grade potassium cyanate, potassium cyanide, anhydrous calcium chloride, calcium bromide dihydrate, barium chloride, anhydrous magnesium chloride,

and calcium cyanamide.

5. Spectroscopy

All spectra were obtained using a Beckman IR7 infrared spectrophotometer. This instrument utilizes a fore-prism for the purpose of primary dispersion or "order sorting" and separates the bands of the prism spectrum with the superior resolving power of a grating. Use of an air dryer to purge the optical compartments reduces waterband absorption to 20 percent. Use of the double beam facilities incorporated in the IR7 enabled the water band to be completely removed from the absorption spectrum of the sample. Some absorption due to the carbon dioxide in the atmosphere still remained, however.

The IR7 is reported (2, 37) to be capable of a frequency reproducibility of 0.25 cm^{-1} from 600 to 1150 cm^{-1} and a frequency reproducibility of 1.0 cm^{-1} from 2000 to 4000 cm. Its frequency accuracy is reported as $\pm$0.5 cm^{-1} at 650 cm^{-1}, $\pm$2.0 cm^{-1} at 1404.96 cm^{-1}, $\pm$2.5 cm^{-1} at 2016.7 cm^{-1}, and $\pm$0.3 cm^{-1} at 1000 cm^{-1}. No frequency calibration of this instrument has been carried out in this laboratory, however. The IR7 is capable of a resolution of 0.3 cm^{-1} at 1000 cm^{-1}.

Scans were made at a speed of 0.8 cm^{-1}/minute on peaks with a period of 32 seconds. The slit width was usually twice that for the

standard program. This gives a resolution varying from 1 to 3 cm^{-1}.

Low temperature spectra were obtained by placing the samples in a conventional low-temperature cell similar to that described by Wagner and Hornig (40, p. 297-298). The cell was sealed and evacuated, then the cold finger was filled with liquid nitrogen.

IV. DISCUSSION AND RESULTS

1. Spectra of Pressed Pellets

Potassium bromide pellets were pressed containing on the order of ten milligrams of potassium cyanide per gram of the alkali halide. An effort was made to determine whether the cyanide would go into solid solution without having to use the freeze-drying technique for forming an intimate mixture of the cyanide and the alkali halide. Use of the freeze-drying technique would not enable potassium cyanide to be quantitatively incorporated into the pellets due to loss of hydrogen cyanide from the aqueous solution prepared during this process.

The spectrum of each pellet was scanned immediately after pressing. Some of the pellets were then heated to 100° C under vacuum for four hours, then rescanned. No change in the spectra occurred.

The spectrum of a pellet pressed from a mixture containing 5.38 mg KCN per gram KBr may be seen in Figure 3, curve (a). This pellet was given two heat treatments, the first at 100° C under vacuum for four hours, and the second at 600° C under an argon atmosphere for four hours. The spectrum following each treatment is shown in Figure 3. After heating to 600° C, sharp narrow absorption

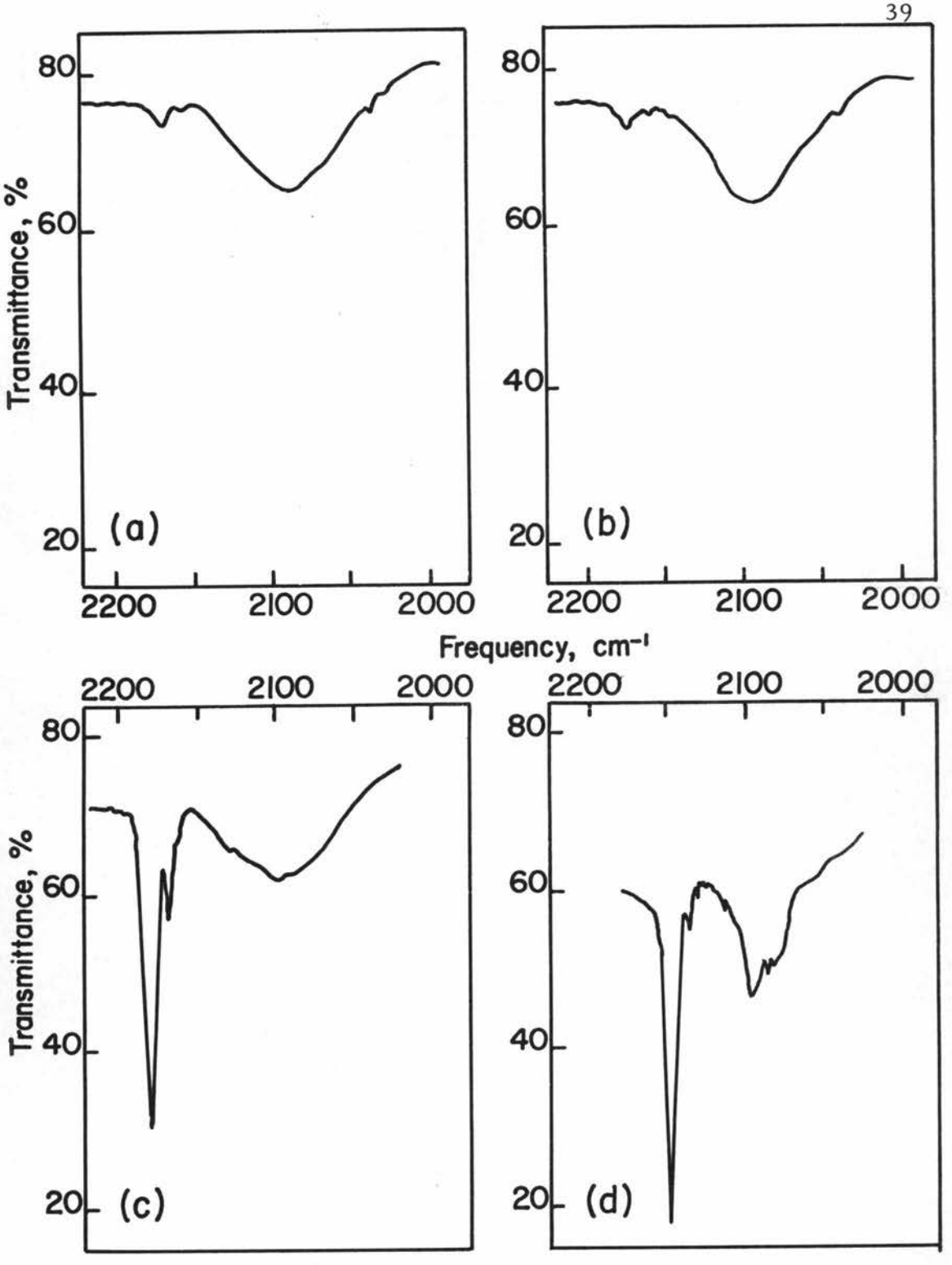

Figure 3. The infrared spectrum of a pellet containing 5.38 mg KCN per gram KBr (a) after pressing the pellets, (b) after four hour heat treatment at 100° C under vacuum, (c) after four hour heat treatment at 600° C under argon atmosphere, and (d) at lowered temperature in a liquid nitrogen cold cell.

peaks of cyanate appeared indicating some oxidation of the sample. However, the cyanide peak remained essentially unchanged. The half width of this band was about 55 to 60 wave numbers, which seemed somewhat broad for a solid solution absorption peak. At liquid nitrogen temperature a sharp peak appeared at 2089 cm^{-1}, 9 cm^{-1} above the center for the main peak. Cooling may have caused sharpening of a solid solution cyanide peak enabling it to be seen.

The force constants of cyanamide ion, $NCN^{=}$, have not as yet been determined. In aqueous solution this ion tends to decompose; therefore, its Raman spectrum is difficult to obtain. Although the cyanamide ion is symmetric, the $N^{15}CN^{14=}$ ion should give an infrared absorption in the symmetric stretching region. With hope that this peak might be observed due to the amount of N^{15} present in nature, several pellets of calcium cyanamide in potassium bromide and in potassium iodide were pressed. The scans of all pellets showed no sharp peak in the symmetric stretching region around 1200 to 1300 cm^{-1}.

One pellet containing 3.3 mg CaNCN per gram KBr was heated to 600° C under an argon atmosphere for 4.5 hours, then cooled to liquid nitrogen temperatures and scanned (see Figure 4). Sharp peaks appeared at 2171.0, 2194.5, 2218.5, and 2239.5 cm^{-1}. in addition to the broad antisymmetric stretching ν_3 peak of cyanamide ion at 2060-2070 cm^{-1}. Another peak not shown in the figure

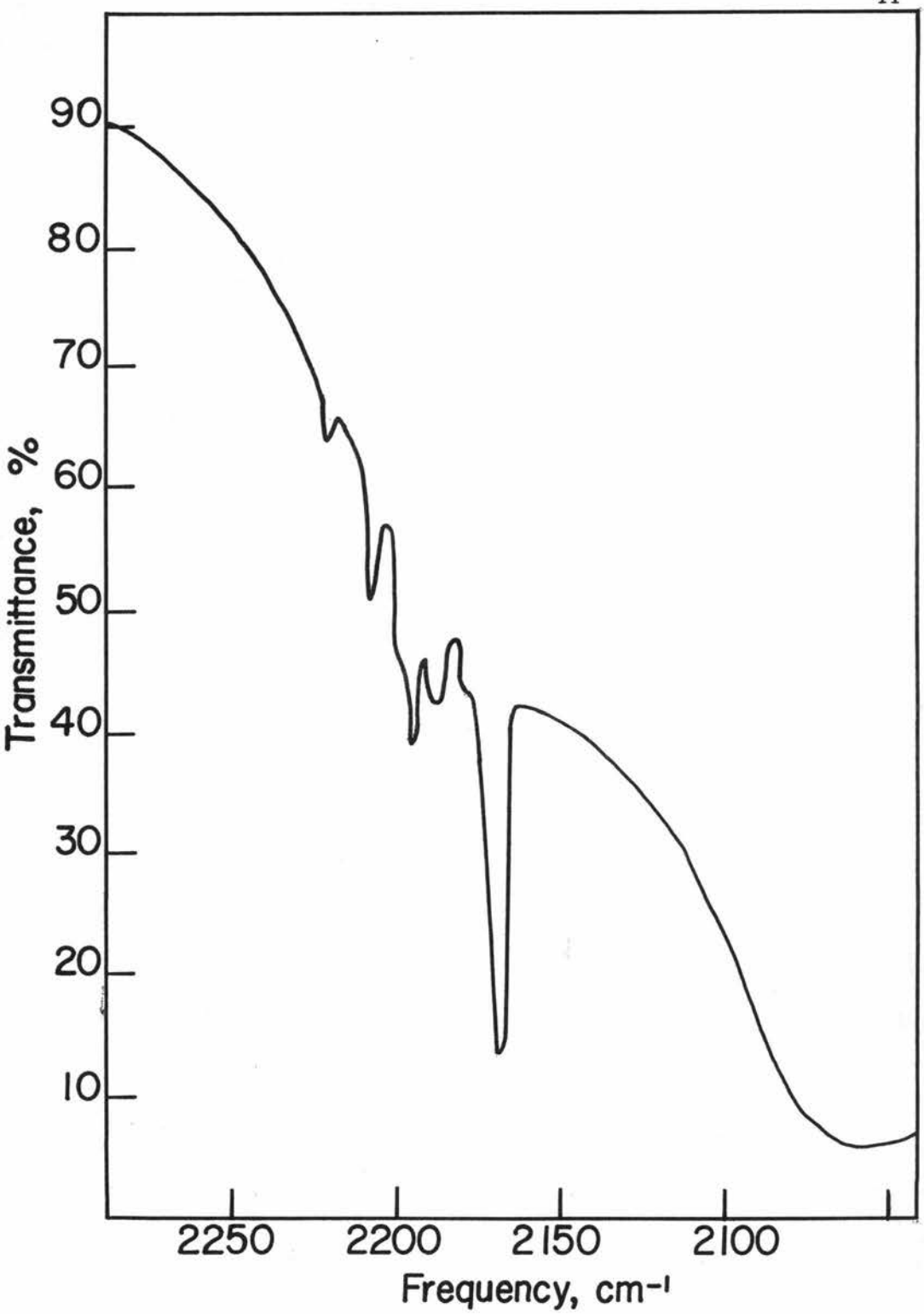

Figure 4. The infrared spectrum of a pellet containing 3.3 mg CaNCN per gram KBr, after 4-1/2 hour heat treatment at 600° C under argon atmosphere, scanned while cooled with liquid nitrogen.

appeared at 671 cm^{-1} corresponding to the bending mode of vibration for cyanamide ion. The broadness of the peaks indicates that most of the cyanamide has not gone into solid solution. The peak at 2170 cm^{-1} appears at the frequency for the ν_3 fundamental absorption of cyanate ion as assigned by Maki and Decius (24, p. 127, p. 123; 26, p. 774).

Peaks appeared at 1201.5 and 1288 cm^{-1} corresponding to a pair of Fermi resonance peaks arising from interaction between ν_1 and the first overtone of the bending frequency $2\,\nu^{\circ}_2$ for cyanate. In addition the cyanate bending fundamental ν_2' appeared at 630 cm^{-1}. The other peaks listed above do not correspond to any absorptions found in potassium bromide. Experimental work to be discussed later in this chapter seems to indicate that calcium ions present near cyanate ions will perturb the vibrating cyanate giving rise to these new peaks.

A surprising degree of sharpening and narrowing of peaks occurred upon cooling two pellets containing CaNCN in KI to liquid nitrogen temperatures. The spectra of these pellets taken first at room temperature, then at lowered temperatures using liquid nitrogen as a coolant are shown in Figure 5. For both pellets the sharp peaks appear at 2092, 2159, and 2171 cm^{-1}. The 2159 cm^{-1} frequency corresponds to that for ν_3 of cyanate ion at lowered temperature in a potassium iodide host lattice. The other two peaks may

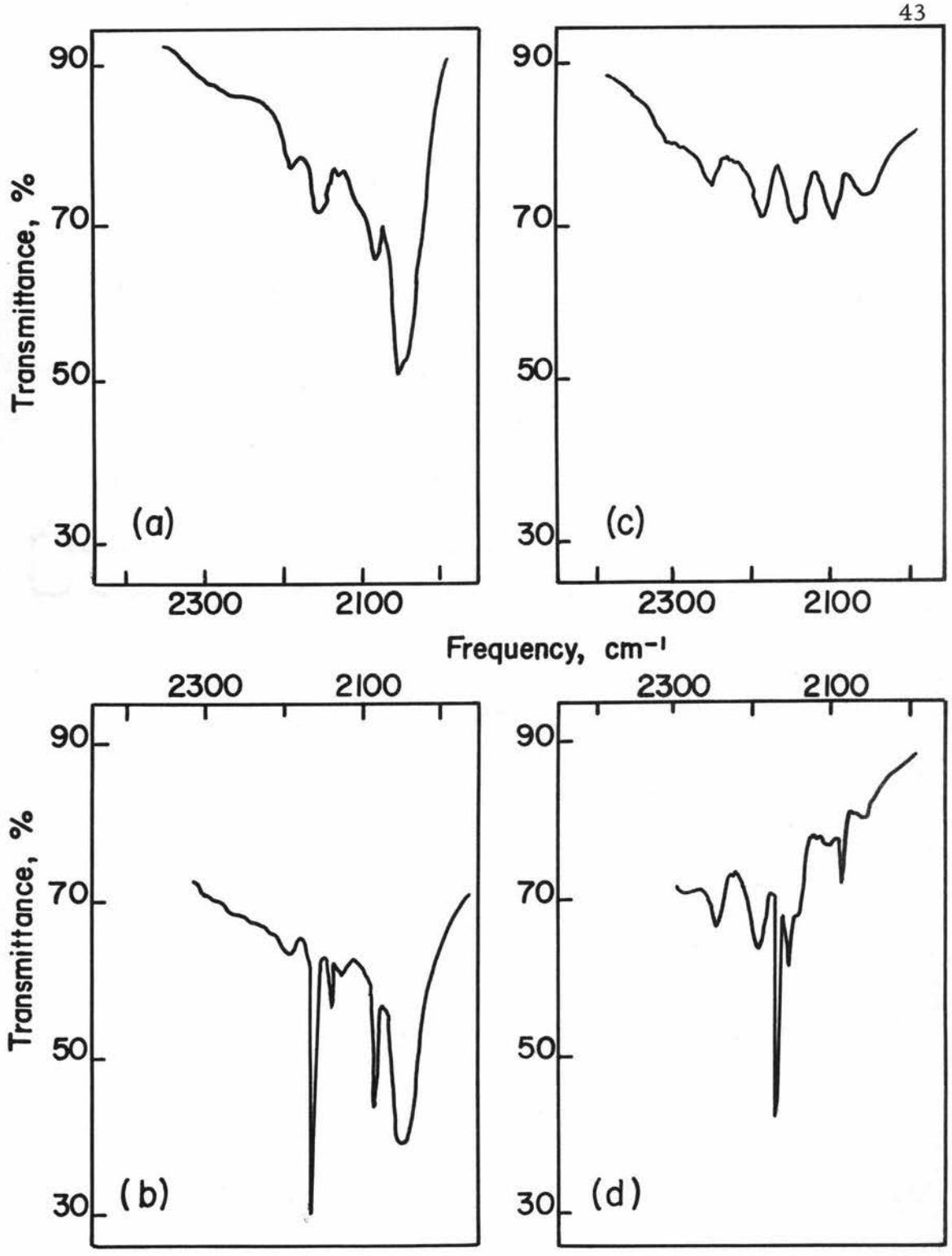

Figure 5. Infrared spectra of a pellet containing 0.22 mg CaNCN per gram KI (a) at room temperature, (b) cooled with liquid nitrogen; infrared spectra of a pellet containing 0.11 mg. CaNCN per gram KI (c) at room temperature, (d) cooled with liquid nitrogen.

be due to cyanate ions paired with calcium ions. The presence of calcium ion should perturb the vibrating cyanate ion giving rise to new peaks.

2. Spectra of Single Crystals

Table 2 contains a list of observed infrared absorption frequencies for potassium chloride and potassium bromide single crystals containing potassium cyanate at room temperature, and spectra of these crystals are given in Figures 6, 7, and 8. Assignments for the absorption bands are the same as those given by Maki and Decius (26, p. 774, p. 777) which were summarized in Table 1. Spectra for alkali halide crystals doped with KNCO and either $CaCl_2$, $CaBr_2$, or $BaCl_2$ are given in Figures 9 through 22. New peaks which appear due to the presence of Ca^{++} ion or Ba^{++} ion are listed in Table 4, the frequencies being reported for liquid nitrogen temperatures. Additional crystals were grown and scanned containing KNCO and either $MgCl_2$, $MgBr_2$, or $BaBr_2$. However, no new peaks appeared due to the M^{++} ion, so no spectra for these crystals have been included.

In the spectrum of a potassium chloride crystal containing Ca^{++} and NCO^- ions, new peaks appeared at 1397, 1427, 1450, 1474, and 1518 cm^{-1} in addition to those new peaks listed in Table 4 for the regions where cyanate absorptions usually appear. A potassium chloride crystal was grown doped with potassium carbonate and

Table 2. Observed frequencies for infrared spectra of cynate ion in single crystals*

Assignment						Isotopic Species	Observed frequencies in cm^{-1} for	
Lower			Upper				KCl	KBr
ν_1	ν_2^{ℓ}	ν_3	ν_1	ν_2^{ℓ}	ν_3			
0	0^0	0	0	1^1	0	C^{13}	613.2	612.0
0	0^0	0	0	1^1	0	...	631.0	629.4
0	0^0	0	1	0^0	0	O^{18}	1180.0	1175.8
0	0^0	0	0	2^0	0	O^{18}	...	...
0	0^0	0	1	0^0	0	N^{15}	1192.8	1188.9
0	0^0	0	0	2^0	0	N^{15}	1287.9	1282.3
0	0^0	0	1	0^0	0	C^{13}	1196.0	1191.0
0	0^0	0	0	2^0	0	C^{13}	1277.4	1272.5
0	0^0	0	1	0^0	0	...	1210.7	1206.0
0	0^0	0	0	2^0	0	...	1297.3	1293.0
0	0^0	0	0	0^0	1	$N^{15}C^{13}$	2107.2	2095.0
0	0^0	0	0	0^0	1	$C^{13}O^{18}$	2117.7	2103.5
0	0^0	0	0	0^0	1	C^{13}	2124.7	2113.0
0	0^0	0	0	0^0	1	N^{15}	2165.0	2153.0
0	0^0	0	0	0^0	1	O^{18}	2178.5	2159.5
0	0^0	0	0	0^0	1	...	2181.8	2169.8
0	0^0	0	2	0^0	0	C^{13}	2370.8	2360.4
0	0^0	0	1	2^0	0	C^{13}	2472.9	2462.6
0	0^0	0	0	4^0	0	C^{13}	2565.0	2554.4
0	0^0	0	2	0^0	0	...	2402.8	2394.6
0	0^0	0	1	2^0	0	...	2498.8	2487.3
0	0^0	0	0	4^0	0	...	2612.8	2602.5

Table 2 (continued)

Assignment						Isotopic	Observed frequencies in cm^{-1} for	
Lower			Upper					
ν_1	ν_2^{ℓ}	ν_3	ν_1	ν_2^{ℓ}	ν_3	Species	KCl	KBr
0	0^0	0	0	1^1	1	C^{13}	2727.5	2714.0
0	0^0	0	0	1^1	1	...	2801.9	2788.1
0	0^0	0	1	0^0	1	C^{13}	3300.8	3284.1
0	0^0	0	0	2^0	1	C^{13}	3384.0	3366.0
0	0^0	0	1	0^0	1	N^{15}	3336.0	3318.0
0	0^0	0	0	2^0	1	N^{15}	3430.5	3414.7
0	0^0	0	1	0^0	1	...	3372.6	3355.0
0	0^0	0	0	2^0	1	...	3458.8	3442.2
0	1^1	0	1	0^0	0	...	...	...
0	1^1	0	0	2^0	0	...	...	664.5
0	1^1	0	1	1^1	0	...	1193.0	1188.0
0	1^1	0	0	3^1	0	...	1314.4	1310.5
0	1^1	0	0	1^1	1	C^{13}	2114.2	2102.2
0	1^1	0	0	1^1	1	...	2170.7	2158.8
0	1^1	0	2	1^1	0	...	...	...
0	1^1	0	1	3^1	0	...	...	...
0	1^1	0	0	5^1	0	...	2638.6	2628.5
0	1^1	0	1	0^0	1	...	2741.0	2725.0
0	1^1	0	0	2^0	1	...	2825.0	2813.0
0	1^1	0	0	2^2	1	...	2790.0	2776.2
0	1^1	0	1	1^1	1	...	3342.1	3325.7
0	1^1	0	0	3^1	1	...	...	...

Table 2 (continued)

Assignment							Observed frequencies in cm^{-1} for	
Lower			Upper			Isotopic		
ν_1	ν_2^{ℓ}	ν_3	ν_1	ν_2^{ℓ}	ν_3	Species	KCl	KBr
0	2^2	0	1	2^2	1	...	1181.9	1177.0
0	2^2	0	0	4^2	0	...	1326.4	1320.6
0	2^2	0	0	2^2	1	...	2161.0	2147.9

* Table 3 gives frequencies for additional peaks observed in the spectra of the single crystals.

Table 3. Frequencies for miscellaneous absorptions observed in the spectra of cyanate ion in single crystals.

Band Identification	Observed frequencies in cm^{-1} for KCl	KBr	Remarks
1	...	1113	
2	...	1390	
3	1974[a]	1960[a]	$B^{11}O^{16}O^{16}$-
4	...	2010	
5	2045[a]	2028.6[a]	$B^{10}O^{16}O^{16}$-
6	...	2074	Difference band for lattice mode
7	...	2128	
8	...	2210.5	
9	...	2248	
10	...	2266	Sum band for lattice mode
11	...	2332	
12	...	2350	
13	...	2378.8	
14	2444	2434	
15	2781	2766	
16	2854	2854	
17	2925	2925	
18	2960	2960	
19	3318	3301.2	
20	...	3536	
21	3580	3565	
22	3695	3676.7	
23	3798	3781.0	

[a] These frequencies correspond closely to values reported by Morgan and Staats (27) for metaborate ion in potassium chloride or potassium bromide host lattices.

Table 4. Observed frequencies for infrared spectra of M^{++} NCO^- ion pairs in single crystals.

	Band Identification	Observed frequencies in cm^{-1} for NCO^- ion with Ca^{++} ion in KCl	KBr	Ba^{++} ion in KCl
Bending	1	650.0	645.8	641.0
	2	654.6	...	645.5
	3	...	...	652.2
Symmetric stetching	4	1232.7	1229.7	1227.2
	5	1234.6	1232.6	1230.5
	6	1239.0	1238.2	1240.7
	7	1247.5	1258.7	1243.2
	8	1256.7	1274.7	1254.7
	9	1264.2	1319.2	1257.2
	10	1325.9	1330.2	1260.5
	11	1335.9	...	1281.7
	12	1341.5	...	1309.6
	13	...	...	1324.6
	14	...	...	1333.8
	13	...	...	1348.6
Anti-symmetric stretching	16	2139.3	2140	2108.3
	17	2188.2	2183	2120.2
	18	2198.8	2189.3	2151.2
	19	2211.3	2198.3	2154.2
	20	2221.8	2210.8	2159.3
	21	2239.2	2228.7	2168.8
	22	2250.1	2236.5	2192.3
Combination	23	3403.3	3392	3360
	24	3407	3406.3	3379
	25	3417.3	3415	3394
	26	3441	3452	3408
	27	3477.7	3484	3430
	28	3486	3507	3453
	29	3493	3538.3	3483
	30	3499	...	3509
	31	3511		
	32	3520		
	33	3543		
	34	3557.2		

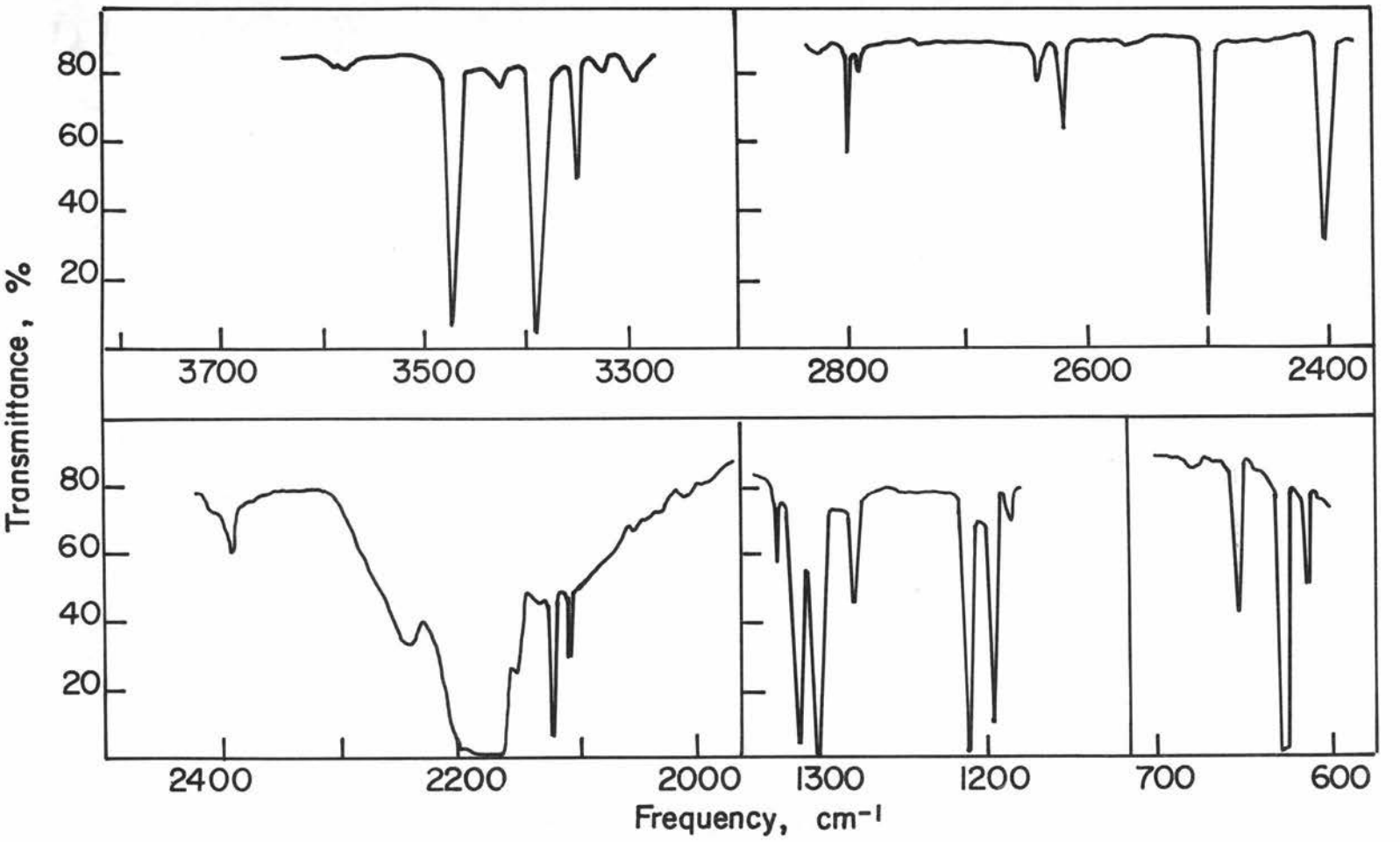

Figure 6. Infrared absorption spectrum of a crystal of 2.65 cm thickness grown from a melt containing 4.60 m moles KNCO per mole KCl scanned at room temperature.

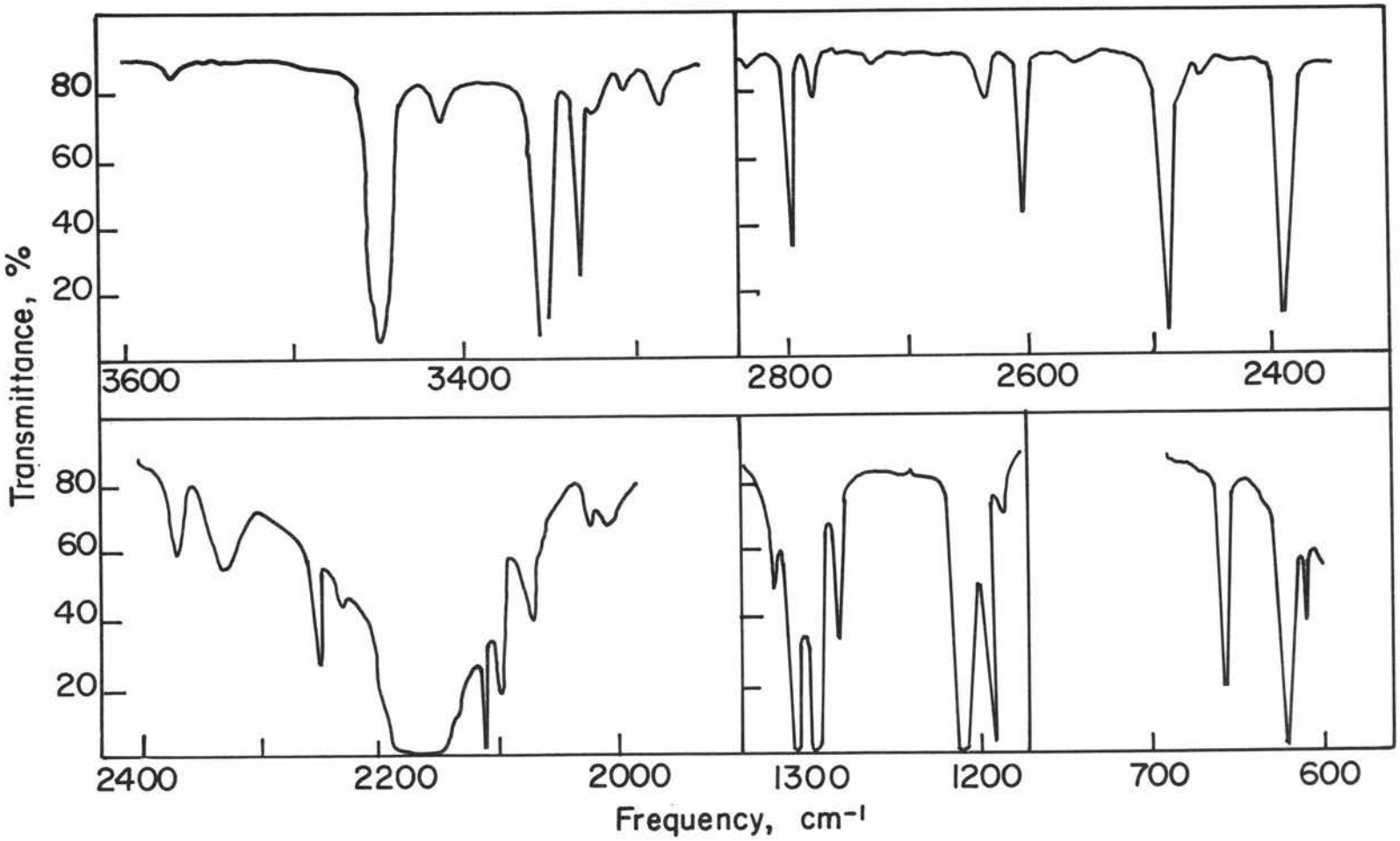

Figure 7. Infrared absorption spectrum of a crystal of 1.75 thickness grown from a melt containing 7.35 m moles KNCO per mole KBr scanned at room temperature.

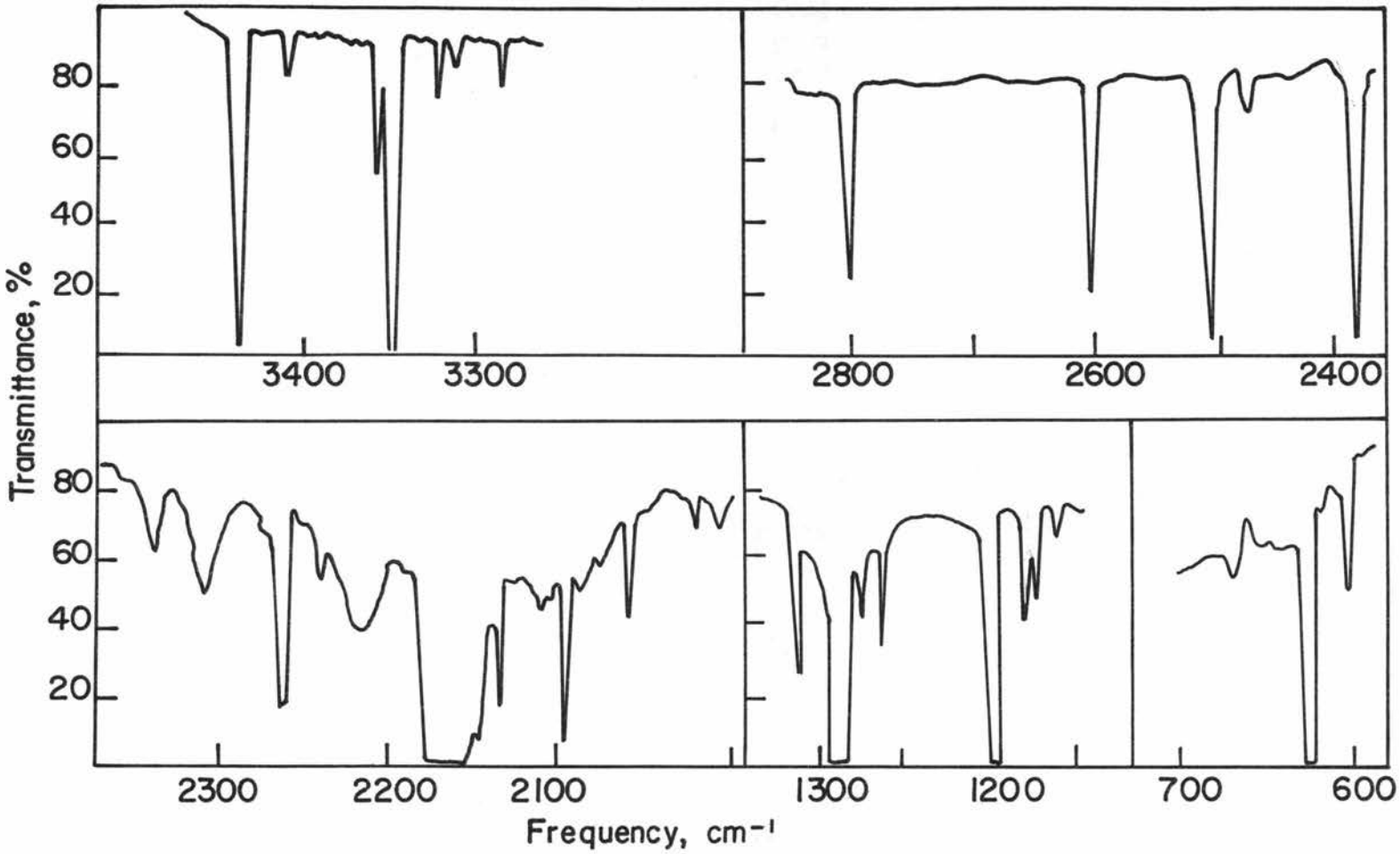

Figure 8. Infrared absorption spectrum of a crystal of 1.75 cm thickness grown from a melt containing 7.35 m moles KNCO per mole KBr scanned while cooled with liquid nitrogen.

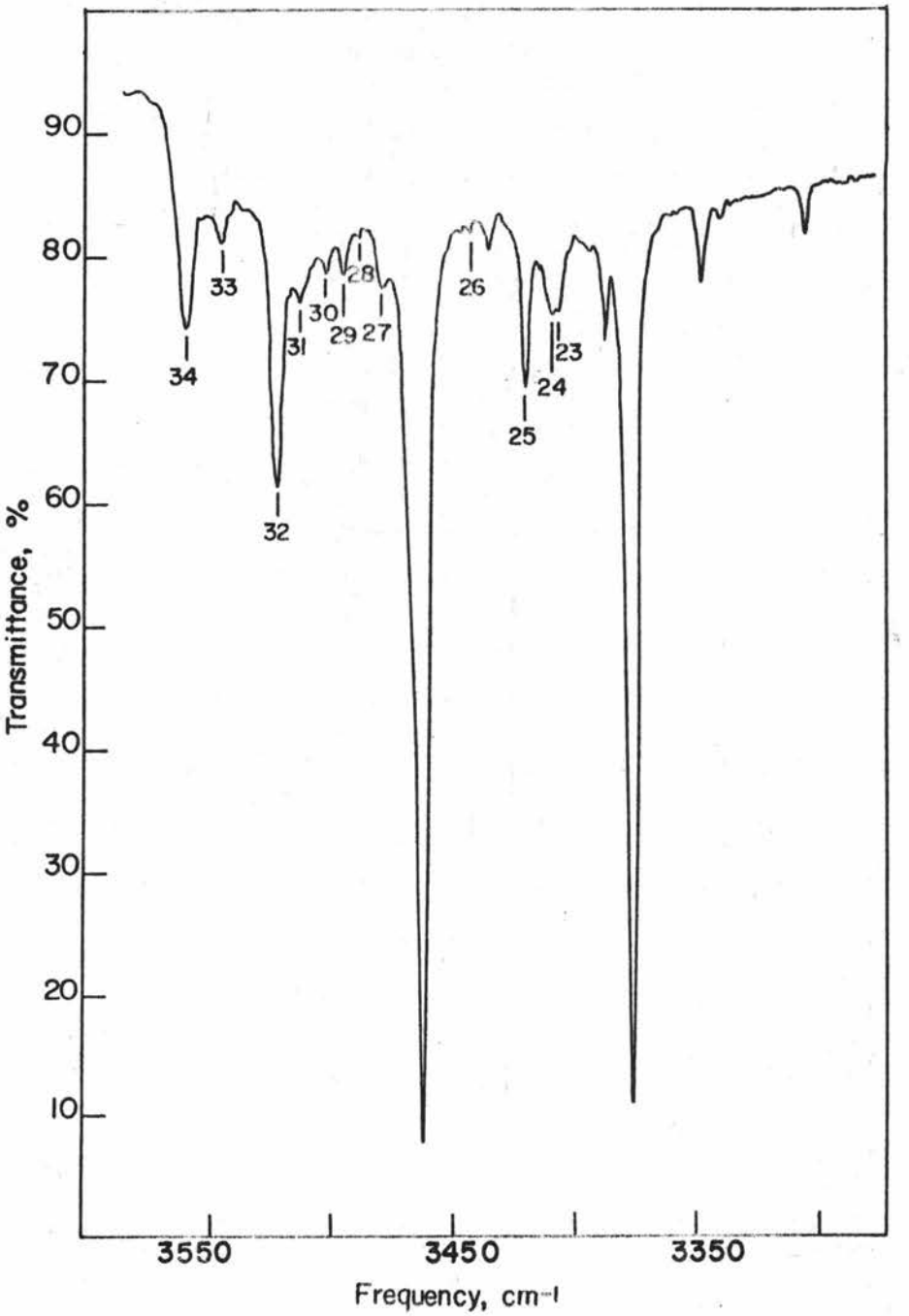

Figure 9. Infrared absorption spectrum of a crystal of 2.30 cm thickness grown from a melt containing 4.60 m moles KNCO and 3.36 m moles $CaCl_2$ per mole KCl scanned while cooled with liquid nitrogen.

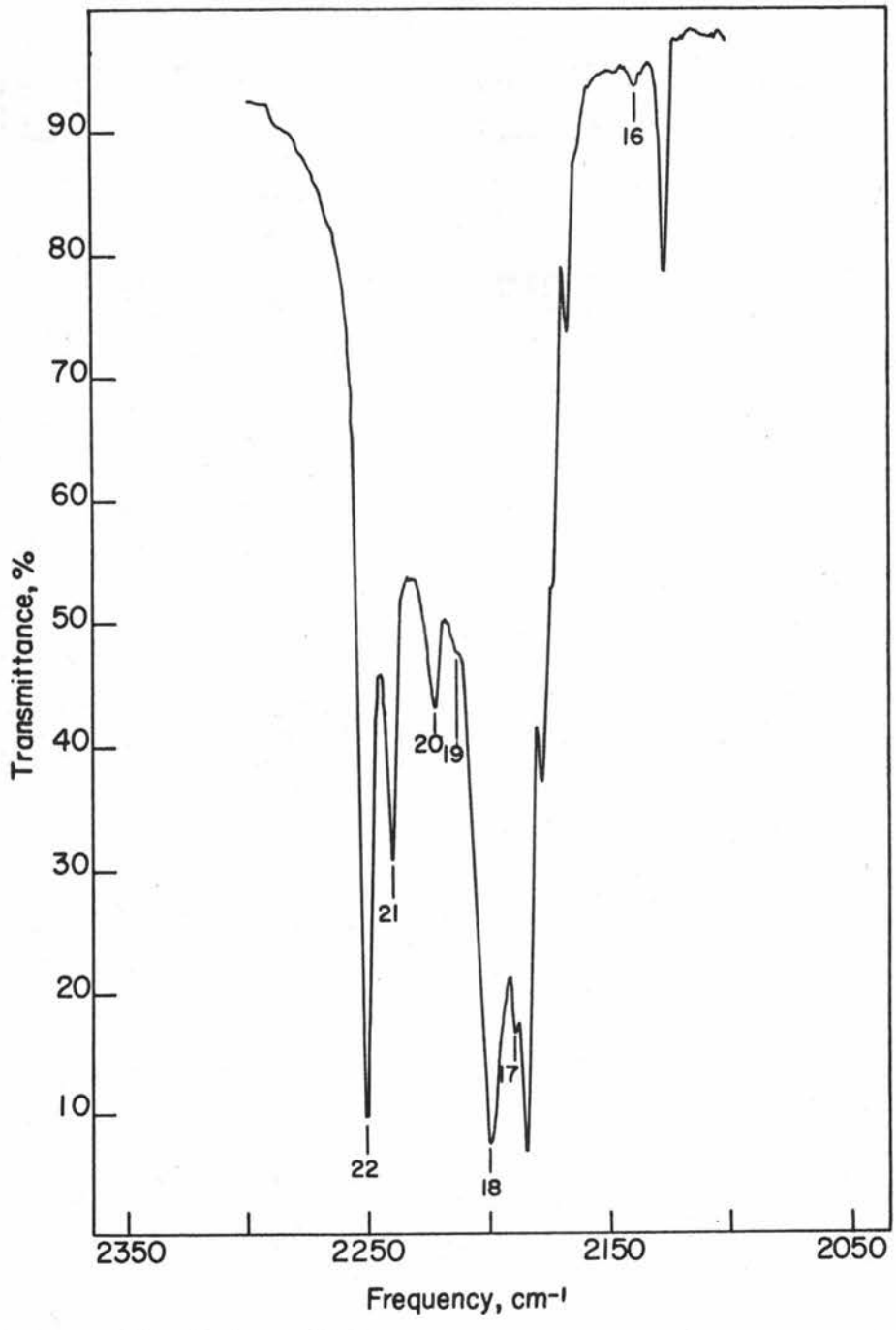

Figure 10. Infrared absorption spectrum of a crystal of 0.32 cm thickness grown from a melt containing 4.60 m moles KNCO and 3.36 m moles $CaCl_2$ per mole Kcl scanned while cooled with liquid nitrogen.

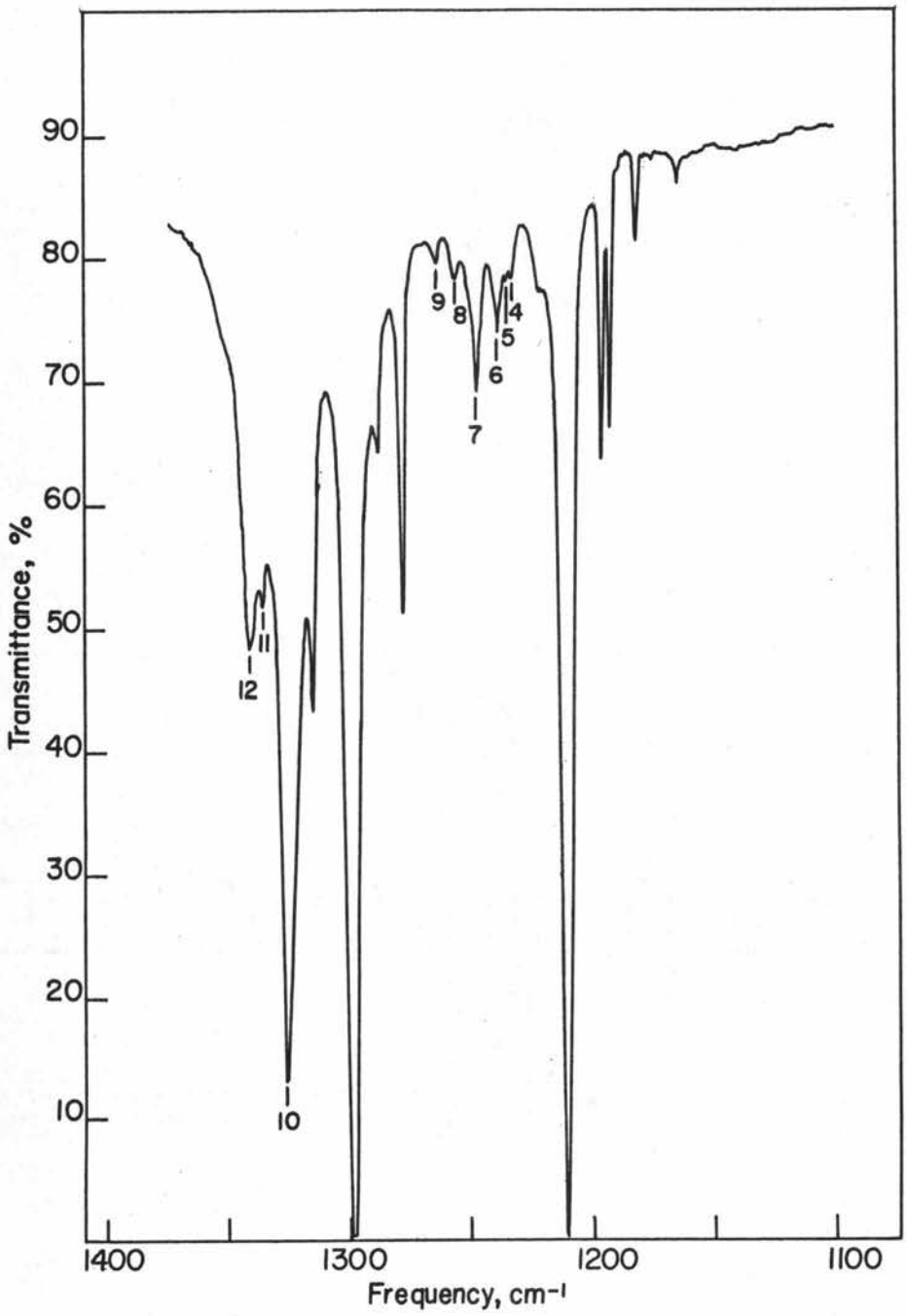

Figure 11. Infrared absorption spectrum of a crystal of 2.30 cm thickness grown from a melt containing 4.60 m moles KNCO and 3.36 m moles $CaCl_2$ per mole KCl scanned while cooled with liquid nitrogen.

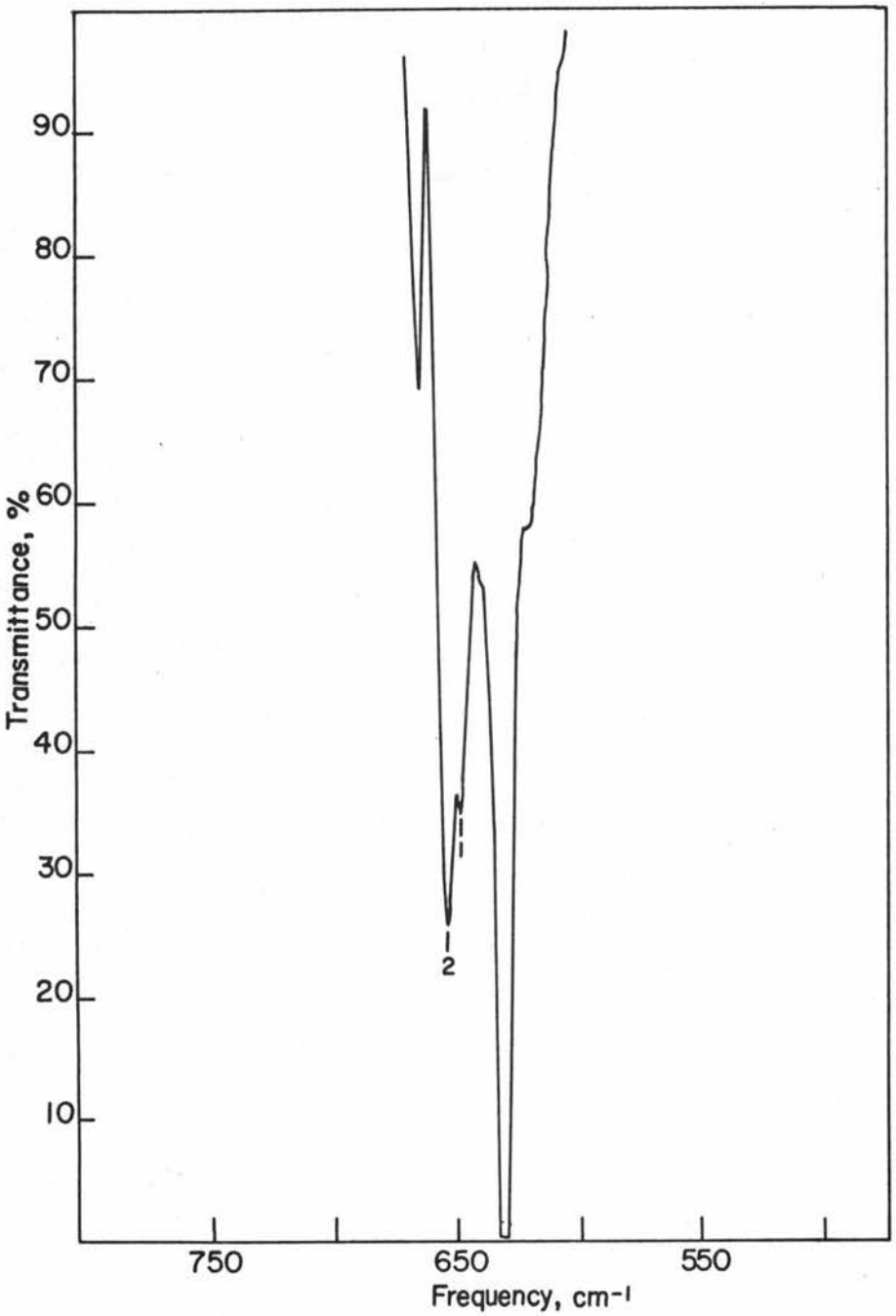

Figure 12. Infrared absorption spectrum of a crystal of 2.30 cm thickness grown from a melt containing 4.60 m moles KNCO and 3.36 m moles $CaCl_2$ per mole KCl scanned while cooled with liquid nitrogen.

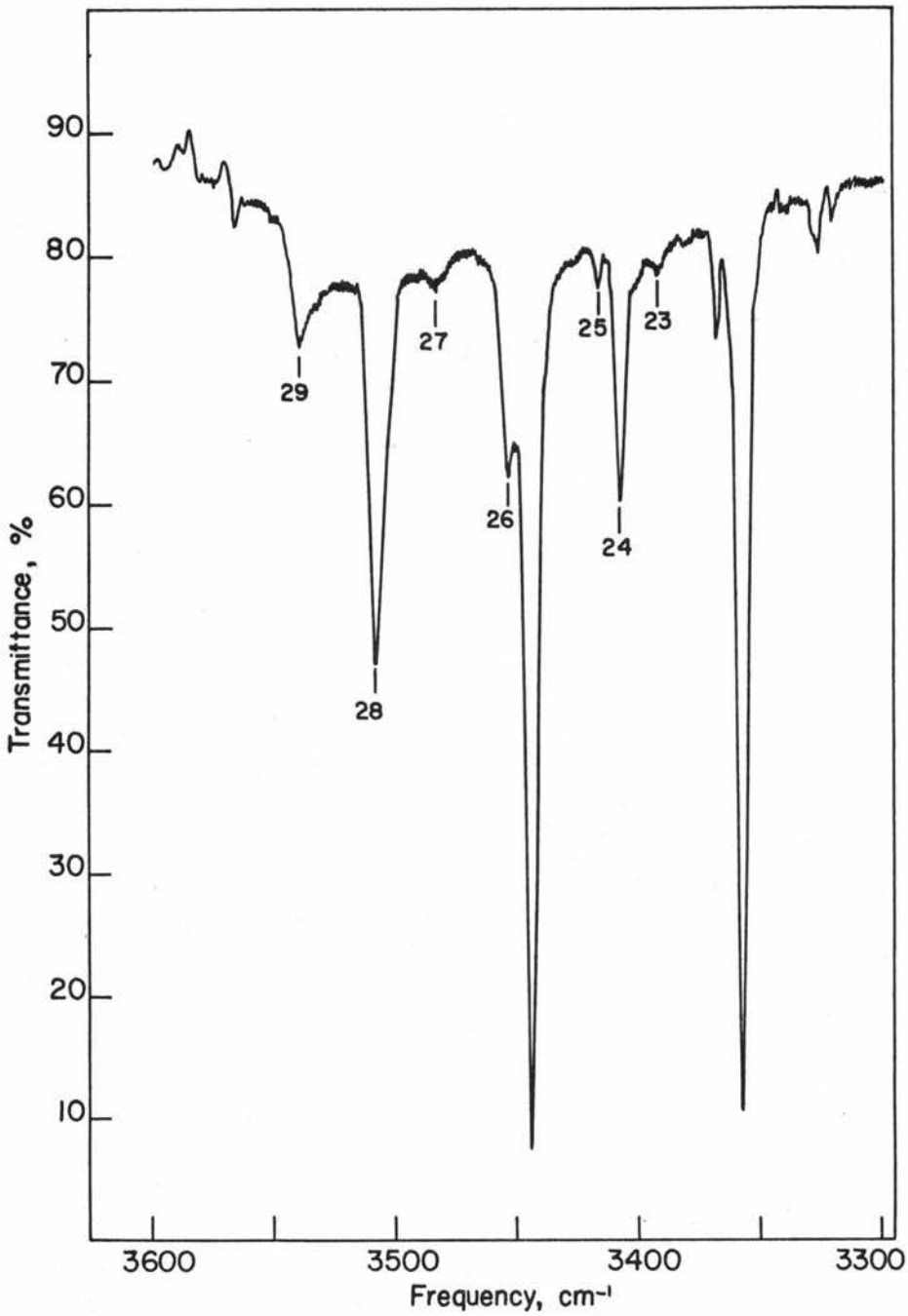

Figure 13. Infrared absorption spectrum of a crystal of 0.92 cm thickness grown from a melt containing 7.35 m moles KNCO and 2.98 m moles $CaBr_2$ per mole KBr scanned while cooled with liquid nitrogen.

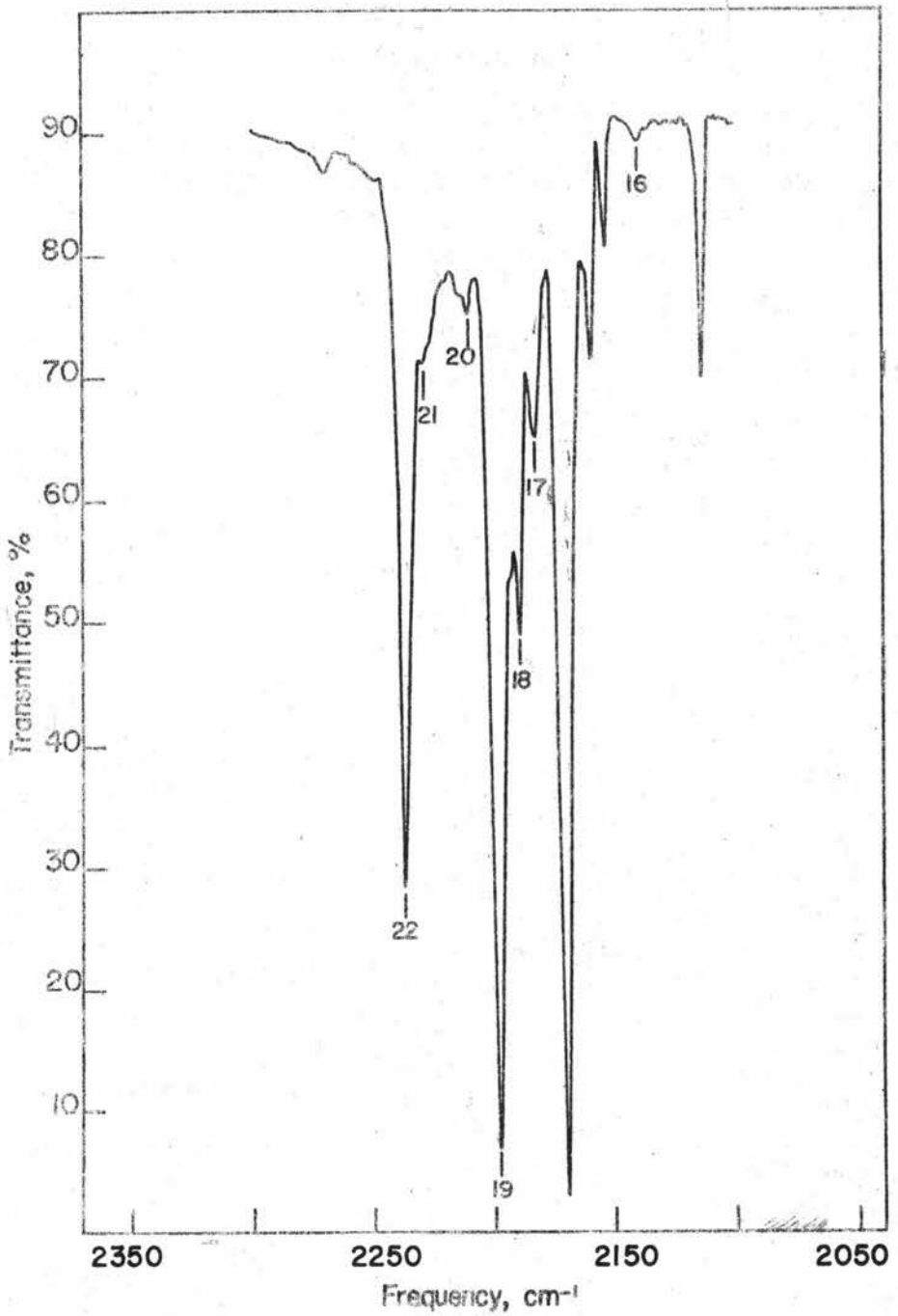

Figure 14. Infrared absorption spectrum of a crystal of 0.12 cm thickness grown from a melt containing 7.35 m moles KNCO and 2.98 m moles $CaBr_2$ per mole KBr scanned while cooled with liquid nitrogen.

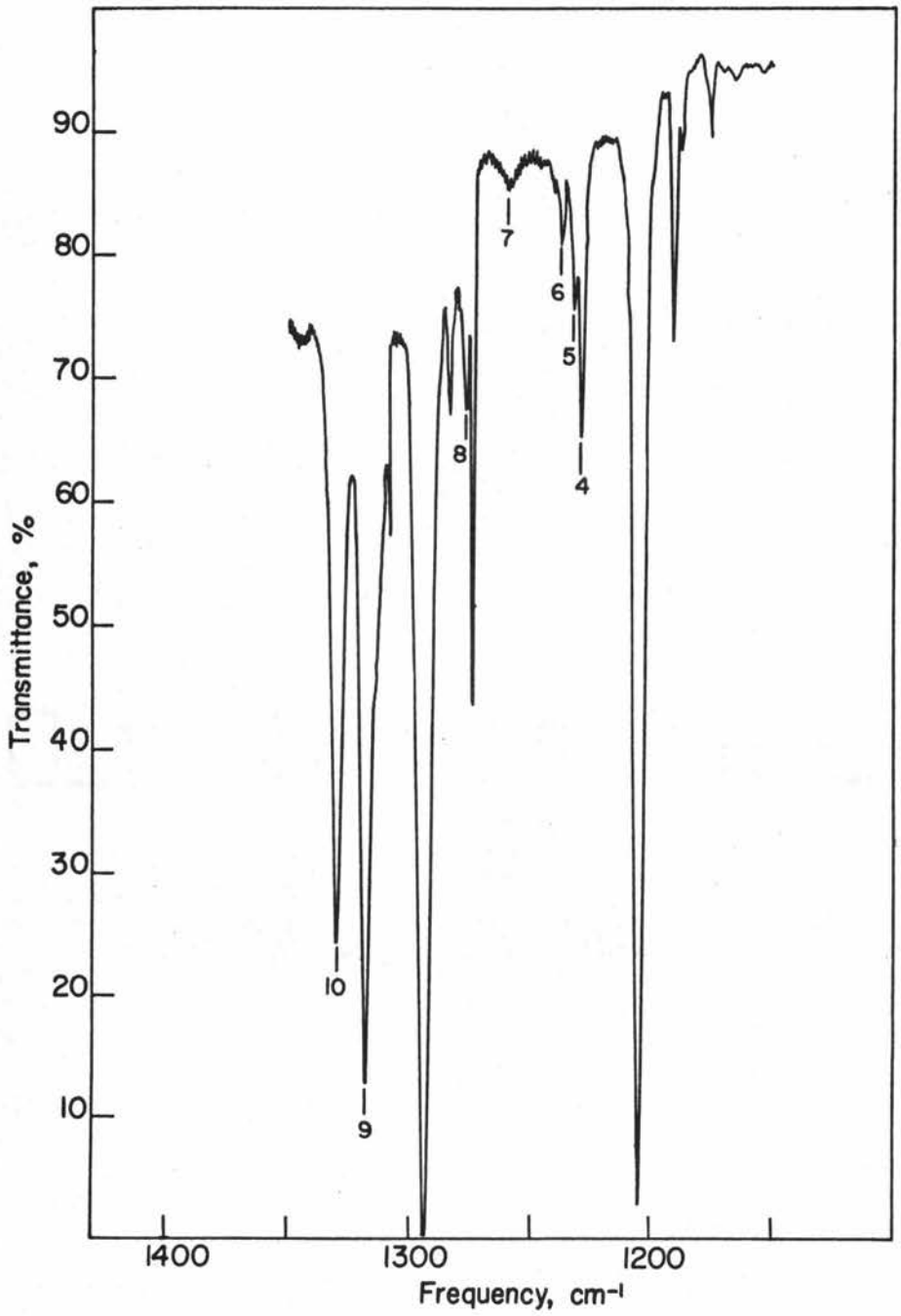

Figure 15. Infrared absorption spectrum of a crystal of 0.92 cm thickness grown from a melt containing 7.35 m moles KNCO and 2.98 m moles $CaBr_2$ per mole KBr scanned while cooled with liquid nitrogen.

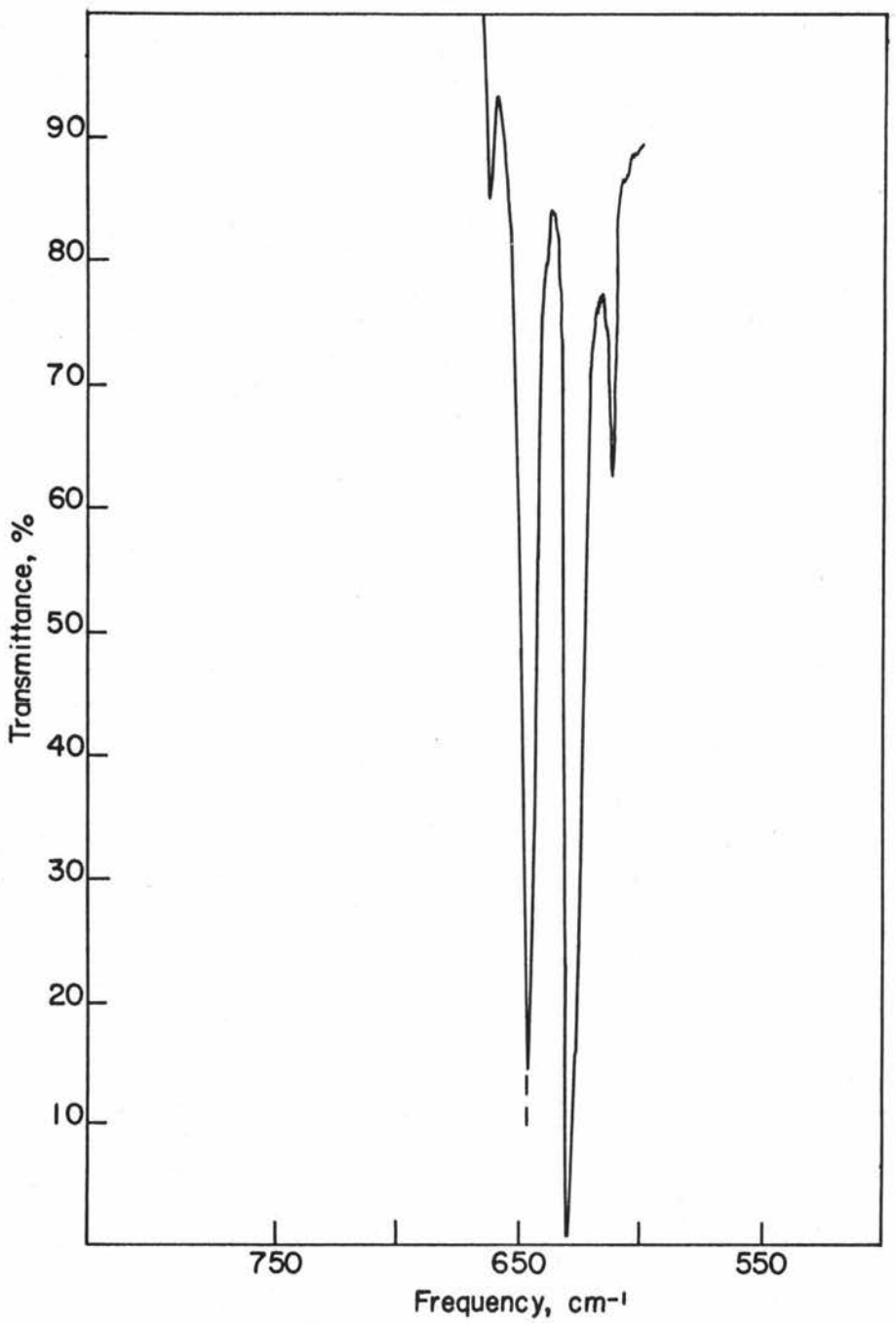

Figure 16. Infrared absorption spectrum of a crystal of 0.92 cm thickness grown from a melt containing 7.35 m moles KNCO and 2.98 m moles $CaBr_2$ per mole KBr scanned while cooled with liquid nitrogen.

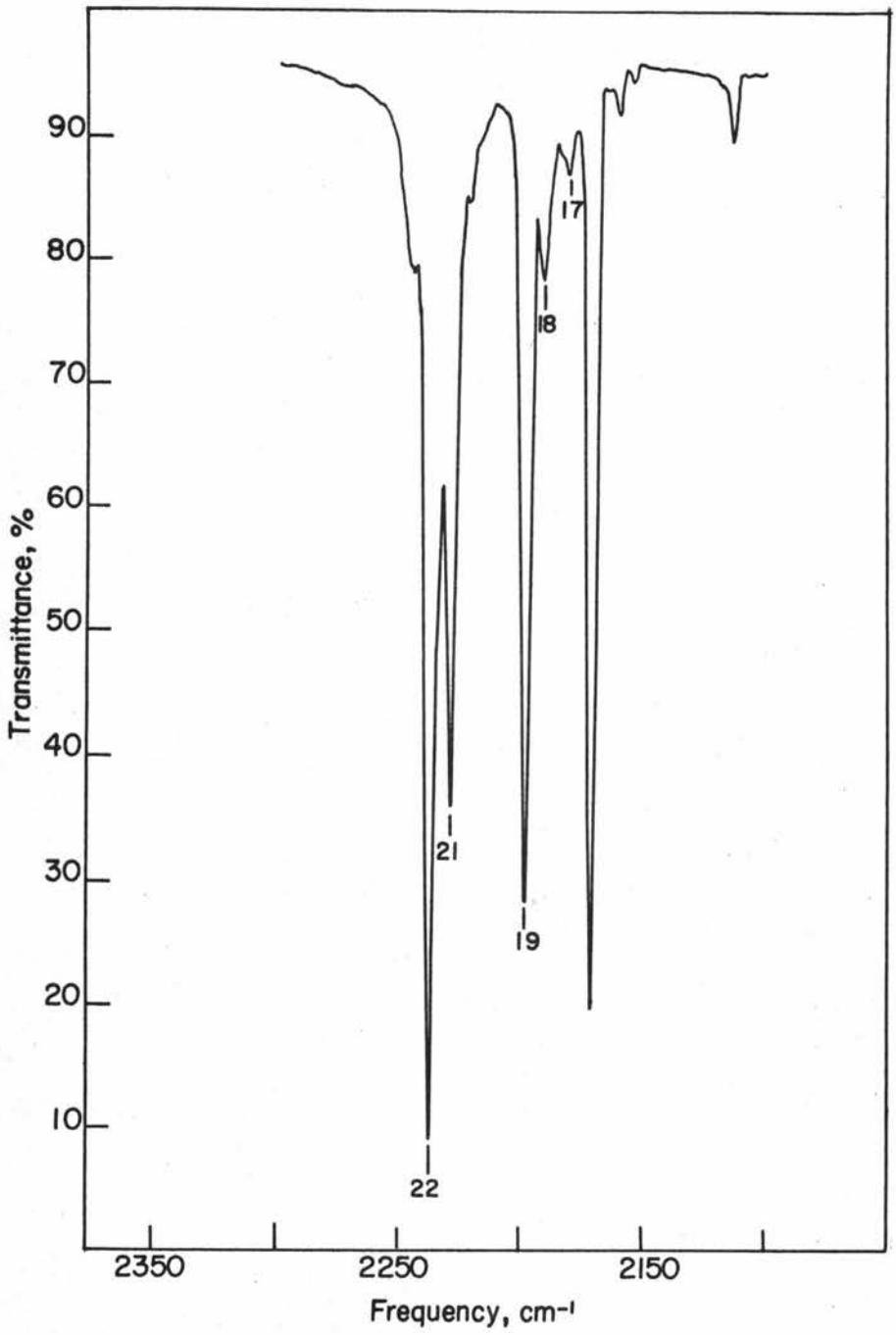

Figure 17. Infrared absorption spectrum of a crystal of 1.02 cm thickness grown from a melt containing 4.41 m moles KNCO and 2.98 m moles $CaBr_2$ per mole KBr scanned while cooled with liquid nitrogen.

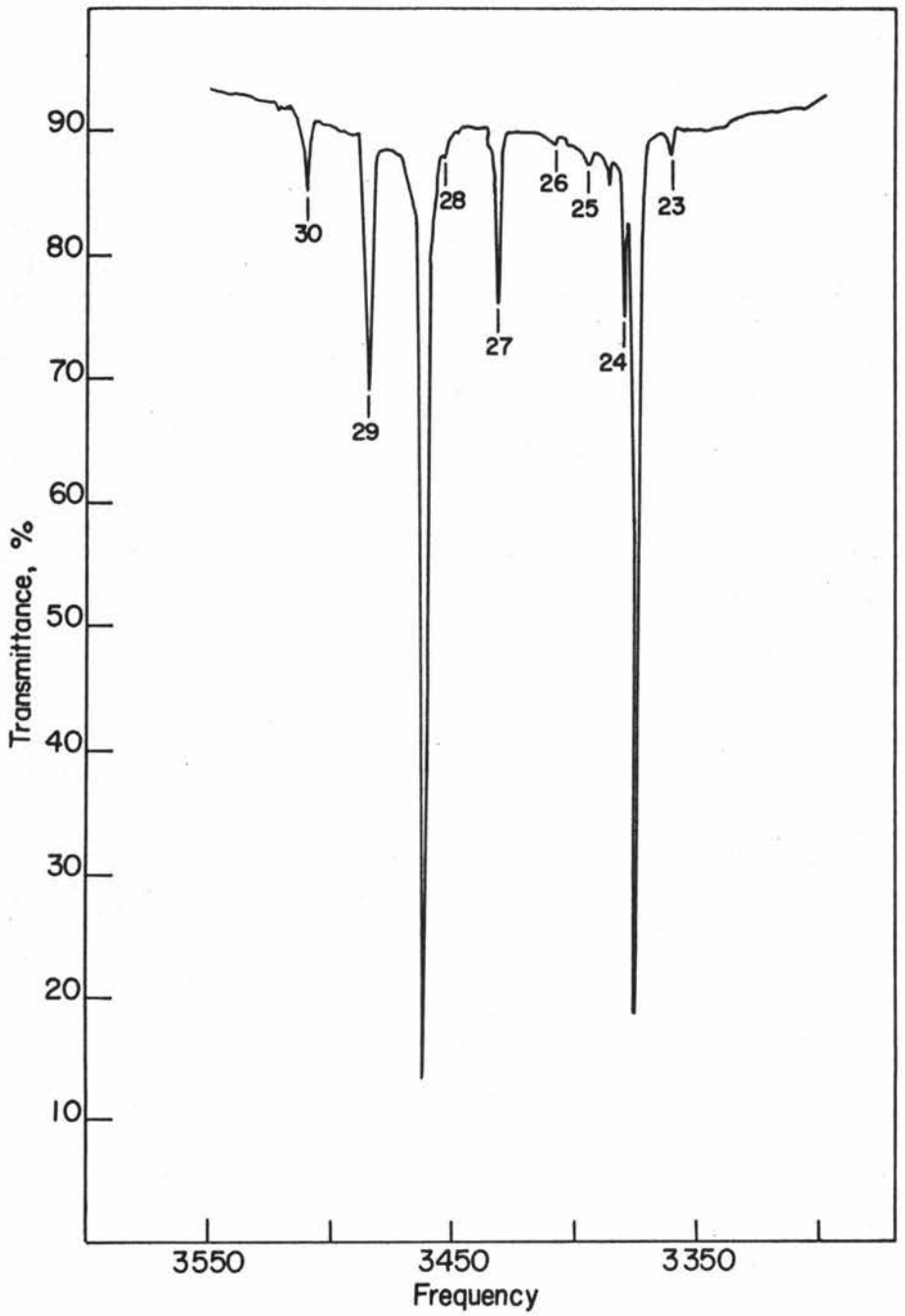

Figure 18. Infrared absorption spectrum of a crystal of 1.95 cm thickness grown from a melt containing 4.60 m moles KNCO and 1.79 m moles $BaCl_2$ per mole KCl scanned while cooled with liquid nitrogen.

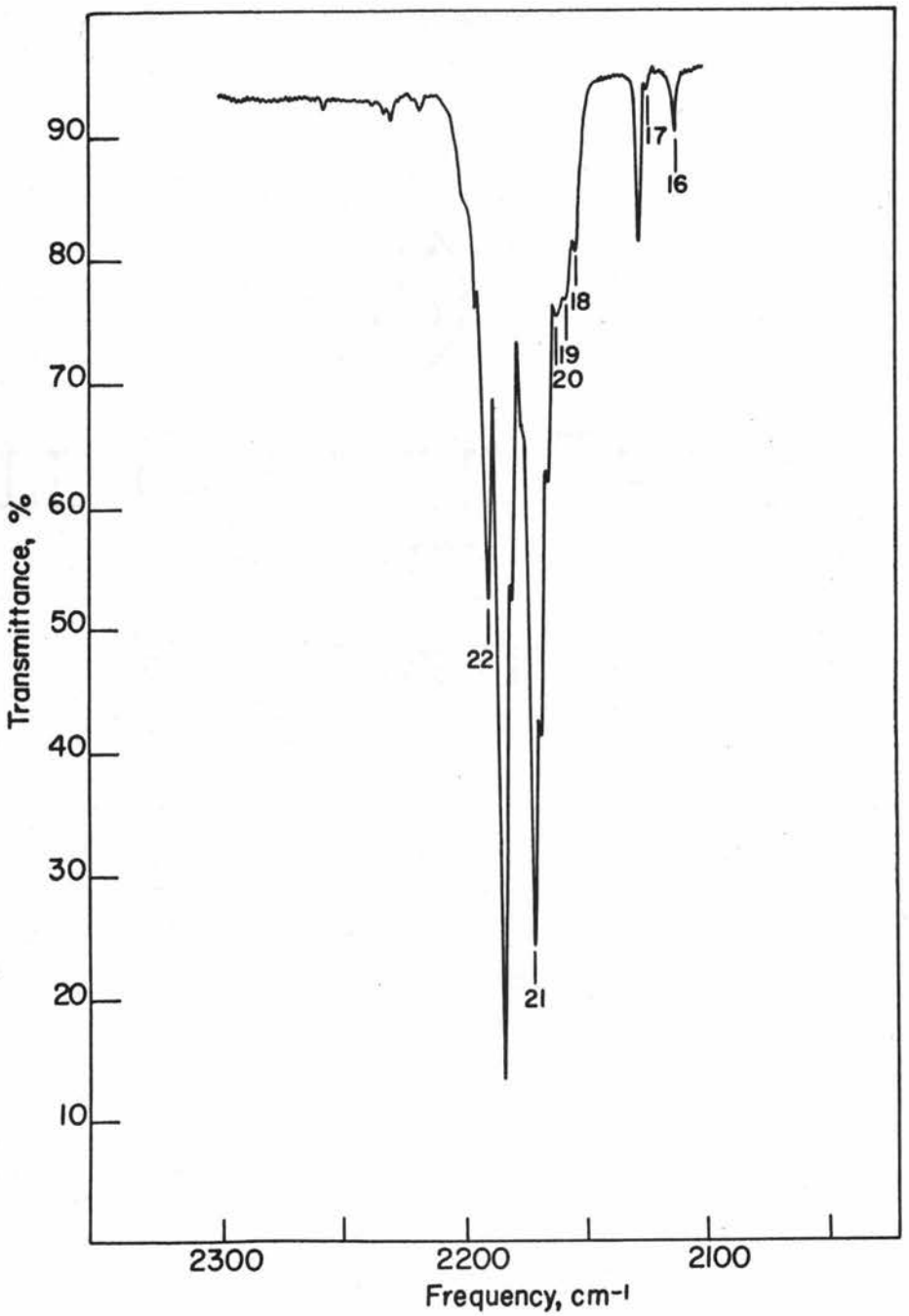

Figure 19. Infrared absorption spectrum of a crystal of 0.32 cm thickness grown from a melt containing 4.60 m moles KNCO and 1.79 m moles $BaCl_2$ per mole KCl scanned while cooled with liquid nitrogen.

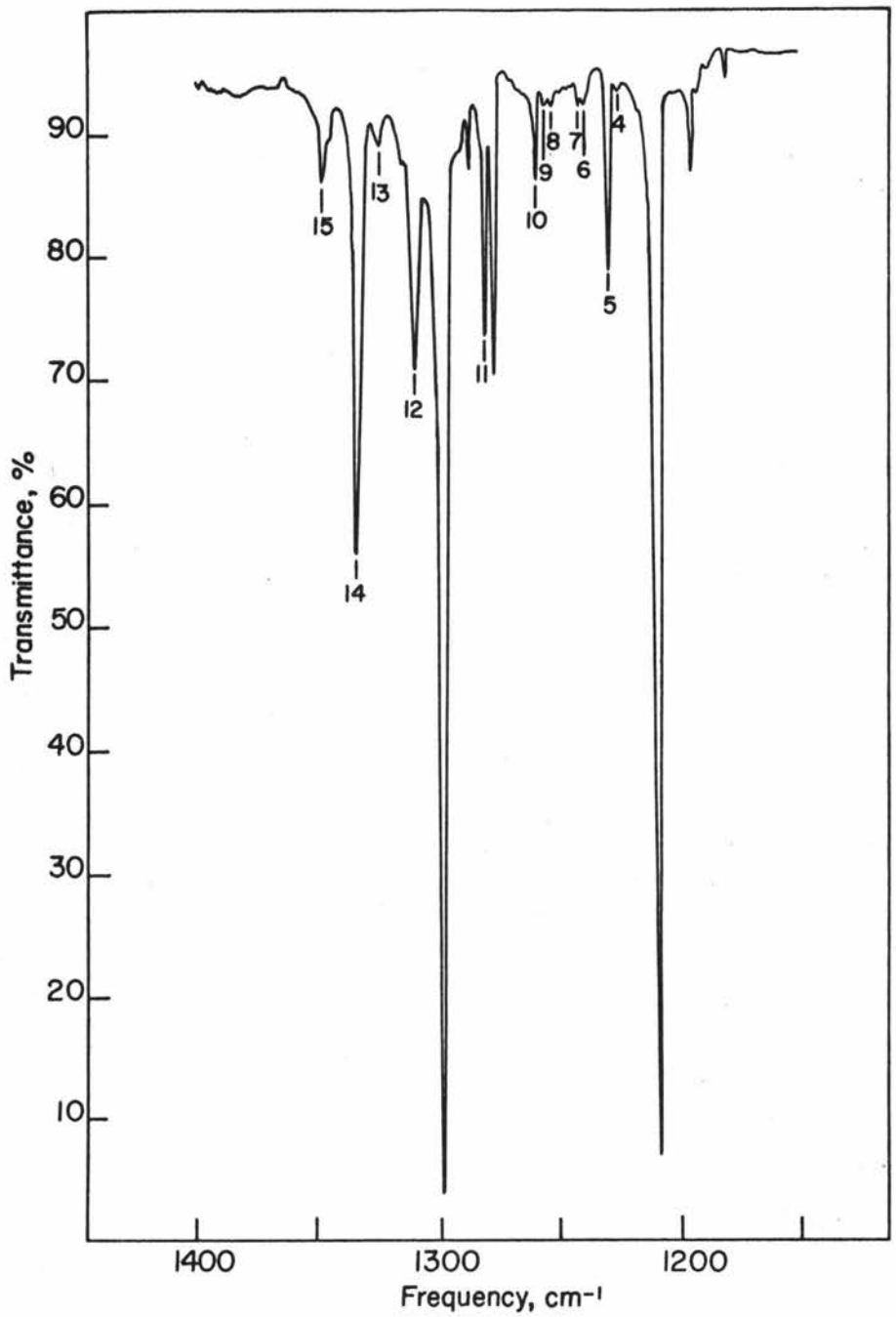

Figure 20. Infrared absorption spectrum of a crystal of 1.95 cm thickness grown from a melt containing 4.60 m moles KNCO and 1.79 m moles $BaCl_2$ per mole KCl scanned while cooled with liquid nitrogen.

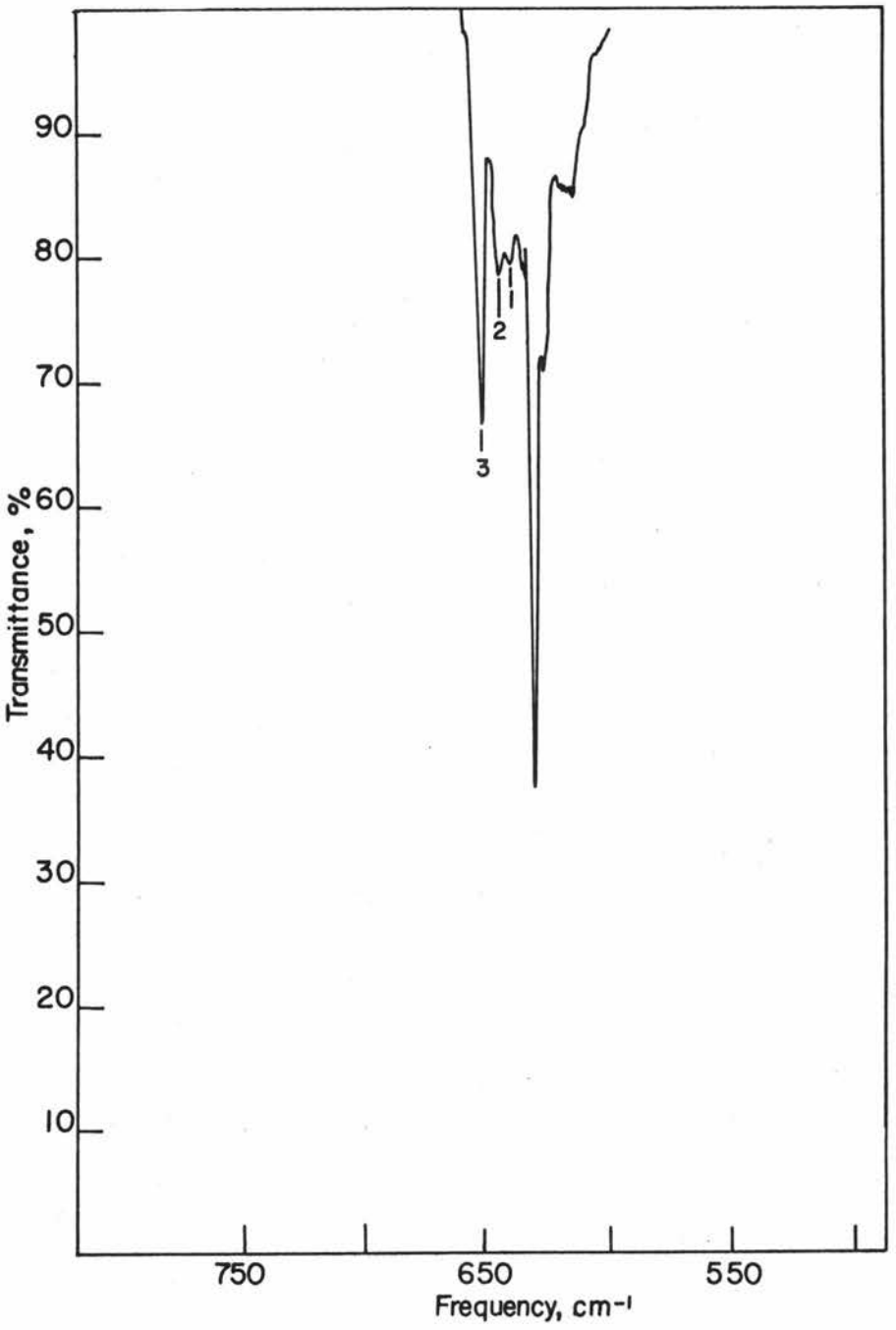

Figure 21. Infrared absorption spectrum of a crystal of 1.95 cm thickness grown from a melt containing 4.60 m moles KNCO and 1.79 m moles $BaCl_2$ per mole KCl scanned while cooled with liquid nitrogen.

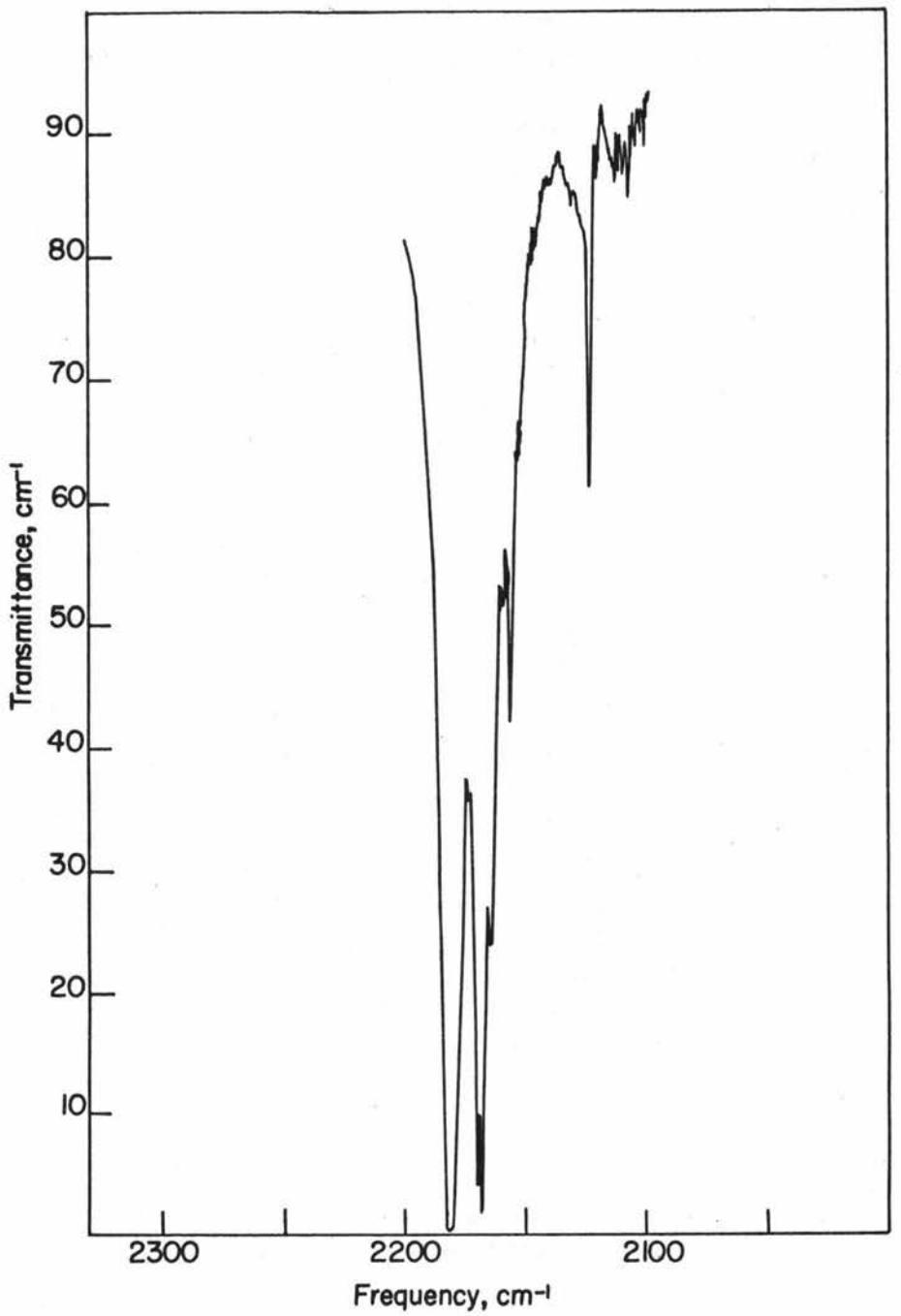

Figure 22. Infrared absorption spectrum of a crystal of 0.32 cm thickness grown from a melt containing 4.60 m moles KNCO and 1.79 m moles $BaCl_2$ per mole KCl scanned at room temperature.

calcium chloride which gave a spectrum with absorptions appearing at the above frequencies. These frequencies are therefore assigned as absorptions for carbonate in the presence of calcium ion. Morgan and Staats (27) have carried out a study of the infrared spectrum of alkali halide crystals doped with calcium and carbonate ions.

Because the new peaks not due to carbonate fall in either the bending, symmetric stretching, anti-symmetric stretching or combination regions of the spectrum, they evidently are caused by cyanate ion which has been perturbed in some manner by the presence of calcium ion. The wealth of new peaks seems to indicate that more than one new species of cyanate ion are present in the crystal.

In order to correlate the peaks in one region with those in another the symmetric stretching and combination regions were examined for possible Fermi resonance doublets arising from transitions from the ground state to $\{\nu_1, 2\nu_2^\circ\}$ and to $\{\nu_1 + \nu_3, 2\nu_2^\circ + \nu_3\}$ for the various species of cyanate ion. For unperturbed cyanate ion the separation of 86.6 cm^{-1} between the Fermi resonance peaks for $\{\nu_1, 2\nu_2^\circ\}$ is different from the separation of 86.2 cm^{-1} between the Fermi resonance peaks for $\{\nu_1 + \nu_3, 2\nu_2^\circ + \nu_3\}$ by only 0.4 cm^{-1}. Using the equation

$$\frac{\nu_0}{h} = E - E_0 = \sum_{i=1}^{3} \omega_i^\circ n_i + \sum_{k \le i=1}^{3} x_{ik} n_i n_k + g_{22} l^2$$

the value for the anharmonicity constant x_{13} is calculated from frequencies listed under KCl in Table 2 to be -18.2 cm^{-1} and that for x_{23} is -11.0 cm^{-1}. The difference between the separation of ν_1 and $2\nu_2^\circ$ and the separation of $\nu_1 + \nu_3$ and $2\nu_2^\circ + \nu_3$ is just $x_{13} - 2x_{23}$ or 3.8 cm^{-1} which is larger than the 0.4 cm^{-1} difference discussed above by almost a factor of ten. This insensitivity of the Fermi resonance peaks to change in the frequencies of the original unperturbed peaks may be explained by examination of the secular equation

$$\begin{vmatrix} W_1^\circ - W & W_{12} \\ W_{12} & W_2^\circ - W \end{vmatrix} = 0$$

This equation has two solutions W_+ and W_-, with the separation between them being

$$W_+ - W_- = \sqrt{(W_1^\circ - W_2^\circ)^2 + 4W_{12}^2}$$

Since W_{12} remains constant and $W_1^\circ - W_2^\circ$ is small compared to $2W_{12}$, the separation of the Fermi resonance energy levels $W_+ - W_-$ will change very little with a change in the separation of the unperturbed energies.

If the assumption is made for the new species of cyanate that the separation of a given Fermi resonance pair in the symmetric stretching region is approximately the same as the separation of its corresponding Fermi resonance pair in the combination region, then some progress can be made toward interpreting the spectrum. An additional assumption that the anharmonicity constants of the new species do not greatly differ from those for the unperturbed cyanate ion has also been made.

Table 5 lists possible assignments for some of the new peaks appearing in the spectrum of a potassium chloride crystal doped with potassium cyanate and calcium chloride. Various parameters calculated as a check on these assignments are also listed. The symbol $(\nu_+)^{\nu_1}_{2\nu_2^\circ}$ refers to the higher Fermi resonant peak arising from resonance between ν_1 and $2\nu_2^\circ$; the symbol $(\nu_+ - \nu_-)^{\nu_1}_{2\nu_2^\circ}$ refers to the separation between the two Fermi resonance peaks; the symbol $(\Delta\nu_+)^{\nu_1}_{2\nu_2^\circ}$ refers to the separation between $(\nu_+)^{\nu_1}_{2\nu_2^\circ}$ for the new species and $({}^\circ\nu_+)^{\nu_1}_{2\nu_2^\circ}$ for unperturbed cyanate ion, or $(\Delta\nu_+)^{\nu_1}_{2\nu_2^\circ} = (\nu_+ - {}^\circ\nu_+)^{\nu_1}_{2\nu_2^\circ}$; also $\Delta\nu_3 = \nu_3 - {}^\circ\nu_3$; and the symbol $({}^\circ\nu_+)^{\nu_1+\nu_3}_{2\nu_2^\circ+\nu_3}$ refers to the higher Fermi resonant peak of unperturbed cyanate arising from resonance between $\nu_1 + \nu_3$ and $2\nu_2^\circ + \nu_3$. Examination of the table reveals that the separation of the Fermi resonance peaks in the symmetric stretching region differs from the separation of the corresponding

Table 5. Tentative correlation of absorption peaks in the various regions of the spectrum for cyanate ion with Ca^{++} ion present in a potassium chloride host lattice.

	Frequencies in cm^{-1} for NCO^{-1} species with designations			
	1	2	3	4
$(\nu_+)^{\nu_1}_{2\nu_2^\circ}$	1341.5	1325.9	1335.9	1321.9
$(\nu_-)^{\nu_1}_{2\nu_2^\circ}$	1239.0	1247.5	1232.7	1264.2
$(\nu_+)^{\nu_1+\nu_3}_{2\nu_2^\circ+\nu_3}$	3520	3557.2	3511	3543
$(\nu_-)^{\nu_1+\nu_3}_{2\nu_2^\circ+\nu_3}$	3417.3	3477.7	3407	3486
ν_3	2198.8	2250.1	2195.3	2239.2
$(\nu_+ - \nu_-)^{\nu_1}_{2\nu_2^\circ}$	102.5	78.4	103.2	57.7
$(\nu_+ - \nu_-)^{\nu_1+\nu_3}_{2\nu_2^\circ+\nu_3}$	102.7	79.5	104	57
$(\Delta\nu_+)^{\nu_1}_{2\nu_2^\circ}$	44.2	28.6	38.6	24.6
$(\Delta\nu_-)^{\nu_1}_{2\nu_2^\circ}$	28.3	36.8	22.0	53.5
$\Delta\nu_3$	17.0	68.3	13.5	57.4
$(^\circ\nu_+)^{\nu_1+\nu_3}_{2\nu_2^\circ+\nu_3} + (\Delta\nu_+)^{\nu_1}_{2\nu_2^\circ} + \Delta\nu_3$	3520.0	3555.7	3510.9	3540.8
$(^\circ\nu_-)^{\nu_1+\nu_3}_{2\nu_2^\circ+\nu_3} + (\Delta\nu_-)^{\nu_1}_{2\nu_2^\circ} + \Delta\nu_3$	3417.9	3477.7	3408.1	3483.5

peaks in the combination region by only a wavenumber at most. Terms of the type $(\Delta\nu_+)^{\nu_1}_{2\nu_2^\circ}$ and $\Delta\nu_3$ were calculated relative to unperturbed cyanate ion and added to the $(^\circ\nu_+)^{\nu_1+\nu_3}_{2\nu_2+\nu_3}$ peak of unperturbed cyanate to give a term $(^\circ\nu_+)^{\nu_1+\nu_3}_{2\nu_2^\circ+\nu_3} + (\Delta\nu_+)^{\nu_1}_{2\nu_2^\circ} + \Delta\nu_3$ which should be the same as the $(\nu_+)^{\nu_1+\nu_3}_{2\nu_2^\circ+\nu_3}$ peak for perturbed cyanate ion in the combination region. The differences between the calculated and the observed values are on the order of from 0.1 to 2.5 cm^{-1}, which is satisfactorily small considering the assumptions that were made. The peaks for perturbed cyanate ion were related back to the corresponding peaks of unperturbed cyanate ion as a convenient method for incorporating the anharmonicity of the unperturbed cyanate into the calculation.

In the symmetric stretching region the separation of the Fermi resonance peaks $(\nu_+ - \nu_-)^{\nu_1}_{2\nu_2^\circ}$ ranges from 103.2 to 57.7 cm^{-1}. The separation for unperturbed cyanate ion is 87.1 cm^{-1}. Since $2\nu_2^\circ - \nu_1$ is only 0.1 cm^{-1} for unperturbed cyanate ion, the separation of its Fermi resonance peaks can be attributed almost entirely to the W_{12} term in the secular equation obtained from applying the linear variation method to the resonance problem. The perturbed forms of cyanate have a ν_2' frequency which evidently shifts very little from species to species, because peaks at 650.0 and 654.6 cm^{-1} were the only new ones to appear with the addition of calcium ion to the crystal, and these are separated by only 5.4 cm^{-1}.

The Fermi resonance peaks for any given perturbed species of cyanate do not have the same intensity, but the peak at the higher frequency has the strongest intensity. This indicates that $2\nu_2^\circ - \nu_1$ is much larger than the 0.1 cm^{-1} separation for the unperturbed cyanate ion and would tend to increase the separation between the Fermi resonance peaks. Since $2\nu_2^\circ$ remains relatively constant, the difference $2\nu_2^\circ - \nu_1$ must be attributed to a variation of ν_1 from species to species. If the assignments are correct for species 2 and 4, the decrease in splitting must be due to a decrease in the W_{12} term caused by the perturbing effect of the near neighbor calcium ions.

The peaks appearing at 3493 and 3499 cm^{-1} in the combination region probably correspond with peaks at 2188.2 and 2239.2 cm^{-1} in the anti-symmetric stretching region. The peak at 2139.3 cm^{-1} is assigned as ν_3 for the C^{13} isotope of cyanate ion species 1 given in Table 5.

Information similar to that in Table 5 is given in Table 6 for cyanate ion with calcium ion present in a potassium bromide host lattice. A peak appearing at 2140 cm^{-1} is assigned as ν_3 for the C^{13} isotope of cyanate ion species 5 of that table.

In the spectrum for the potassium chloride crystal containing cyanate and barium ions, no direct correlation of Fermi resonance pairs in the various regions was apparent. Although Fermi resonance pairs could not be determined, individual peaks in the symmetric

Table 6. Tentative correlation of absorption peaks in the various regions of the spectrum for cyanate ion with Ca^{++} ion present in a potassium bromide host lattice.

	Frequencies in cm^{-1} for NCO^- species with designations	
	5	6
$(\nu_+)^{\nu_1}_{2\nu_2^\circ}$	1330.2	1319.2
$(\nu_-)^{\nu_1}_{2\nu_2^\circ}$	1229.7	1238.2
$(\nu_+)^{\nu_1+\nu_3}_{2\nu_2^\circ+\nu_3}$	3507	3538.3
$(\nu_-)^{\nu_1+\nu_3}_{2\nu_2^\circ+\nu_3}$	3406	(3457.3)
ν_3	2198.3	2236.5
$(\nu_+ - \nu_-)^{\nu_1}_{2\nu_2^\circ}$	100.5	81.0
$(\nu_+ - \nu_-)^{\nu_1+\nu_3}_{2\nu_2^\circ+\nu_3}$	100.7	(81.0)
$(\Delta\nu_+)^{\nu_1}_{2\nu_2^\circ}$	37.2	26.2
$(\Delta\nu_-)^{\nu_1}_{2\nu_2^\circ}$	23.7	32.2
$\Delta\nu_3$	28.5	66.7
$(^\circ\nu_+)^{\nu_1+\nu_3}_{2\nu_2^\circ+\nu_3} + (\Delta\nu_+)^{\nu_1}_{2\nu_2^\circ} + \Delta\nu_3$	3507.9	3535.1
$(^\circ\nu_-)^{\nu_1+\nu_3}_{2\nu_2^\circ+\nu_3} + (\Delta\nu_-)^{\nu_1}_{2\nu_2^\circ} + \Delta\nu_3$	3407.2	3453.9

stretching region could be related with a peak in the anti-symmetric stretching region to yield frequencies the same as various peaks appearing in the combination region. These correlations were:

$$1333.8 + 2168.8 + \text{anharmonicity} = 3484 - 0.7$$

$$1309.6 + 2168.8 + \text{anharmonicity} = (3458.8) - 0.7$$

$$1281.7 + 2168.8 + \text{anharmonicity} = 3430 + 0.6$$

$$1230.5 + 2168.8 + \text{anharmonicity} = 3379 + 0.4$$

The peak 3458.8 cm^{-1} appearing in parentheses falls under a strong unperturbed cyanate ion absorption of the same frequency. A peak appearing at 2108.3 cm^{-1} is assigned as ν_3 for the C^{13} isotope of the cyanate ion species for which the C^{12} ν_3 absorption appears at 2168.8 cm^{-1}.

For a given position that the cyanate ion might occupy in an alkali halide lattice, the ion may be oriented with either the nitrogen atom or else the oxygen atom nearest to a neighboring calcium ion. If cyanate ion is represented by the two resonance structures

$$\bar{O} - C \equiv N \qquad (A)$$

$$O = C = \bar{N} \qquad (B)$$

then calcium ion nearest the oxygen atom would cause structure A to predominate, whereas calcium ion nearest the nitrogen atom would cause structure B to predominate. Since the assymmetric stretching vibration is predominantly a carbon-nitrogen stretching mode, the

presence of calcium ion nearest the oxygen atom in a cyanate ion would cause structure A to predominate, increasing the overall bond order of the carbon-nitrogen bond, thus increasing the frequency of vibration for ν_3 . Similarly, calcium ion nearest the nitrogen atom would tend to decrease the frequency of ν_3 . In the symmetric stretching region the predominance of structure B would lead to a more symmetrical vibration, decreasing $\left(\frac{\partial \mu}{\partial Q_1}\right)_0$, and consequently reducing the intensity of absorption for this mode. For cyanate ion occupying a particular position in the alkali halide lattice relative to a neighboring calcium ion, then, one of two sets of peaks would be expected depending upon which end of the cyanate ion was nearest the calcium. If cyanate ions were equally distributed between the two possible orientations, both sets of peaks would appear. The higher ν_3 peak would correspond to the stronger ν_1 peak according to the previous discussion. Actually, the oxygen atom in unperturbed cyanate is more negative than is the nitrogen, so that the orientation with calcium ion nearest the oxygen is probably preferred.

Examination of the spectra for species 1 and 2 in the potassium chloride crystal and species 5 and 6 in the potassium bromide crystal with reference to the above discussion yields further evidence in support of the assignments found in Tables 4 and 5 for these species. In the potassium chloride crystal species 2 has a ν_3 peak (shown in Figure 10 as peak 22) which is higher than that (peak 18,

Figure 10) for species 1. Also, the Fermi resonance pair (peaks 7 and 10, Figure 11) in the symmetric stretching region for species 2 are of greater intensity than those (peaks 6 and 12, Figure 11) for species 1. Since peak 13 is stronger than peak 22 in Figure 11, the combination Fermi resonance peaks $(\nu_-)^{\nu_1+\nu_3}_{2\nu_2^\circ+\nu_3}$ and $(\nu_+)^{\nu_1+\nu_3}_{2\nu_2^\circ+\nu_3}$ (peaks 25 and 32, Figure 9) for species 1 are stronger than those (peaks 27 and 34, Figure 9) for species 2.

Perhaps species 5 and 6 in potassium bromide correspond to species 1 and 2 in potassium chloride. Examination of peaks 22 (species 6) and 19 (species 5) of Figure 14 and of peaks 22 (species 2) and 18 (species 1) of Figure 10 indicates that the ratio of the amounts present of species 6 to species 5 is less than the ratio of the amounts present of species 2 to species 1. A corresponding decrease in the intensity of the Fermi resonance peaks in the $\nu_1 + 2\nu_2^\circ$ region for species 6 relative to species 5 would be expected. Indeed, when these peaks are examined, the ratio of the intensities of the Fermi resonance pair (peaks 6 and 9, Figure 15) for species 6 to those (peaks 4 and 10, Figure 15) for species 5 is less than the ratio for the corresponding pairs (species 2: peaks 7 and 10, Figure 11 and species 1: peaks 6 and 12, Figure 11) appearing in the potassium chloride spectrum. Since peak 19 (species 5) of Figure 14 is stronger than peak 22 (species 6), the combination Fermi resonance peaks

$(\nu_-)^{\nu_1+\nu_3}_{2\nu_2^0+\nu_3}$ and $(\nu_+)^{\nu_1+\nu_3}_{2\nu_2^0+\nu_3}$ (peaks 24 and 28, Figure 13) for species 5 are stronger than those (peak under unperturbed cyanate absorption and peak 29, Figure 13) for species 6.

Although the previous discussion has been based upon the assumption that the new peaks which appeared upon doping with calcium ion were due to cyanate ion-calcium ion pairs in solid solution within the alkali halide lattice, the possibility exists that solid solution of some of the calcium and cyanate ions may not have occurred, and the new peaks may arise from small calcium cyanate crystals interspersed throughout the alkali halide crystal. Good evidence against such a supposition, however, is the narrowness of the new absorption peaks and the fact that the peaks for cyanate in the potassium chloride lattice appear at much different frequencies than those for cyanate in the potassium bromide lattice.

3. Interaction of Cyanate Ion with Divalent Cations in Alkali Halide Crystals

In the spectra of both the potassium chloride crystal and the potassium bromide crystal containing cyanate and calcium ions, the new peaks which appeared in the anti-symmetric region were higher than the ν_3 frequency for unperturbed cyanate ion. An increase in compressional forces acting on the ends of the cyanate ion was thought to be the cause. If the presence of calcium ion with its

double positive charge near a cyanate ion would cause the cyanate to be reoriented so that the carbon and nitrogen atoms would lie on the cell edge rather than on the body diagonal (as in unperturbed cyanate), then the nearest neighbors for the carbon and the nitrogen atoms would lie along the longitudinal axis of the cyanate ion and give the expected increase in compressional forces acting on them.

Figures 23 and 24 illustrate cyanate ion lying along the body diagonal of a potassium chloride unit cell, the cyanate ion having replaced a chloride ion. A calcium ion, which has replaced a potassium ion in the lattice, also lies along the body diagonal and is opposite an end atom of the cyanate ion. Calculations to be discussed later indicate that in this orientation the compressional forces acting on the end atoms are not sufficiently large to cause the frequency shifts for ν_3 observed in the spectrum.

Figures 25 and 26 illustrate cyanate ion lying on the cell edge, the reorientation having been caused by a nearest neighbor calcium ion. In this orientation the length of the cyanate ion is greater than the space available, and some distortion of the lattice must take place in order to accomodate it. In this case, compressional forces on the end atoms should be fairly large. If a potassium ion vacancy is situated nearest the end atom not associated with the calcium ion, then sufficient space for the cyanate ion along the cell edge is available. A potassium ion vacancy would be expected somewhere in

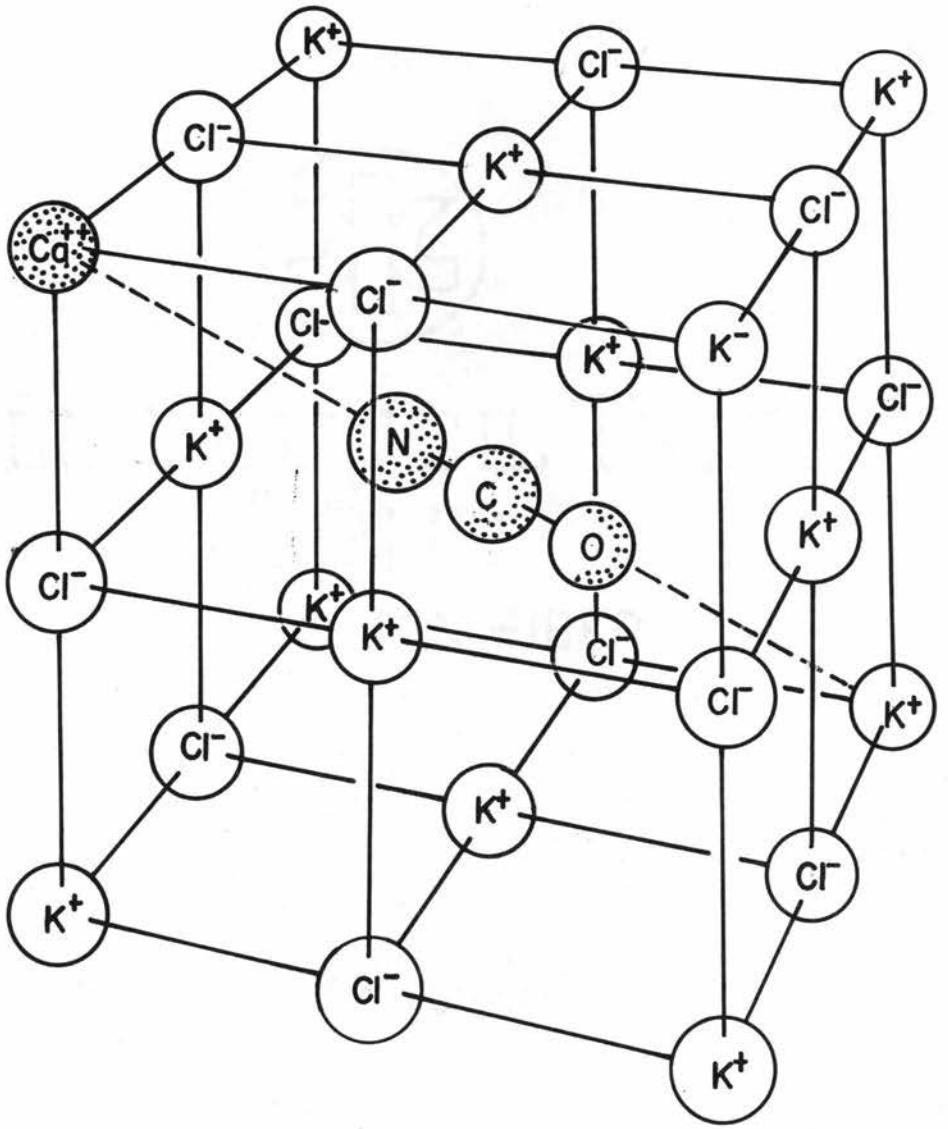

Figure 23. Cyanate and calcium ions in a KCl host lattice. Configuration A: The cyanate ion is substituted for a chloride ion, with the nitrogen and oxygen atoms lying on the body diagonal of the KCl unit cell. The calcium ion is substituted for a potassium ion and is nearest to the nitrogen atom of the cyanate ion.

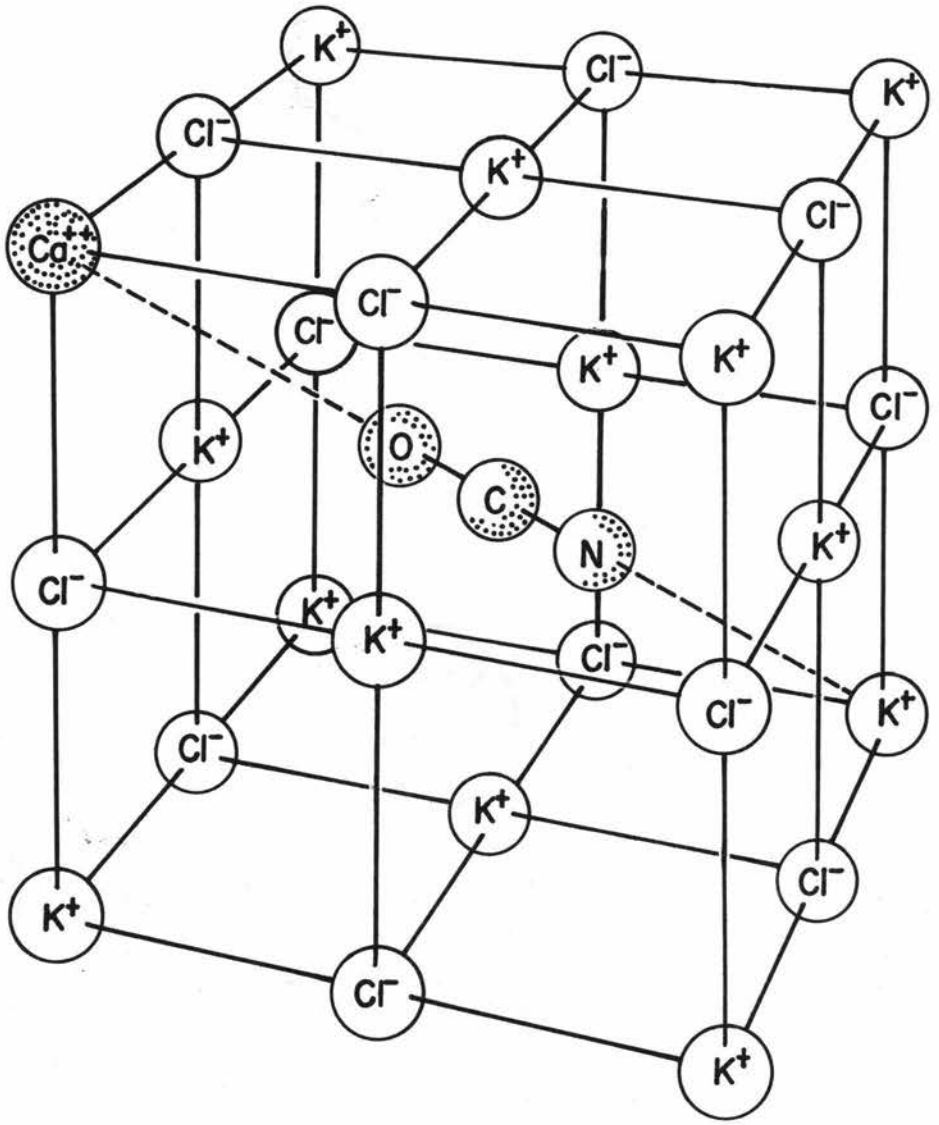

Figure 24. Cyanate and calcium ions in a KCl host lattice. Configuration B: The cyanate ion is substituted for a chloride ion, with the nitrogen and oxygen atoms lying on the body diagonal of the KCl unit cell. The calcium ion is substituted for a potassium ion and is nearest to the oxygen atom of the cyanate ion.

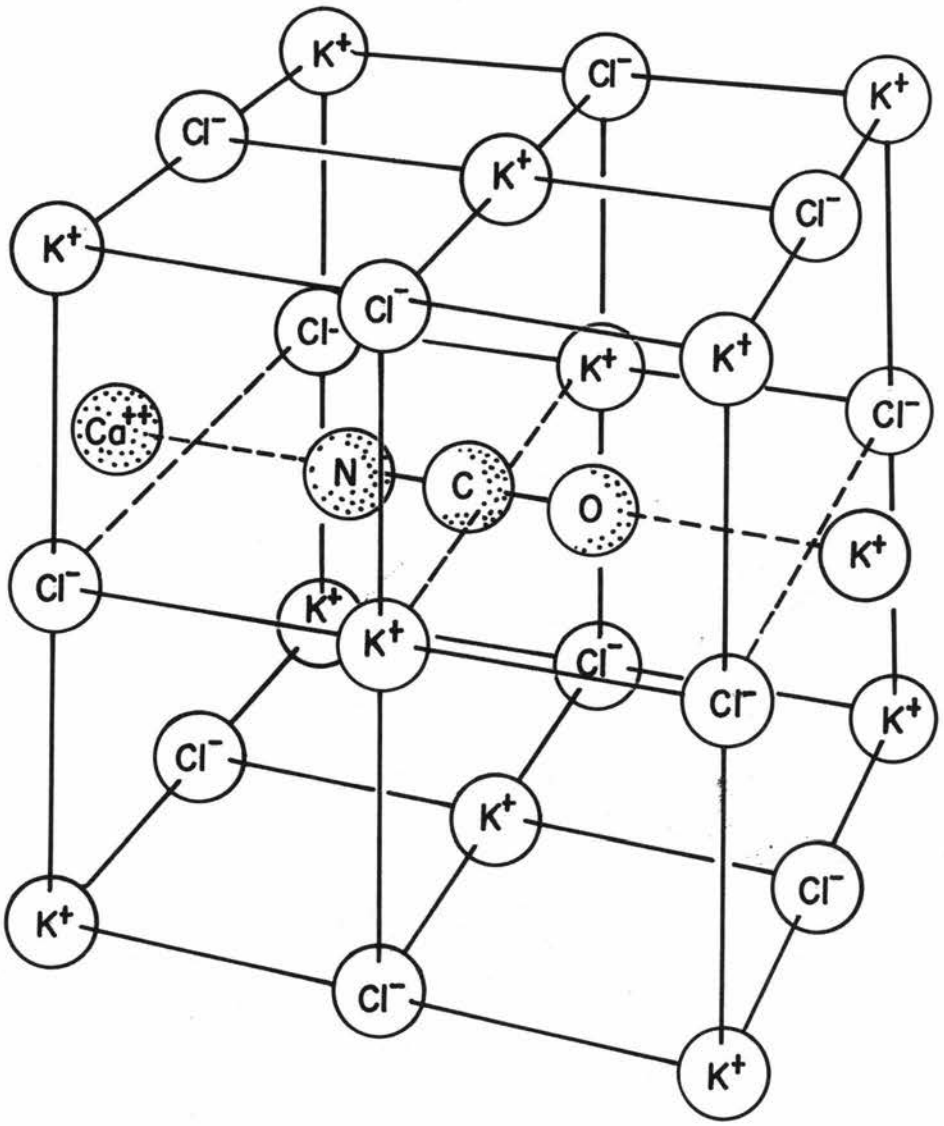

Figure 25. Cyanate and calcium ions in a KCl host lattice. Configuration C: The cyanate ion is substituted for a chloride ion, with the nitrogen and oxygen atoms lying on the cell edge of a KCl unit cell. The calcium ion is substituted for a potassium ion and is nearest to the nitrogen atom of the cyanate ion. The length of the cyanate ion distorts the lattice, forcing the calcium ion and a potassium ion away from their lattice points.

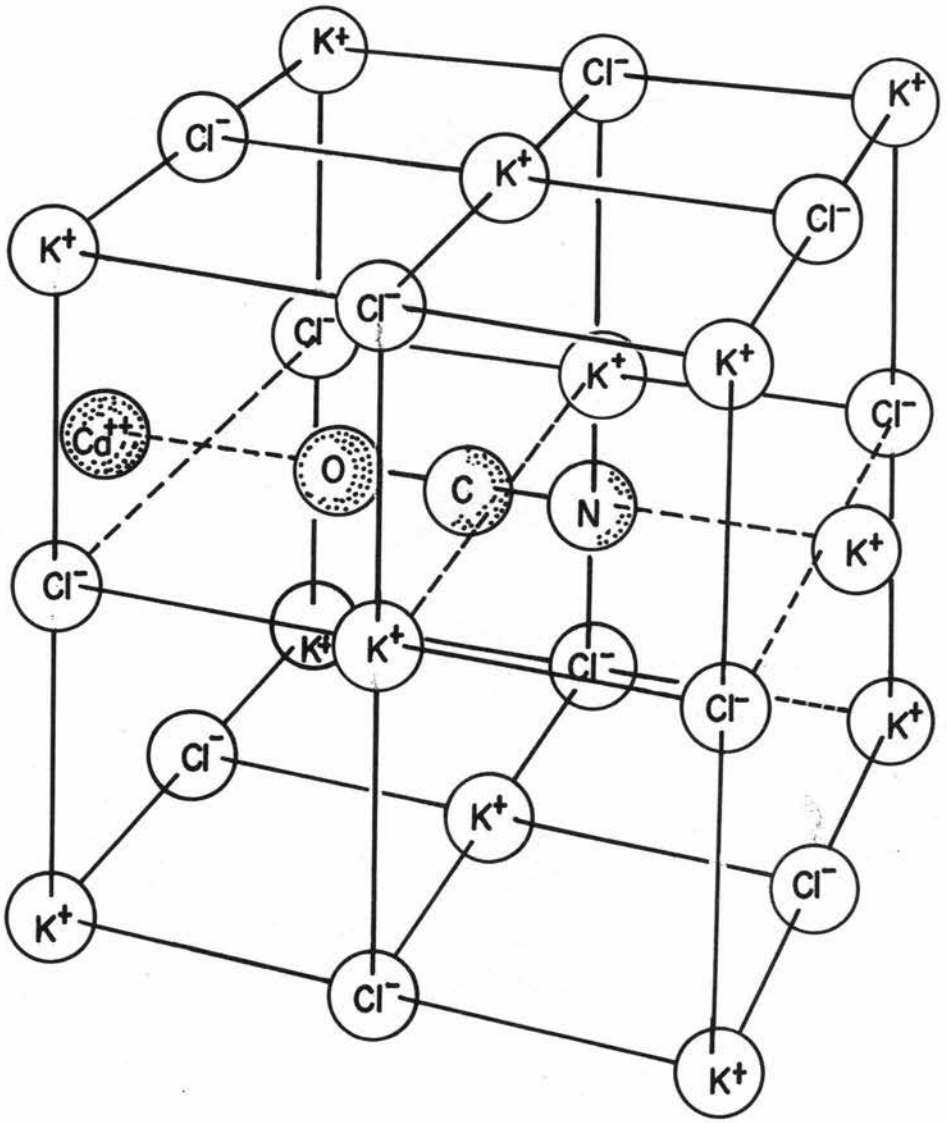

Figure 26. Cyanate and calcium ions in a KCl host lattice. Configuration D: The cyanate ion is substituted for a chloride ion, with the nitrogen and oxygen atoms lying on the cell edge of a KCl unit cell. The calcium ion is substituted for a potassium ion and is nearest to the oxygen atom of the cyanate ion. The length of the cyanate ion distorts the lattice, forcing the calcium ion and a potassium ion away from their lattice points.

the vicinity of the calcium ion in order to preserve electrical neutrality for the crystal. This type of substitution in the lattice is illustrated in Figures 27 and 28. The nearest neighbor calcium ion, in this case, would still act on a cyanate end atom with greater compressional force than would be the case for cyanate ion in its usual orientation when no calcium ion is present.

In order to estimate the effect of these various configurations upon the cyanate spectrum, theoretical calculations were made. The first step in these calculations was to determine a potential function between ion pairs which, if applied to a crystal lattice of these ion pairs, would yield the repulsive energy for the crystal. The potential function used to describe the energy of a crystal has been discussed in Chapter II and is given by the equation

$$\mathcal{E}_T(r) = -\alpha^2 A \frac{e^2}{r} + B e^{(n+1)\left(1-\frac{r}{a_0}\right)}$$

where

$$B = \frac{\alpha^2 A e^2}{(n+1) a_0} .$$

Since B is the coefficient of the exponential term for the repulsive energy, the assumption has been made that its magnitude depends upon the types of ions involved in each ion pair and upon the nature of the crystal lattice according to the relation

$$B = f_c \sqrt{f_\beta \cdot f_\gamma}$$

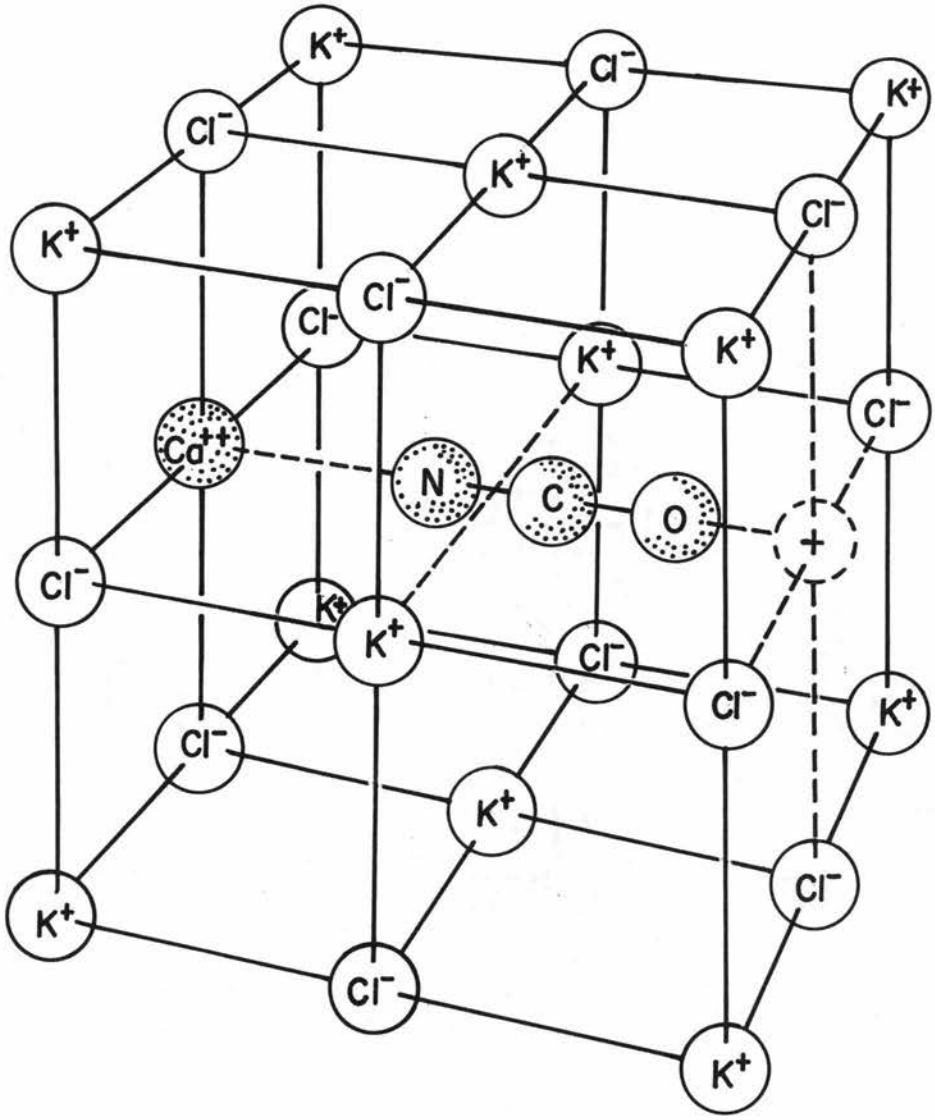

Figure 27. Cyanate and calcium ions in a KCl host lattice. Configuration E: The cyanate ion is substituted for a chloride ion, with the nitrogen and oxygen atoms lying on the cell edge of a KCl unit cell. The calcium ion is substituted for a potassium ion and is nearest to the nitrogen atom of the cyanate ion. A potassium ion vacancy is the nearest neighbor of the cyanate ion.

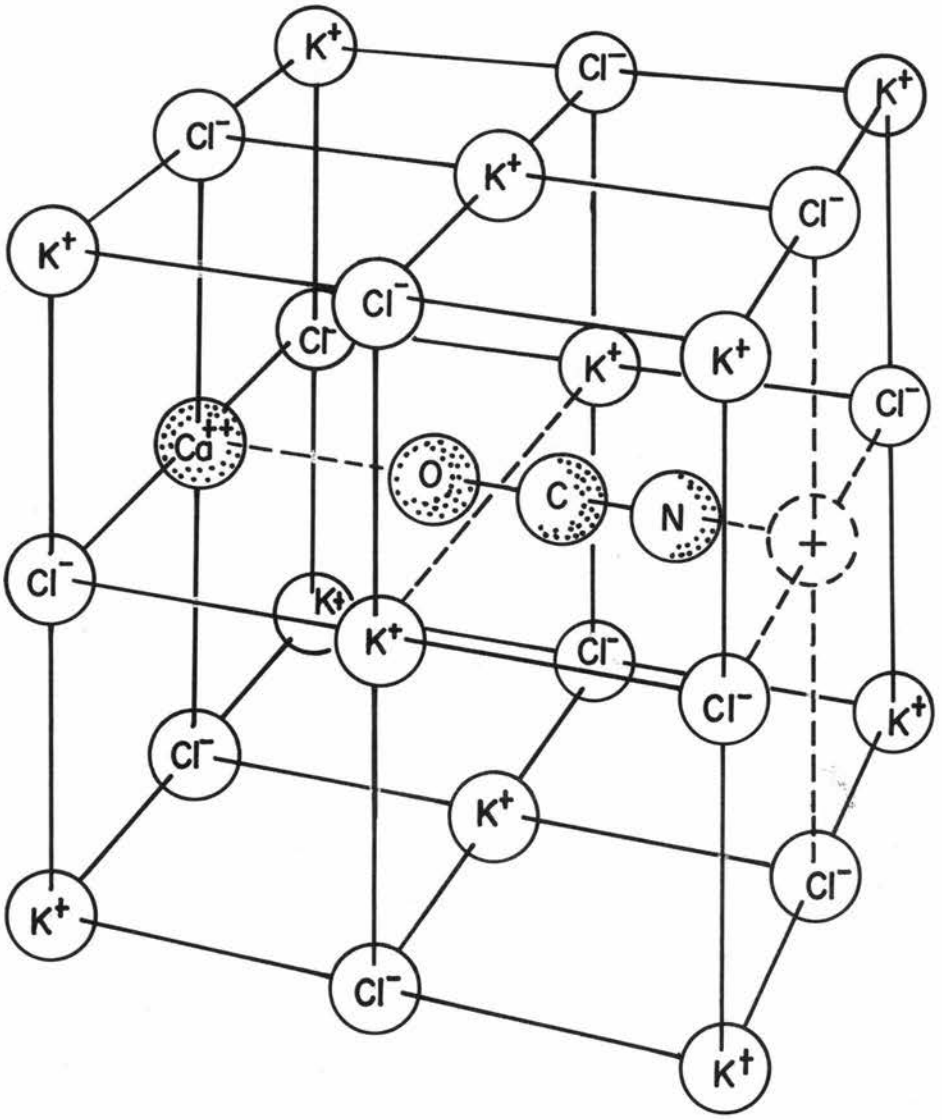

Figure 28. Cyanate and calcium ions in a KCl host lattice. Configuration F: The cyanate ion is substituted for a chloride ion, with the nitrogen and oxygen atoms lying on the cell edge of a KCl unit cell. The calcium ion is substituted for a potassium ion and is nearest to the oxygen atom of the cyanate ion. A potassium ion vacancy is the nearest neighbor of the cyanate ion.

where: (a) f_c is a constant determined by the crystal structure and is given by the equation

$$f_c = \frac{m_{\beta_u \gamma_v} e^2 b_{\beta\gamma}}{(n+1) a_0} \quad ;$$

(b) f_β is a constant determined by the nature of ion β in an ion pair and is calculated from some reference $\beta_i \gamma_j$ crystal according to the equation

$$f_\beta = \frac{d^2_{\beta_i \gamma_j} A_{\beta_i \gamma_j}}{b_{\beta\gamma} m_{\beta_i \gamma_j}}$$

(c) f_γ is a constant determined by the nature of the other ion, γ, of the ion pair and is calculated from a reference $\eta_k \gamma_\ell$ crystal according to the equation

$$f_\gamma = \frac{d^2_{\eta_k \gamma_\ell} A_{\eta_k \gamma_\ell}}{b_{\eta\gamma} m_{\eta_k \gamma_\ell}} \quad ;$$

(d) $b_{\theta\phi}$, a parameter derived from quantum mechanical calculations by Pauling (33, p. 383), is calculated according to the equation

$$b_{\theta\phi} = 1 + \frac{Z_\theta}{N_\theta} + \frac{Z_\phi}{N_\phi} \quad ;$$

(e) N_θ is the number of outer electrons in ion θ and is usually 8 or 18;

(f) N_ϕ is the number of outer electrons in ion ϕ;

(g) $m_{\theta_s \phi_t}$ is the number of nearest neighbors for ion θ in the crystal $\theta_s \phi_t$ multiplied by the number of times,

s, that ion Θ appears in the formula for a stoichiometric molecule of the crystal.

Accordingly, for a particular crystal the value for $\frac{a^2_{\beta u \gamma v} A_{\beta u \gamma v} e^2}{(n+1) a_o}$ should be the same as $f_c \sqrt{f_\beta \cdot f_\gamma}$. In order to test the accuracy of the assumed ion pair potential function, $f_{Ca^{++}}$ was determined from a calcium sulfide lattice and f_{F^-} was determined from a potassium fluoride crystal lattice. The resulting values were used to determine the repulsive potential constant B for a calcium sulfide crystal. The value for $\frac{a^2_{CaF_2} A_{CaF_2} e^2}{(n+1) a_o}$ calculated from the calcium fluoride lattice was compared to the value for

$$\frac{m_{CaF_2} e^2 b_{Ca^{++}F^-} a_{CaS} a_{KF}}{(n+1) a_o} \sqrt{\frac{A_{CaS} A_{KF}}{b_{Ca^{++}S} b_{K^+F^-} m_{CaS} m_{KF}}} .$$

Cancelling terms, $a^2_{CaF_2} A_{CaF_2}$ should be approximately the same as

$$m_{CaF_2} b_{Ca^{++}F^-} a_{CaS} a_{KF} \sqrt{\frac{A_{CaS} A_{KF}}{b_{Ca^{++}S} b_{K^+F^-} m_{CaS} m_{KF}}} .$$

Substituting in the numerical values yields

$$a^2_{CaF_2} A_{CaF_2} = (1)^2 (5.0) = 5.0$$

and

$$m_{CaF_2}\, b_{Ca^{++}}\, \alpha_{CaS}\, \alpha_{KF} \sqrt{\frac{A_{CaS}\, A_{KF}}{b_{Ca^{++}S} = b_{K^+F} - m_{CaS}\, m_{KF}}}$$

$$= (8)(1.125)(2)(1)\sqrt{\frac{(1.7)(1.7)}{(1)(1)(6)(6)}} = 5.1 \ .$$

The agreement between the results has inspired some confidence in this potential function for calculating repulsive forces acting between ion pairs. For one ion pair consisting of ions β and γ the repulsive potential is then given by the equation

$$\epsilon_{\beta\gamma}^{rep.} = \frac{e^2 b_{\beta\gamma}}{(n+1)\, a_0}\, \alpha_{\beta_i \gamma_j}\, \alpha_{\eta_k \gamma_\ell} \sqrt{\frac{A_{\beta_i \gamma_j}\, A_{\eta_k \gamma_\ell}}{b_{\beta\gamma}\, b_{\eta\gamma}\, m_{\beta_i \gamma_j}\, m_{\eta_k \gamma_\ell}}}\; e^{(n+1)\left(1 - \frac{r}{a_0}\right)}$$

$$= B_{\beta\gamma}\, e^{(n+1)\left(1 - \frac{r}{a_0}\right)} \ .$$

For an end atom of cyanate ion in an alkali halide host lattice, with a calcium ion substituted for a near neighbor potassium ion, the potential energy is given by the expression

$$\epsilon_\sigma = -\frac{e^2}{a_{\eta\gamma}} \sum_{\theta}{}' \left(z_\theta z_\sigma \frac{a_{\eta\gamma}}{r_{\theta\sigma}} \right) + B_{\theta\sigma}\, e^{(n+1)\left(1 - \frac{r_{\theta\sigma}}{a_{\theta\sigma}}\right)}$$

where: (a) σ is either the nitrogen or the oxygen atom of the cyanate ion;

(b) $\eta\gamma$ is either KCl or KBr;

(c) ζ is the nearest neighbor ion of σ lying along the longitudinal axis of cyanate ion;

(d) the sum extends over all ions of the alkali halide lattice except for the term with $\theta = \phi$ NCO^-

The change in the force constants of λ_1 and λ_3 for cyanate ion due to this potential function may be determined by taking the second derivative of the potential with respect to the normal coordinates Q_1 and Q_3, respectively. The contribution to $\Delta\lambda_1$ and $\Delta\lambda_3$ by the nitrogen atom is then

$$\Delta\lambda_1^N = \frac{\partial^2 \epsilon_N}{\partial Q_1^2} = \frac{\partial^2 \epsilon_N}{\partial r_{NC}^2}\left(\frac{\partial r_{NC}}{\partial Q_1}\right)^2$$

and

$$\Delta\lambda_3^N = \frac{\partial^2 \epsilon_N}{\partial Q_3^2} = \frac{\partial^2 \epsilon_N}{\partial r_{NC}^2}\left(\frac{\partial r_{NC}}{\partial Q_3}\right)^2$$

The interatomic distance r_{NC} is related to Q_1 and Q_3 by the relation

$$r_{NC} = r_{NC}^\circ + \left(L_{11} + \frac{0.09}{1.26} L_{21}\right) Q_1 + \left(L_{13} + \frac{0.09}{1.26} L_{23}\right) Q_3$$

where $r_{NC}^\circ = 1.17\,\text{Å}$, $r_{CO}^\circ = 1.26\,\text{Å}$, and the center of gravity for the cyanate ion is 1.17 Å from the oxygen atom. The equilibrium interatomic distances in the cyanate ion were determined from molecular orbital calculations given in Appendix I. A similar contribution

is made by the oxygen atom to $\Delta\lambda_1$ and $\Delta\lambda_3$ with r_{CO} being given by the relation

$$r_{CO} = r_{CO}^{\circ} + \frac{1.17}{1.26}\left(L_{21} Q_1 + L_{23} Q_3\right)$$

Force constants for cyanate ion in a potassium bromide host lattice given by Maki and Decius (26, p. 780) were used to calculate values for the L_{tk}'s used above. The values for the internal coordinate force constants were

$$f_1 = f_{NC} = 15.879$$
$$f_2 = f_{CO} = 11.003$$
$$f_{12} = f' = 1.422,$$

and the calculated values obtained for the L matrix constants were

$$L_{11} = 0.11846 \quad , \qquad L_{13} = -0.37494$$
$$L_{21} = 0.23898 \quad , \qquad L_{23} = 0.29756$$

In order to evaluate the coulombic portion of the term $\frac{\partial^2 \epsilon_\sigma}{\partial r^2}$, second derivatives of the coulombic potential for a sodium chloride type crystal lattice with a vacancy at the origin were calculated using an ALWAC IIIE digital computer. The details of this calculation are given in Appendix II. After the computer calculation had been made, the results were modified to include the effect of a calcium ion substituting for a potassium ion in the lattice.

The second derivative of the repulsive potential energy is given by the equation

$$\left[\frac{\partial^2 \epsilon_\sigma^{rep.}}{\partial r_{s\sigma}^2}\right]_{r_{s\sigma}=a_{s\sigma}} = B_{s\sigma}\frac{(n+1)^2}{a_{s\sigma}^2}$$

$$= \frac{(n+1)}{a_{s\sigma}^3} b_{s\sigma} a_{s\beta} a_{r\sigma}\sqrt{\frac{A_{s\beta} A_{r\sigma}}{b_{s\beta} b_{r\sigma} m_{s\beta} m_{r\sigma}}}$$

where β is a sulfide ion if s is a calcium or barium ion, and β is a chloride ion if s is a potassium. In other words, calcium sulfide was used as a reference crystal for calcium ion, barium sulfide was used as a reference crystal for barium ion, and potassium chloride was used as a reference crystal for potassium ion. Since the cyanate ion has a unit negative charge, the f_σ constant was given the same value as for a chloride ion in potassium chloride; i.e.,

$$A_{r\sigma} = 1.75 \;,\; a_{r\sigma} = 1 \;,\; b_{r\sigma} = 1 \;,\; m_{r\sigma} = 6.$$

The value of n was estimated to be eight for an ion with an electronic configuration of the neon type interacting with an ion having an electronic configuration of the argon type. The equilibrium interatomic distance $a_{s\sigma}$ was set equal to the sum of the radius of ion s and the radius of atom σ in cyanate ion. In order to estimate the radii of the oxygen and the nitrogen atoms in cyanate ion, the distance from the nitrogen atom to a nearest neighbor sodium ion and the distance from the oxygen atom to a nearest neighbor sodium ion in a sodium cyanate lattice was calculated. Wykoff (45, Chapter

VI, text page 8, table page 7) indicates that sodium cyanate has a rhombohedral structure with $\alpha = 38^{o}\ 22'$ and $a_o = 5.44$ Å.

Also

$u\,(Na) = 0$, $u\,(N) = 0.575$

$u\,(C) = 0.495$, $u\,(O) = 0.420$.

Using these values, the nearest neighbor distances are $d_{NaN} = 2.48$ Å and $d_{NaO} = 2.44$ Å. Substracting the 1.01 Å radius of the sodium ion gives $r_{N \text{ in } NCO^-} = 1.47$ Å and $r_{O \text{ in } NCO^-} = 1.43$ Å.

In order to calculate the constant $b_{s\sigma} = 1 + \frac{Z_s}{N_s} + \frac{Z_\sigma}{N_\sigma}$ a knowledge of the charge on the nitrogen and the oxygen atoms was required. Maki (24, p. 139) using valence bond structures, indicates that cyanate ion should have the charge distribution

-0.42e	0e	-0.58e
N	C	O

It is interesting to note the significant difference in these values obtained by the valence bond method to those of -0.61, 0.31, -0.70, for N, C, and O atoms, respectively, obtained by the molecular orbital calculation in Appendix I.

Under the influence of the field due to a calcium ion carrying an additional unit of positive charge compared to the potassium ions of the host lattice on one side of the cyanate ion and a possible vacancy on the other, the electronic distribution should change. In an attempt to estimate this shift in charge the polarizability of the

cyanate ion was calculated from refractive indices listed in the x-ray Powder Data File (5, card 8-471) for potassium cyanate. The values given were $n_1 = 1.412$ and $n_2 = 1.575$. The crystal structure of potassium cyanate is the same type as the tetragonal structure of potassium azide described by Wyckoff (45, Chapter VI, illustration page 1). The unit cell contains four cyanate ions with longitudinal axes parallel to the xy- plane. The longitudinal axes for two of the cyanate ions are parallel to each other and perpendicular to the axes for the remaining two cyanate ions. The polarizability of the four ions relative to a field applied in the xy-plane is therefore $2\alpha''_{NCO^-} + 2\alpha^{\perp}_{NCO^-}$ and the polarizability of the four ions relative to a field applied perpendicular to the xy-plane is $4\alpha^{\perp}_{NCO^-}$ where $\alpha^{\perp}_{NCO^-}$ is the polarizability of a cyanate ion perpendicular to its longitudinal axis and α''_{NCO^-} is the polarizability of the cyanate ion parallel to this axis. The polarizability can then be calculated from the refractive indices according to the equations

$$\frac{n_1^2 - 1}{n_1^2 + 2} = \frac{4\pi}{3}\frac{1}{V}\left(4\alpha_{K^+} + 4\alpha^{\perp}_{NCO^-}\right)$$

and

$$\frac{n_2^2 - 1}{n_2^2 + 2} = \frac{4\pi}{3}\frac{1}{V}\left(4\alpha_{K^+} + 2\alpha''_{NCO^-} + 2\alpha^{\perp}_{NCO^-}\right)$$

where V is the volume of the unit cell. The X-ray Powder Data File (5, card 8-471) gives values of $a_o = 6.084$ Å and $C_o = 7.034$ Å for

the lattice constants of the potassium cyanate crystal. Thus $V = 260.4 \times 10^{-24}$ cm^3. The polarizability of the potassium ion according to Schockley, Tessman, and Kahn as recorded by Kittel (20, p. 97) is 1.326×10^{-24} cm^3, so that the polarizability of the cyanate ion can be determined. Solution of the above equations gives for the polarizabilities: $\alpha^{\perp}_{NCO^-} = 2.542 \times 10^{-24}$ cm^3 and $\alpha^{\parallel}_{NCO^-} = 5.076 \times 10^{-24}$ cm^3. These values compare favorably with those values listed by Hirschfelder, Curtiss, and Bird (16, p. 950) of 1.97×10^{-24} and 4.86×10^{-24} cm^3 for N_2O.

The field applied at the center of the cyanate ion in the direction of its longitudinal axis due to the surrounding ions was calculated. Using this information, the separation in charge δ caused by the field was calculated according to the equation

$$\alpha F = \delta e d_{NO} \qquad or \qquad \delta = \frac{\alpha F}{d_{NO} e}$$

where d_{NO} is the interatomic NO distance in the cyanate ion and e is the unit electronic charge. The value obtained for δe was added to the -0.42e charge on the nitrogen atom of unperturbed cyanate ion and was subtracted from the -0.58e charge on the oxygen atom to yield the charge distribution for perturbed cyanate ion. From this information b_{so} can be determined and then the contribution to $\Delta\lambda_1$ and $\Delta\lambda_3$ from the repulsive forces in the crystal.

In addition to the coulombic and repulsive contributions to

$\Delta\lambda_1$ and $\Delta\lambda_3$, the change in the charge distribution of cyanate ion changes its internal force constants. In order to estimate the magnitude of this effect, the percentages of the structures $\bar{N}=C=O$ and $N\equiv C-\bar{O}$ used to describe the resonance structure of a given species were determined from the values calculated for the charge on the nitrogen and carbon atoms of the cyanate ion for that species. From the percentages of these structures the bond orders for the NC and CO bonds were calculated. Information listed by Wilson, Decius, and Cross (44, p. 175, 178), Maki (24, p. 135), and Somayajulu (38) has lead to the use of the equations

$$f_{CN} = 6.48\, n_{CN} - 0.84$$

and

$$f_{CO} = 7.76\, n_{CO} - 0.02$$

for calculating the force constants of the NC and CO bonds of the new species from the bond orders N_{CN} and N_{CO}. From these values the changes, Δf_{CN} and Δf_{CO}, in the force constants relative to unperturbed cyanate were calculated. The changes in the normal coordinate force constants were finally calculated using the usual equations

$$\Delta\lambda_1 = L_{11}^2\,\Delta f_{CN} + L_{21}^2\,\Delta f_{CO},$$

$$\Delta\lambda_2 = L_{13}^2\,\Delta f_{CN} + L_{23}^2\,\Delta f_{CO}.$$

Here, the assumption has been made that $\Delta f'$ is small compared to

Δf_{CN} and to Δf_{CO} and may be neglected.

Preliminary calculations indicated that in configurations C and D, if the lattice was not allowed to distort, but rather the nitrogen-calcium and oxygen-potassium interatomic distances or else the oxygen-calcium and nitrogen-potassium interatomic distances were compressed in order to squeeze the cyanate ion along the cell edge, the change in the force constants were about one order of magnitude larger than the observed shift. Therefore, the calculations whose results are listed in Tables 7, 8, 9, and 10 were made with the assumption for configurations C and D that the lattice distorted to an extent which would allow the interionic distances between the cyanate ion and its nearest neighbors to be equal to the sum of the ionic radii for each pair under consideration.

The calculations were made taking the positive direction as being from the calcium ion directed toward the cyanate ion. The $\Delta\lambda^{0}$'s in Table 10 are the differences between the $\Delta\lambda$'s for each configuration and $\Delta\lambda$ for the unperturbed cyanate ion in the host lattice under consideration. Configuration U in the tables refers to unperturbed cyanate ion which is oriented along the body diagonal of the unit cell surrounded only by ions of the host lattice. The values for the theoretical changes in force constants for ν_3 in Table 9 and 10 may be compared to the experimental values listed in Table 11 in order to gain some idea of the accuracy of the calculations. The

Table 7. Positions of the N, C, and O atoms of cyanate ion and of the nearest neighbor K^+ and Ca^{++} ions relative to their assigned lattice points for each configuration.

Host Lattice	Configuration	Positions (Å)				
		K^+	Ca^{++}	C	N	O
KCl	U	0	--	-0.04	-1.21	1.22
KCl	A	0	0	-0.04	-1.21	1.22
KCl	B	0	0	+0.04	+1.21	-1.22
KCl	C	0.52	-0.85	-0.36	-1.53	0.90
KCl	D	0.52	-0.85	-0.31	0.86	-1.57
KCl	E	--	0	0.49	-0.68	1.75
KCl	F	--	0	0.54	1.71	-0.72
KBr	U	0	--	-0.04	-1.21	1.22
KBr	A	0	0	-0.04	-1.21	1.22
KBr	B	0	0	+0.04	1.21	-1.22
KBr	C	0.37	-0.72	-0.37	-1.54	0.89
KBr	D	0.37	-0.72	-0.32	0.85	-1.58
KBr	E	--	0	0.35	-0.82	1.61
KBr	F	--	0	0.40	1.57	-0.86

Table 8. Field at the center of cyanate ion, charges on the N and O atoms, and bond orders for the NC and CO bonds for each configuration.

Host Lattice	Configuration	Field (e/cm^2) X 10^{-14}	Charge (e) N	Charge (e) O	Bond Order NC	Bond Order CO
KCl	U	0	0.42	0.58	2.58	1.42
KCl	A	- 3.40	0.49	0.51	2.51	1.49
KCl	B	- 3.40	0.35	0.65	2.65	1.35
KCl	C	- 4.44	0.51	0.49	2.49	1.51
KCl	D	- 4.45	0.33	0.67	2.67	1.33
KCl	E	-21.32	0.86	0.14	2.14	1.86
KCl	F	-21.26	0.00	1.00	3.00	1.00
KBr	U	0	0.42	0.58	2.58	1.42
KBr	A	- 3.1	0.48	0.52	2.52	1.48
KBr	B	- 3.1	0.36	0.64	2.64	1.36
KBr	C	- 4.85	0.52	0.48	2.48	1.52
KBr	D	- 4.91	0.32	0.68	2.68	1.32
KBr	E	-19.13	0.82	0.18	2.18	1.82
KBr	F	-19.06	0.02	0.98	2.98	1.02

Table 9. Change in force constants due to the attractive and compressional forces of the lattice surrounding cyanate ion for each configuration.

Host Lattice	Configuration	Force Constant Change (millidynes/Å) Δf_{NC}	Δf_{CO}	$\Delta \lambda_1$	$\Delta \lambda_3$
KCl	U	0.00	0.00	0.000	0.000
KCl	A	-0.46	0.54	0.024	-0.017
KCl	B	0.45	-0.54	-0.024	0.016
KCl	C	-0.58	0.70	0.032	-0.020
KCl	D	0.58	-0.70	-0.032	0.020
KCl	E	-2.85	3.41	0.155	-0.099
KCl	F	2.72	-3.26	-0.148	0.094
KBr	U	0.00	0.00	0.000	0.000
KBr	A	-0.40	0.46	0.021	-0.016
KBr	B	0.39	-0.47	-0.021	0.013
KBr	C	-0.65	0.78	0.035	-0.022
KBr	D	0.65	-0.78	-0.035	0.022
KBr	E	-2.59	3.10	0.141	-0.090
KBr	F	2.59	-3.10	-0.141	0.090

Table 10. Change in force constants due to the shift in charge within the cyanate ion induced by the surrounding lattice for each configuration.

Host Lattice	Configuration	Force Constant Change (millidynes/Å) $\Delta\lambda_1$	$\Delta\lambda_3$	$\Delta\lambda_1^\circ$	$\Delta\lambda_3^\circ$
KCl	U	0.0087	0.0246	0	0
KCl	A	0.0035	-0.0001	-0.0052	-0.0245
KCl	B	-0.0028	0.0016	-0.0071	-0.0230
KCl	C	0.0080	0.0335	-0.0007	0.0089
KCl	D	0.0148	0.0312	0.0061	0.0066
KCl	E	0.0059	0.0642	-0.0028	0.0396
KCl	F	0.0308	0.0476	0.0221	0.0230
KBr	U	0.0073	0.0204	0	0
KBr	A	0.0028	-0.0004	-0.0045	-0.0208
KBr	B	-0.0024	0.0010	-0.0097	-0.0194
KBr	C	0.0072	0.0315	-0.0001	0.0111
KBr	D	0.0140	0.0291	0.0067	0.0087
KBr	E	0.0054	0.0576	-0.0019	0.0372
KBr	F	0.0309	0.0528	0.0236	0.0324

Table 11. Force constants calculated from frequencies observed experimentally.

Host Lattice	Species	λ_3	$\Delta\lambda_3$ (millidynes/Å)	$\Delta(\Delta\lambda_3)$
KCl	unperturbed	2.8037	0	
	1	2.8476	0.0439	0.1342
	2	2.9818	0.1781	
	3	2.8386	0.0349	0.1146
	4	2.9532	0.1495	
KBr	unperturbed	2.7725	0	
	5	2.8463	0.0738	0.0998
	6	2.9461	0.1736	

information in Table 9 indicates that, for a given position of the cyanate ion in an alkali halide lattice, the change in force constant for the nitrogen atom with calcium ion as a nearest neighbor is the same as the change in force constant for the oxygen atom with a nearest neighbor calcium ion except for change in sign. Also the Δf_3 force constants in Table 10 do not change a great deal upon going from an orientation with calcium ion nearest the nitrogen to an orientation with calcium ion nearest the oxygen if the center of the cyanate ion remains in about the same position of the lattice. Therefore, it would be expected that the shift in force constant f_3 would approximately obey the relation

$$f_3^{\text{perturbed}} = f_3^{\text{unperturbed}} + \Delta f_3^{\text{lattice}} \pm \Delta f_3^{\text{inductive}}$$

where the positive sign is taken if calcium ion is nearest the oxygen atom of the cyanate ion. Applying this equation to the information in Table 11 leads to values of 0.1110 millidynes/Å for $\Delta f_3^{\text{lattice}}$ and 0.0671 millidynes/Å for $\Delta f_3^{\text{inductive}}$ of species 1 and 2, 0.0922 millidynes/Å for $\Delta f_3^{\text{lattice}}$ and 0.0573 millidynes/Å for $\Delta f_3^{\text{inductive}}$ of species 3 and 4, and 0.1227 millidynes/Å for $\Delta f_3^{\text{lattice}}$ and 0.0489 millidynes/Å for $\Delta f_3^{\text{inductive}}$ of species 5 and 6. Configurations E and F in Table 10 give the largest values of $\Delta f_3^{\text{lattice}}$ obtained from the theoretical calculations, and these are about three times smaller than the observed values.

However, as has been mentioned previously, configurations C and D can give values for $\Delta\lambda_3^{\text{lattice}}$ up to ten times larger than the observed values if the host lattice does not distort appreciably. The truth must lie somewhere between the two extremes. Configurations E and F in Table 9 give the largest values of $\Delta\lambda_3^{\text{inductive}}$ obtained from the theoretical calculations, and these are about one and one-half times larger than the largest observed experimental value. Configurations C and D give values one-third the size of the observed value. This disparity between the experimental and theoretical values prevents an assignment being made for any species with respect to its probable configuration in the host lattice. Nevertheless, it will be mentioned that species 1 and 2 of the KCl host lattice give the largest values for $\Delta\lambda_3^{\text{lattice}}$ and for $\Delta\lambda_3^{\text{inductive}}$. Also of the theoretical changes in force constant, configurations E and F give the largest values for $\Delta\lambda_3^{\text{lattice}}$ and $\Delta\lambda_3^{\text{inductive}}$; so perhaps species 1 and 2 have configurations E and F.

The negative values of $\Delta\lambda_3^{\text{lattice}}$ obtained for configurations A and B of a potassium chloride lattice in Table 10 seem to indicate that the shift toward lower frequency of ν_3 with barium is a result of cyanate ion remaining along the body diagonal, even when barium ion is a nearest neighbor. The increased size of the barium ion compared with calcium ion probably prevents cyanate from assuming an orientation along the cell edge.

The reason for no new peaks appearing when crystals were doped with magnesium ion is not known. Perhaps the small size of the ion enables it to occupy an interstitial position in preference to a lattice point so that it does not tend to pair up with cyanate ion.

4. Summary

The spectra of several alkali halide pressed pellets containing small amounts of potassium cyanide or of calcium cyanamide have been examined. Heating the pellets caused some of the impurity ions to be oxidized to cyanate. The spectra of the pellets cooled with liquid nitrogen showed the appearance of several sharp peaks not evident in the room temperature spectra some of which are probably due to calcium ion-cyanate ion pairs dissolved in the alkali halide lattice.

Potassium chloride and potassium bromide crystals doped with potassium cyanate and either calcium chloride or calcium bromide have been grown. The spectra of these crystals scanned while cooled with liquid nitrogen contained many new peaks which do not appear in the spectra of cyanate doped potassium chloride or bromide crystals having no divalent cations present. Because of the narrowness of these new absorption peaks and the fact that the new peaks in the spectra of the potassium chloride crystal appeared at much different frequencies from those in the spectra of the potassium

bromide crystal, these new absorptions were assumed to arise from calcium ion-cyanate ion pairs in solid solution rather than from small calcium cyanate crystals distributed throughout the alkali halide crystal.

The assumption was made for cyanate ion perturbed by a near neighbor calcium ion that the separation of the Fermi resonance pair appearing in the symmetric stretching region of its spectrum is approximately the same as the separation of its corresponding Fermi resonance pair in the combination region. An additional assumption that the anharmonicity constants of the perturbed cyanate ion do not greatly differ from those for the unperturbed cyanate ion was also made. With the aid of these assumptions many of the new peaks in the symmetric stretching, anti-symmetric stretching, and combination regions of the spectrum were correlated and assigned to various species of cyanate ion-calcium ion pairs, although just what the configuration of the pairs for each species is has not been determined.

Theoretical calculations based upon several possible configurations for calcium ion-cyanate ion pairs in an alkali halide lattice have been made which indicate that the field of a near neighbor calcium is strong enough to bring about the observed shift in frequencies. However, the values obtained theoretically were not close enough to the observed shifts to allow an assignment of the new absorption peaks to a particular calcium ion-cyanate ion pair configuration in

the lattice.

Potassium chloride and potassium bromide crystals were also grown doped with potassium cyanate and either magnesium chloride, magnesium bromide, barium chloride, or barium bromide. New peaks appeared only in the spectrum of the barium chloride doped crystal. The reasons why no new peaks appeared for crystals doped with the other salts are not known.

PART II. METHOD FOR OBTAINING MINIMAL KINEMATICALLY COMPLETE SETS OF INTERNAL COORDINATES

I. INTRODUCTION

In the calculation of normal modes and frequencies of vibration the use of symmetry coordinates can often lead to a great reduction in labor. Symmetry coordinates are coordinates which form the basis of a completely reduced unitary representation of the point group of a molecule, and sets of these coordinates of the same degenerate symmetry species must have identical transformation coefficients (44, p. 115). The easiest method for obtaining internal symmetry coordinates is to construct them from sets of internal coordinates which are exchanged by the symmetry operations of the molecules. Each set contains all the coordinates resulting from the application of all symmetry operations of the molecule to some arbitrarily chosen coordinate and is termed a "symmetrically complete" set of internal coordinates. In many cases not all of the coordinates in a symmetrically complete set are independent. In such cases the coordinates are said to form a redundant set, with one or more redundancy conditions connecting them. The use of redundant coordinates will introduce as many zero roots into the secular equation as there are redundancy conditions. The redundancies are usually removed after the factoring of the secular equation has been

accomplished by omitting the rows and columns in the symmetry $\underset{\sim}{G}$ matrix corresponding to the symmetry coordinates which have been declared redundant (44, p. 145).

In order to determine which symmetry coordinates are redundant the symmetry analyses of both cartesian and internal coordinates are carried out. The symmetry species for the cartesian coordinates diminished by the species for translation and rotation yields the number of independent internal coordinates that will be expected for each. Comparison of these species with those generated by the internal coordinates will indicate where the redundancies occur. Unfortunately, many times, more than one symmetrically complete set of internal coordinates will contribute to a symmetry species which contains a redundancy. The question of which set contributes to the redundancy and which does not, then arises. At present, reference must be made to the elements of the symmetry $\underset{\sim}{G}$ matrix to determine this. A linear combination of rows or columns for the redundant species in this matrix must be found which is equal to zero. The symmetry coordinate corresponding to any row or column with a non-zero coefficient in the linear combination may be declared redundant and be omitted. For complex molecules this procedure may be difficult. In addition, although 3n-6 or more internal coordinates may have been used, essential internal coordinates may have been inadvertantly omitted. A method for selecting a sufficient set of

internal coordinates has been described by J. C. Decius (10).

The purpose for developing the method to be described was to eliminate redundant coordinates without having to refer to the G_{MV} matrix. This method will also yield a set of internal coordinates which includes all essential vibrational motions.

II. PROCEDURE

Only three types of internal coordinates, bond stretching, valence angle bending, and a special type of torsion, will be used in this development. The dihedral angle of the torsion will be either 0° or 180° for the equilibrium position of the molecule. It is necessary, at this point, to define a set of vectors $\underset{\sim}{s}_{\sim t\alpha}$ such that the direction of $\underset{\sim}{s}_{\sim t\alpha}$ is the direction in which a given displacement of atom α will produce the greatest increase of the internal coordinate S_t, and the magnitude of $\underset{\sim}{s}_{\sim t\alpha}$ is equal to the increase in S_t produced by a unit displacement of the atom in this most effective direction (43, p. 55). Two torsions τ_1 and τ_2 shall be defined as equivalent if $\underset{\sim}{s}_{\sim \tau_1 \alpha} = \underset{\sim}{s}_{\sim \tau_2 \alpha}$ for every atom of the molecule. If $\underset{\sim}{s}_{\sim \tau_1} = -\underset{\sim}{s}_{\sim \tau_2}$ for every atom of the molecule, τ_1 is defined as being equivalent to the negative of τ_2.

Five different cases will now be considered. "N" is the number of atoms in the molecule under consideration.

(1) If N = 1, no internal coordinates are necessary.

(2) If N = 2, one bond stretching internal coordinate should be used.

(3) For linear molecules with N = 3, use (N-1) bond stretching and 2(N-2) valence angle bending internal coordinates with (N-2) angle bending coordinates in the

zx-plane and (N-2) in the yz plane. (Note: (N-1) + 2(N-2) = 3N-5 internal coordinates for linear molecules)

(4) For atoms lying in a plane use (2N-3) bond stretching and (N-3) torsion internal coordinates. (Note: (2N-3) + N-3 = 3N-6 internal coordinates for planar molecules)

(5) For atoms not lying in a plane with three or more atoms use (3N-6) bond stretches.

Many different sets of internal coordinates will usually satisfy the above conditions. In addition, however, they should be kinematically complete in order to include all essential vibrational motions. In order to be certain of obtaining a kinematically complete set proceed in the following manner.

For nonlinear molecules start with any three atoms and join them with three bond stretching coordinates. Connect a fourth atom of the molecule to each of the first three with bond stretches if the fourth atom does not lie in the same plane as the original three. If the fourth atom is coplanar with the three, connect it to two of the three original atoms with bond stretches and connect all four with a torsion coordinate. If the values of the internal coordinates are fixed, the four atoms now form a rigid structure. A fifth atom may be attached to three of the four in this structure following the same procedure that was used in attaching the fourth atom to the original three.

A five atom rigid configuration would then be obtained. This process can be continued until all the atoms of the molecule have been joined to the structure. The internal coordinates used in this formation will be a minimal kinematically complete set of internal coordinates.

Different kinematically complete sets of coordinates can be obtained by this method for the same molecule depending upon the manner in which the structure was constructed. If the symmetry operations of the point group for this molecule are applied to a set of coordinates obtained as described above, symmetrically complete sets of internal coordinates will be generated. It is generally desirable to use a set of symmetrically complete sets containing the least number of internal coordinates possible. Although this may not always be achieved, a reduced set may be obtained by adding each new internal coordinate to the structure (according to the method above) which will generate the least possible increase in symmetrically complete sets if the symmetry operations of the point group were applied.

Once a satisfactory set of internal coordinates has been obtained redundancies in the symmetry coordinates constructed from them can immediately be removed. The internal coordinates generated by the symmetry operations which were not present in the original minimal kinematically complete set are declared redundant. The symmetrically complete sets will yield as many redundancies as

there are redundant internal coordinates contained in them. When a redundancy has been found to appear in a certain symmetry species and a symmetrically complete set containing a redundancy contributes to this species, the symmetry coordinate corresponding with this species and this set of internal coordinates is omitted.

III. EXAMPLES

The chlorinated cyclobutane molecule shown in (k) of Figure 29 will be used for the first example. Without the use of the method described in Chapter II it is still possible to find a kinematically complete set of internal coordinates for this molecule. One such set would be four carbon-carbon stretchings (R's) of the carbon one-carbon two type, four (carbon one-hydrogen one type) carbon-hydrogen stretchings (r's), four (carbon one-chlorine one type) carbon-chlorine stretchings (r̲'s), eight (carbon two-hydrogen one type) carbon-hydrogen stretchings (r*'s), eight (carbon two-chlorine one type) carbon-chlorine stretchings (r̲*'s), four (hydrogen one-chlorine one type) hydrogen-chlorine stretchings (R*'s), and four (carbon one-carbon two-carbon three-carbon four type) torsions (τ's) as described by Wilson et al. (44, p. 60) without the special properties of equivalence described in this dissertation. This is a set of 36 internal coordinates while only 3N-6, or 30, are required; so the set must contain six redundancies.

Application of symmetry theory to the chlorinated cyclobutane molecule leads to the information listed in Table 12. The symbol "u" refers to the cartesian displacement coordinates. One redundancy of species A_1, one of species B_1, and four of species E are expected. Since the set of four torsions makes a contribution to each of the A_1,

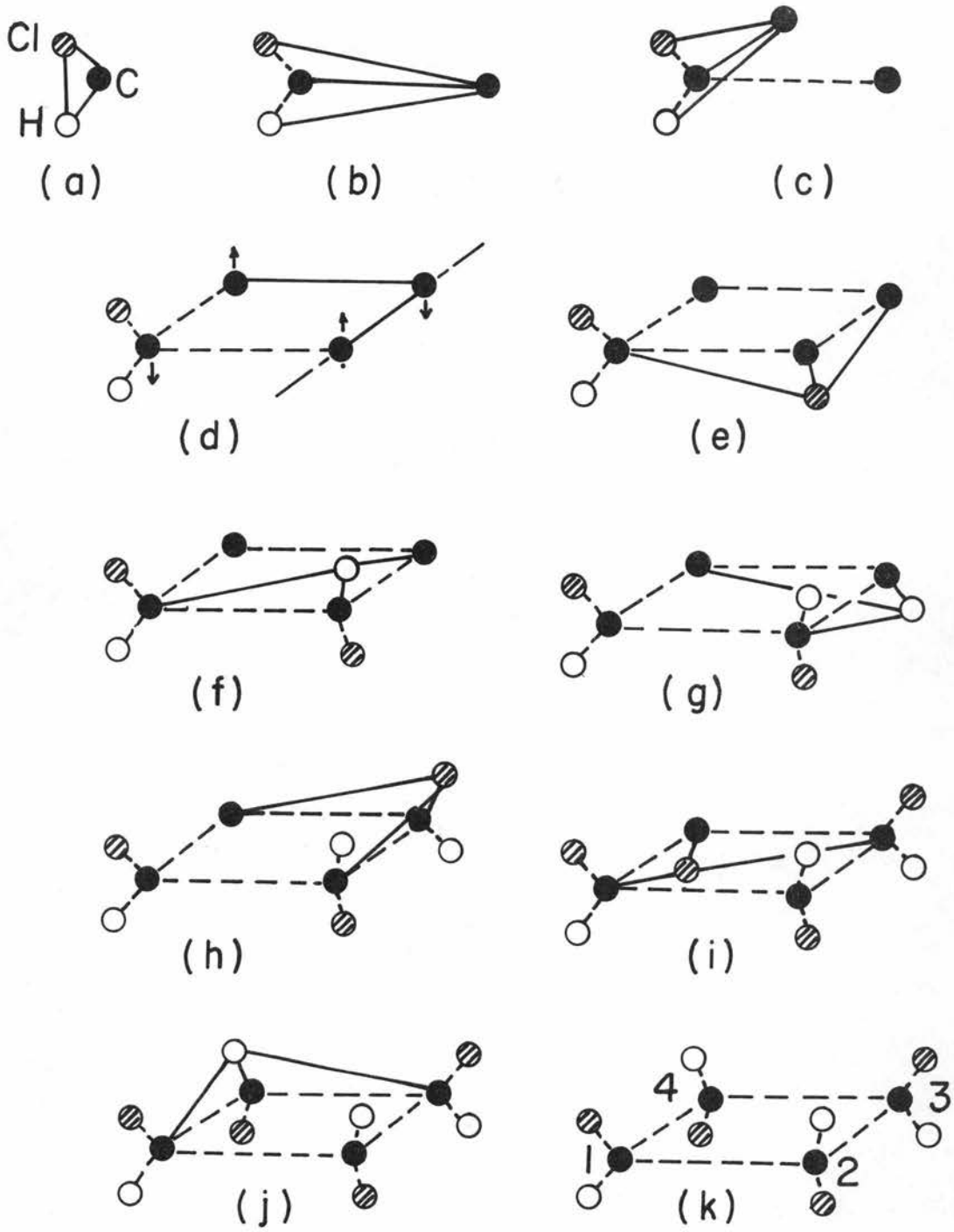

Figure 29. Construction of a rigid chlorinated cyclobutane molecule.

Table 12. Symmetry species for the vibrations of chlorinated cyclobutane.

D_{2d}	E	$2S_4$	C_2	$2C_2'$	$2\sigma_d$	$n^{(u)}$	n_T	n_R	n_v	$n^{(S)}$	$n^{(redundant)}$
A_1	1	1	1	1	1	6	0	0	6	7	1
A_2	1	1	1	-1	-1	3	0	1	2	2	0
B_1	1	-1	1	1	-1	3	0	0	3	4	1
B_2	1	-1	1	-1	1	6	1	0	5	5	0
E	2	0	-2	0	0	9	1	1	7	9	2
$\chi_j(u)$	36	0	0	0	6						

Symmetrically complete internal coordinate set	Invarient subgroup	Irreducible Representations
4R's	$C_s = \{E, C_2'\}$	$A_1 + B_1 + E$
4r's	$C_s = \{E, \sigma_d\}$	$A_1 + B_2 + E$
4r's	$C_s = \{E, \sigma_d\}$	$A_1 + B_2 + E$
8r*'s	$C_1 = \{E\}$	$A_1 + A_2 + B_1 + B_2 + 2E$
8r*'s	$C_1 = \{E\}$	$A_1 + A_2 + B_1 + B_2 + 2E$
4R*'s	$C_s = \{E, \sigma_d\}$	$A_1 + B_2 + E$
4τ's	$C_2 = \{E, C_2'\}$	$A_1 + B_1 + E$

B_1, and E species, the question arises as to whether this complete set of internal coordinates could be eliminated and still be able to include all essential vibrational motions in the remaining sets. At this point reference is generally made to the $\underset{\sim}{G}$ matrix for the symmetry coordinates to resolve the question.

If, for the moment, torsions of the above type are used, a minimal kinematically complete set of internal coordinates can be obtained from the 36 coordinates listed above. The steps are illustrated in Figure 29.

In step (a) hydrogen atom one, carbon atom one, and chlorine atom one are connected by bond stretchings. In steps (b) and (c) carbon atoms two and four are attached to the original three atoms by bond stretchings. In step (d) carbon atom three is attached to carbon atoms two and four by bond stretchings, and carbon atoms one, two, three, and four are connected with a torsion since all four lie in a plane. In steps (e) through (j) the remaining atoms are brought into the rigid configuration with bond stretchings. In this process four of the four R's, four of the four r's, four of the four $\underline{r}$'s, eight of the eight r*'s, eight of the eight $\underline{r}$*'s, one of the four R*'s, and one of the four τ 's were used. This set of internal coordinates is then a minimal kinematically complete set. Thus, when symmetrically complete sets are used, three redundancies are expected to appear in the set of torsions and three in the set of hydrogen-chlorine

stretchings. In Table 3 the R*'s are shown to contribute to the A_1, B_2, and E species, and the τ's are listed as contributing to the A_1, B_1, and E species. One redundancy appears in the A_1 species, one in the B_1 species, and four in the E species. Therefore, the R*'s must contribute one redundancy to the A_1 species and two redundancies to the E species. The τ's contribute one redundancy to the B_1 species and two to the E species. The question posed previously is then answered. The set of four torsions may not be eliminated and still be able to include all essential vibrational motions in the remaining sets.

Further evidence in support of the last statement is obtained upon examining the cyclobutane molecule. Application of symmetry theory to this molecule leads to the information listed in Table 13. The contribution of the torsion set to the B_{1u} species is necessary to obtain the required number of contributions to this species for kinematic completeness. In this case the set of torsions contributes one redundancy to the A_{1u} species and two to the E_g species, and the set of hydrogen-hydrogen stretchings ($\underline{R}$*'s) contributes one redundancy to the A_{1g} species and two to the E_u species. The redundancies would be expected to appear among the same symmetrically complete sets since the general structures of the cyclobutane and the chlorinated cyclobutane molecules are the same.

A reduced set of symmetrically complete sets of internal

Table 13. Symmetry species for the vibrations of cyclobutane.

D_{4h}	E	$2C_4$	C_2	$2C_2'$	$2C_2''$	i	$2S_4$	σ_h	$2\sigma_v$	$2\sigma_d$	$n^{(u)}$	n_T	n_R	n_v	$n^{(S)}$	$n^{(redundant)}$
A_{1g}	1	1	1	1	1	1	1	1	1	1	3	0	0	3	4	1
A_{2g}	1	1	1	-1	-1	1	1	1	-1	-1	2	0	1	1	1	0
B_{1g}	1	-1	1	1	-1	1	-1	1	1	-1	2	0	0	2	2	0
B_{2g}	1	-1	1	-1	1	1	-1	1	-1	1	3	0	0	3	3	0
E_g	2	0	-2	0	0	2	0	-2	0	0	4	0	1	3	4	1
A_{1u}	1	1	1	1	1	-1	-1	-1	-1	-1	1	0	0	1	2	1
A_{2u}	1	1	1	-1	-1	-1	-1	-1	1	1	3	1	0	2	2	0
B_{1u}	1	-1	1	1	-1	-1	1	-1	-1	1	3	0	0	3	3	0
B_{2u}	1	-1	1	-1	1	-1	1	-1	1	-1	1	0	0	1	1	0
E_u	2	0	-2	0	0	-2	0	2	0	0	5	1	0	4	5	1
$\chi_{j(u)}$	36	0	0	0	-2	0	0	4	0	6						

Symmetrically complete internal coordinate set	Invarient Subgroups	Irreducible Representations
4R's	$C_{2v} = \{E, C_2', \sigma_h, \sigma_v\}$	$A_{1g} + B_{1g} + E_u$
8r's	$C_s = \{E, \sigma_d\}$	$A_{1g} + B_{2g} + E_g + A_{2u} + B_{1u} + E_u$
16r*'s	$C_1 = \{E\}$	$A_{1g} + A_{2g} + B_{1g} + B_{2g} + 2E_g + A_{1u} + A_{2u} + B_{1u} + B_{2u} + 2E_u$
4R*'s	$C_{2v} = \{E, C_2'', \sigma_h, \sigma_d\}$	$A_{1g} + B_{2g} + E_u$
4r's	$C_{2v} = \{E, C_2', \sigma_h, \sigma_v\}$	$E_g + A_{1u} + B_{1u}$

coordinates of the type used in this discussion was not obtained for the chlorinated cyclobutane molecule because of the lack of selectivity in choosing a kinematically complete set. Such a set will now be obtained by proceeding with a little more care.

Figure 30 illustrates the procedure that must be followed. The first step is to connect three atoms in the molecule with bond stretchings in such a manner that applying all of the symmetry operations of the point group D_{2d} to the bond stretchings will generate the least possible number of new coordinates. In step (a) three carbon atoms are joined together. After applying the symmetry operations, a set of four (carbon one-carbon two type) carbon-carbon bond stretchings (R's) and a set of two (carbon one-carbon three type) carbon-carbon bond stretchings ($\underline{R}$'s) for a total of six internal coordinates are obtained. This is the least possible number that can be obtained in the first step. For instance, if the hydrogen one, carbon one, and chlorine one atoms had been joined, four r's, four $\underline{r}$'s, and four R*'s would have been obtained after application of the symmetry operations yielding a total of twelve internal coordinates which is a larger number than the six coordinates obtained from step (a). In step (b) a fourth carbon atom is added increasing the number of symmetrically complete sets by the addition of a torsion set. Here the special properties of equivalence for torsions described in Chapter II are used to eliminate any extra torsions that would be generated by the

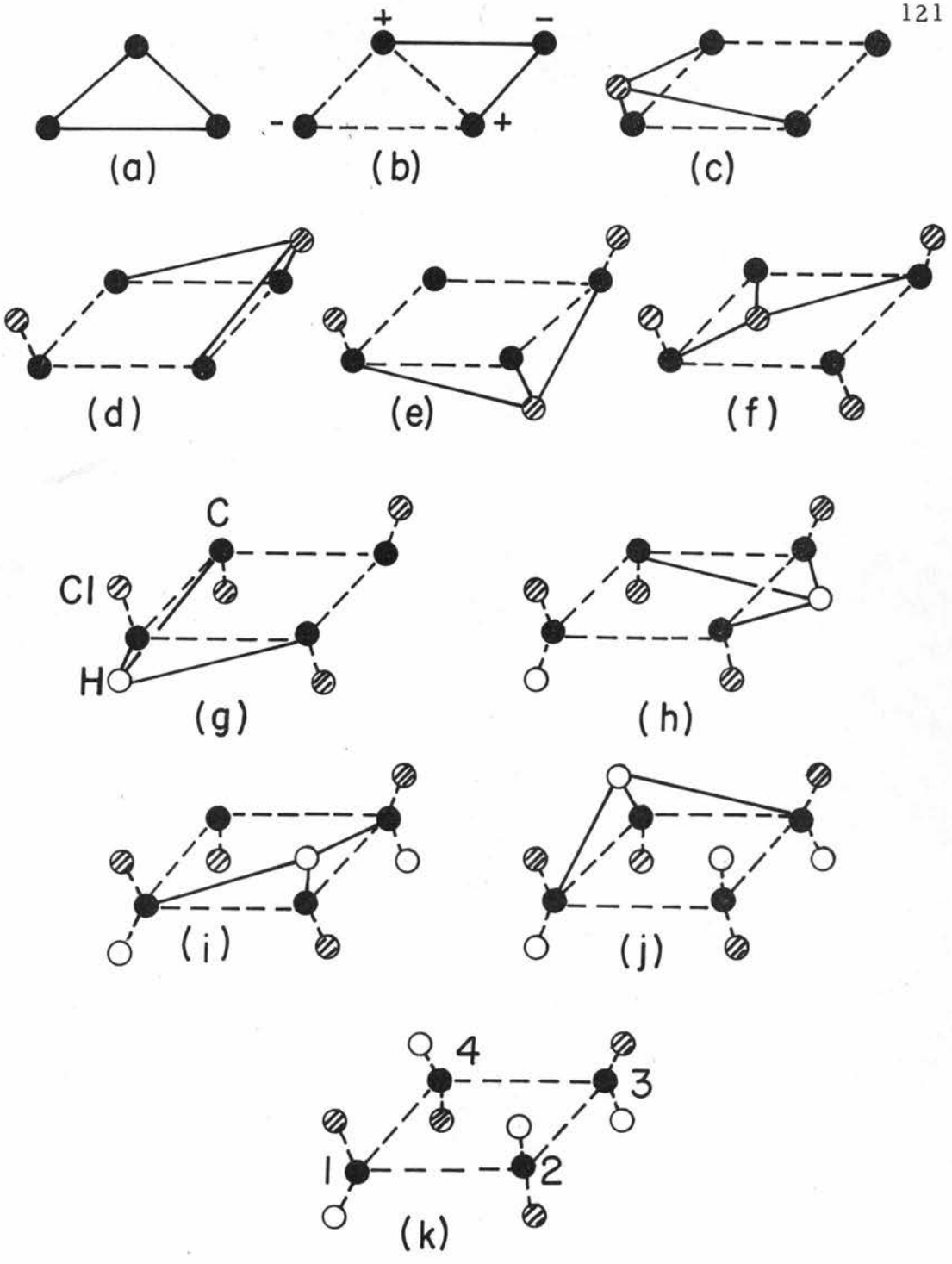

Figure 30. Construction of a rigid chlorinated cyclobutane molecule in a manner that will yield a minimum of redundancies for symetrically complete sets of internal coordinates.

symmetry operations of D_{2d}. Therefore the torsion set contains just one member. In step (c) the $\underline{r}^*$ set of eight carbon-chlorine bond stretchings and the $\underline{r}$ set of four carbon-chlorine stretchings is added. In step (g) the $\underline{r}^*$ set of eight carbon-hydrogen bond stretchings and the r set of four carbon-hydrogen stretchings is added bringing the total to 31 internal coordinates. This set will yield only one redundancy which appears in the set of two $\underline{R}$'s.

The benzene molecule shown in (k) of Figure 31 will be used for the final example. In step (a) of the same figure three carbon atoms are joined together. After applying the symmetry operations of the point group D_{6h} to the resulting three carbon-carbon stretchings, a set of six (carbon two-carbon four type) carbon-carbon stretchings (R's) is obtained. In step (b) a fourth carbon atom is added increasing the number of symmetrically complete sets by the addition of a set of six (carbon one-carbon two type) carbon-carbon stretchings (r's) and a set of six carbon-carbon-carbon-carbon torsions (τ_b's). In step (e) a set of 12 (carbon two-hydrogen one type) carbon-hydrogen stretchings (r*'s) and a set of six carbon-hydrogen-carbon-carbon torsions (τ_b's) are added, bringing the total to 36 internal coordinates. Only 3N-6 internal coordinates are required; therefore six redundancies are expected. Three of these are declared to be among the set of R's since only three of the six were used to construct the rigid molecule. Three of the redundancies will

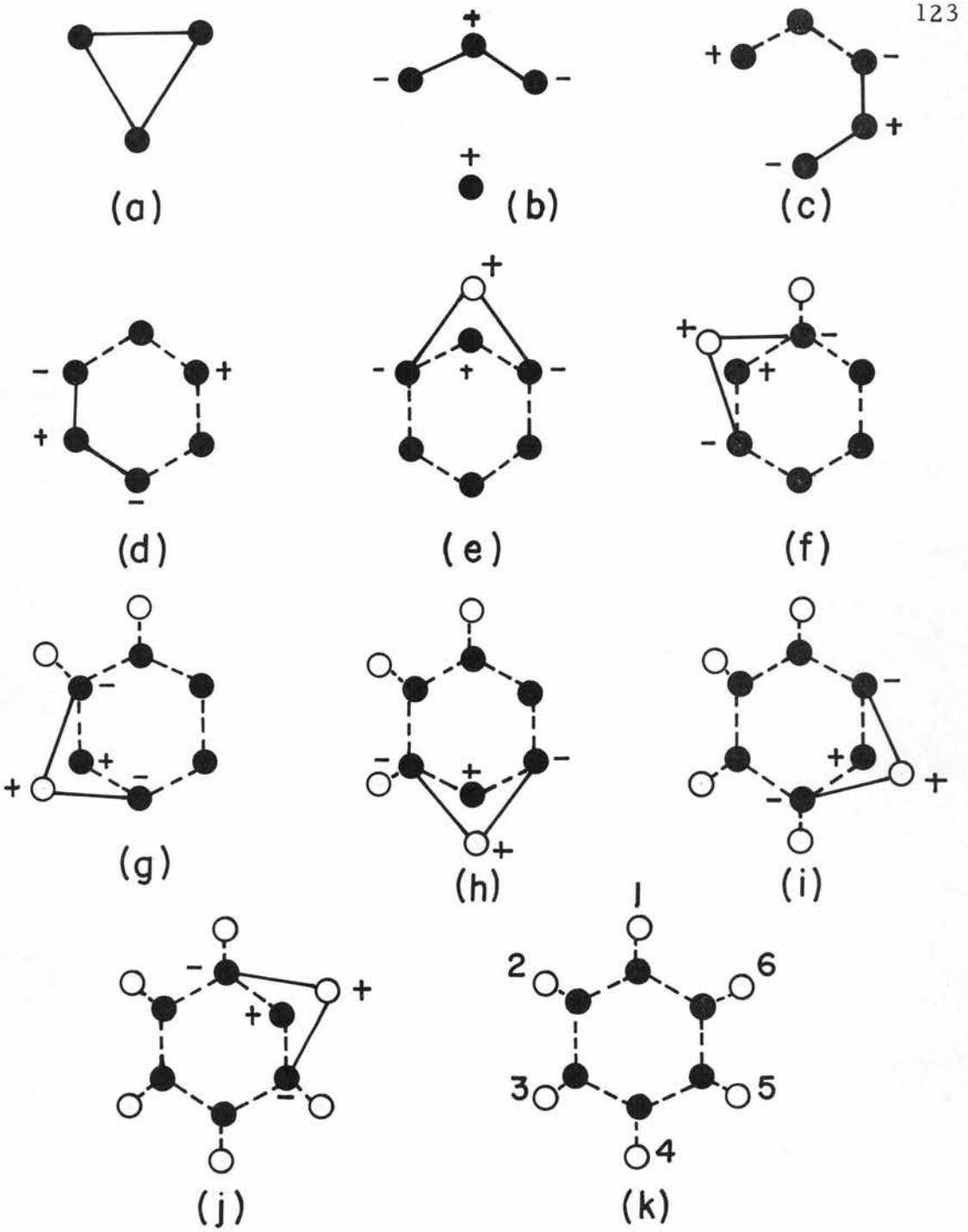

Figure 31. Construction of a rigid benzene molecule in a manner that will yield a minimum of redundancies for symmetrically complete sets of internal coordinates.

appear among the set of τ_a's because only three of the six were used for the construction of the rigid molecule.

Application of symmetry theory to the benzene molecule leads to the information listed in Table 14. Examination of this table indicates that the set of torsions, τ_a's, contributes two redundancies to the E_{1g} species and one to the A_{2u} species. The set of R's contributes one redundancy to the A_{1g} species and two to the E_{1u} species.

Table 14. Symmetry species for the vibrations of benzene.

D_{6h}	E	$2C_6$	$2C_3$	C_2	$3C_2'$	$3C_2''$	i	$2S_3$	$2S_6$	σ_h	$3\sigma_d$	$3\sigma_v$	$n^{(u)}$	n_T	n_R	n_v	$n^{(S)}$	$n^{(red)}$
A_{1g}	1	1	1	1	1	1	1	1	1	1	1	1	2	0	0	2	3	1
A_{2g}	1	1	1	1	-1	-1	1	1	1	1	-1	-1	2	0	1	1	1	0
B_{1g}	1	-1	1	-1	1	-1	1	-1	1	-1	1	-1	0	0	0	0	0	0
B_{2g}	1	-1	1	-1	-1	1	1	-1	1	-1	-1	1	2	0	0	2	2	0
E_{1g}	2	1	-1	-2	0	0	2	1	-1	-2	0	0	2	0	1	1	2	1
E_{2g}	2	-1	-1	2	0	0	2	-1	-1	2	0	0	4	0	0	4	4	0
A_{1u}	1	1	1	1	1	1	-1	-1	-1	-1	-1	-1	0	0	0	0	0	0
A_{2u}	1	1	1	1	-1	-1	-1	-1	-1	-1	1	1	2	1	0	1	2	1
B_{1u}	1	-1	1	-1	1	-1	-1	1	-1	1	-1	1	2	0	0	2	2	0
B_{2u}	1	-1	1	-1	-1	1	-1	1	-1	1	1	-1	2	0	0	2	2	0
E_{1u}	2	1	-1	-2	0	0	-2	-1	1	2	0	0	4	1	0	3	4	1
E_{2u}	2	-1	-1	2	0	0	-2	1	1	-2	0	0	2	0	0	2	2	0
$\chi_j^{(u)}$	36	0	0	0	-4	0	0	0	0	12	0	4						

Symmetrically Complete Internal Coordinate Set	Invarient Subgroups	Irreducible Representations
6R's	$C_{2v} = \{E, C_2', \sigma_v, \sigma_h\}$	$A_{1g} + E_{2g} + B_{1u} + E_{1u}$
6r's	$C_{2v} = \{E, C_2'', \sigma_d, \sigma_h\}$	$A_{1g} + E_{2g} + B_{2u} + E_{1u}$
12r*'s	$C_S = \{E, \sigma_h\}$	$A_{1g} + A_{2g} + 2E_{2g} + B_{1u} + B_{2u} + 2E_{1u}$
$6\tau_a$'s	$C_{2v} = \{E, C_2', \sigma_v, \sigma_h\}$	$B_{2g} + E_{1g} + A_{2u} + E_{2u}$
$6\tau_b$'s	$C_{2v} = \{E, C_2', \sigma_v, \sigma_h\}$	$B_{2g} + E_{1g} + A_{2u} + E_{2u}$

IV. SUMMARY

By a step-by-step process of constructing a rigid structure which fixes the positions of a molecule, a minimal kinematically complete set of internal coordinates is obtained. When additional internal coordinates are added to the above set in order to obtain symmetrically complete sets, these added coordinates are declared redundant. This facilitates the removal of redundancies from the symmetry $\underset{\sim}{G}$ matrix after factorization of the secular equation. A judicious choice of coordinates used in the kinematically complete set will lead to a reduction in redundancies when the set is expanded to obtain symmetric completeness.

Examples of chlorinated cyclobutane, cyclobutane, and benzene have been given to illustrate the method. The symmetrically complete sets of internal coordinates used to describe vibrations of these molecules contained one redundancy in the cases of chlorinated cyclobutane and cyclobutane, and six redundancies in the case of benzene.

BIBLIOGRAPHY

1. Anno, Tosinobu et al. Relations among bond order, force constant and bond length for the C-C and C-N bond in conjugated molecules. Bulletin of the Chemical Society of Japan 30:638-647. 1957.

2. Beckman Instruments, Inc. Scientific and Process Instruments Division. I. R. 7 Infrared spectrophotometer instruction manual. Fullerton, California, 1960. 83 p.

3. Bernstein, H. J. A relation between bond order and bond distance. Journal of Chemical Physics 15:284-289. 1947.

4. Born, Max and Maria Goppert-Mayer. Dynamische Gittertheorie der Kristalle. In: H. Bethe et al.'s Handbuch der Physik, vol. 24, 2. Berlin, Springer-Verlag, 1933. p. 623-795.

5. Brindley, George W. (ed.) X-ray powder data file. Philadelphia, American Society for Testing Materials, 1958. N.p. (Special Technical Publication No. 48-G) (Cards)

6. Bryant, James I. and George C. Turrell. Infrared spectra of the azide ion in alkali-halide lattices. Journal of Chemical Physics 24:1069-1077. 1962.

7. Cleveland, Forest F. Raman spectrum of an aqueous solution of potassium cyanate. Journal of the American Chemical Society 63:622-623. 1941.

8. Coker, Earl Howard. Interactions of sulfate ions in potassium chloride crystals. Ph. D. thesis. Corvallis, Oregon State University, 1963. 144 numb. leaves.

9. Coker, Earl Howard, J. C. Decius and A. B. Scott. Stretching vibrations of sulfate ion in potassium chloride: formation of M^{++} $SO_4^{=}$ pairs. Journal of Chemical Physics 35:745-746. 1961.

10. Decius, J. C. Complete sets and redundancies among small vibrational coordinates. Journal of Chemical Physics 17: 1315-1318. 1949.

11. Evjen, H. M. On the stability of certain heteropolar crystals. Physical Review 39:675-687. 1932.

12. Ewald, P. P. Die Berechnung optischer und elektrostatischer Gitterpotentiale. Annalen der Physik 64:253-287. 1921.

13. Fermi, Enrico. Uber den Ramaneffect des Kohlendioxyds. Zeitschrift fur Physik 71:250-259. 1931.

14. Goubeau, J. Raman-effect und das Konstitutions-problem des Cyanat-restes. (XXX. Mitteil) Zur Kenntnis der Pseudo-halogene. Berichte der Deutschen Chemischen Gesellschaft 68: 912-919. 1935.

15. Hendricks, Sterling B. and Linus Pauling. The crystal structures of sodium and potassium trinitrides and potassium cyanate and the nature of the trinitride group. Journal of the American Chemical Society 47:2904-2920. 1925.

16. Hirschfelder, Joseph O., Charles F. Curtise and R. Byron Bird. Molecular theory of gases and liquids. New York, Wiley, 1954. 1219 p.

17. Jenkins, H. O. Bond order-length relationships. Journal of the American Chemical Society 77:3168-3169. 1955.

18. Jonathan, N. B. H. Relations between force constants, bond orders, bond lengths, and bond frequencies for some nitrogen-oxygen bonds. Journal of Molecular Spectroscopy 4:75-83. 1960.

19. Ketelaar, J. A. A., C. Haas and J. van der Elsken. Infrared absorption spectra of bifluorides in alkali halide disks: The Formation of mixed crystals. Journal of Chemical Physics 24:624-625. 1956.

20. Kittel, Charles. Introduction to solid state physics. New York, Wiley, 1953. 396 p.

21. Kyropoulos, S. Ein Verfahren zur Herstellung groszer kristalle. Zeritschrift fur Anorganische und Algemaine Chemie 154:308-313. 1926.

22. Madelung, E. Das elektrische Field in Systemen von regelmassig angeordneten Punktladungen. Physikalische Zeitschrift 19:524-533. 1918.

23. Madelung, E. Molekulare Eigenschwingungen. Physikalische Zeitschrift 11:898-905. 1910.

24. Maki, Arthur George. The infrared spectrum of cyanate ion in different environments. Ph. D. thesis. Corvallis, Oregon State University, 1960. 151 numb. leaves.

25. Maki, Arthur George and J. C. Decius. Infrared spectrum of cyanate ion as a solid solution in a potassium iodide lattice. Journal of Chemical Physics 28:1003-1004. 1958.

26. Maki, Arthur George and J. C. Decius. Vibrational spectrum of cyanate ion in various alkali halide lattices. Journal of Chemical Physics 31:772-782. 1959.

27. Morgan, H. W. and P. A. Staats. Infrared spectra of dilute solid solutions. Journal of Applied Physics 33:364-366. 1962.

28. Mulliken, R. et al. Formulas and numerical tables for overlap integrals. Journal of Chemical Physics 2:1248-1267. 1949.

29. Nagakura, Saburo. On the electronic structure of the carbonyl and the amide groups. Bulletin of the Chemical Society of Japan 25:164-168. 1952.

30. Nagakura, Saburo and Toichiro Hosoya. Studies on the conjugated double bond systems. VIII. On the electronic structures of furan, pyrrole and thiophen. Bulletin of the Chemical Society of Japan 25:179-182. 1952.

31. Pal, N. N. and P. N. Sen Gupta. Raman effect in some organic and inorganic substances. Indian Journal of Physics 5: 13-34. 1930.

32. Pauling, Linus. The nature of the chemical bond. 2d ed. Ithaca, Cornell University Press, 1948. 450 p.

33. Pauling, Linus. The sizes of ions and their influence on the properties of salt-like compounds. Zeitschrift fur Kristallographie 67:377-404. 1928.

34. Price, W. C. et al. The influence of environment upon the spectra of molecules in liquids and crystals. Proceedings of the Royal Society of London, ser. A, 255:5-21. 1960.

35. Price, W. C., W. F. Sherman and G. R. Wilkinson. Infrared studies on polyatomic ions isolated in alkali-halide lattices. Spectrochimica Acta 16:663-676. 1960.

36. Rao, C. N. R., J. Ramachandran and P. S. Shankar. Characteristic infrared frequencies of inorganic cyanides, cyanates and thiocyanates. Journal of Scientific and Industrial Research 18B:169-170. 1959.

37. Sandorfy, Camille. Etude sur le role des substituants et des heteroatomes dans le noyau benzenique. Bulletin de la Societe Chimique de France, ser. 5, 16:615-626. 1949.

38. Somayajulu, G. R. Correlation of physical properties. VII. Dependence of force constant on electronegativity, bond strength, and bond order. Journal of Chemical Physics 28: 814-821. 1958.

39. Stimson, Miriam Michael and Marie Joannes O'Donnell. The infrared and ultraviolet absorption of cytosine and isocytosine in the solid state. Journal of the American Chemical Society 74:1805-1808. 1952.

40. Wagner, E. L. and Donald F. Hornig. The vibrational spectra of molecules and complex ions in crystals. III. Ammonium chloride and deutero-ammonium chloride. Journal of Chemical Physics 18:296-304. 1950.

41. Wheland, G. W. A quantum mechanical investigation of the orientation of substituents in aromatic molecules. Journal of the American Chemical Society 64:900-908. 1942.

42. Wheland, G. W. and Linus Pauling. A quantum mechanical discussion of orientation of substituents in aromatic molecules. Journal of the American Chemical Society 57:2086-2095. 1935.

43. Williams, Dudley. The infrared spectrum of potassium cyanate solution. Journal of the American Chemical Society 62: 2442-2444. 1940.

44. Wilson, E. Bright, Jr., John Courtney Decius and Paul C. Cross. Molecular vibrations. New York, McGraw-Hill, 1955. 388 p.

45. Wyckoff, Ralph W. G. Crystal structures. Vol. 2. New York, Interscience, 1960. N.p.

APPENDICES

APPENDIX I

Bond Orders of Ions and Molecules Isoelectronic to Cyanate

The purpose of this appendix is to present the "self-consistent" molecular orbital method described by Nagakura (29, 2) as it has been applied to the electronic structures of NCO^-, OCO, ONO^+, NNO, NNN^-, and $NCN^=$ and the results obtained from calculations performed with the aid of an ALWAC IIIE digital computer. A brief description of this method as applied to the cyanate ion will be given.

Cyanate ion is linear, hence the central carbon atom must be sp hybridized. It has two sp hybrids containing one electron each which are used for forming $p\sigma$ bonds. If an electron is gained by the nitrogen atom, the expected configuration for the ground state of cyanate ion is

$$NCO^- \Sigma: \quad (2s)^2(2s)^2(\sigma_g 2p)^2(\sigma_u 2p)^2(\pi_u 2p)^4(\pi_g 2p)^4$$

The initial M. O. approximation was based on the representation shown in Figure 32.

Experimental data for cyanate ion discussed by Jonathan (18) indicate the presence of delocalized π -bonding. The assumption was made that the σ -bonding may be described, to a good degree

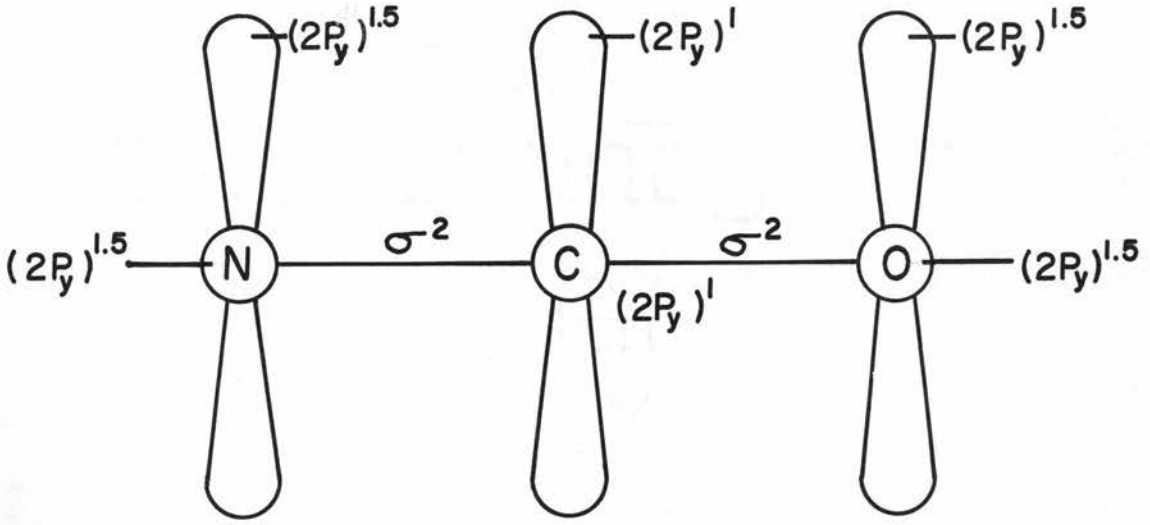

Figure 32. Electronic state of NCO^-.

of approximation, by means of two localized molecular orbitals, each of which describes the σ -bonding between either the nitrogen or the oxygen and the carbon atom. Assuming, therefore, that the contribution to the bond order from the σ -bonds is unity, only the eight π -electrons were considered.

The molecular orbital calculation was carried out for the y-plane with the assumptions that similar results are valid for the z-plane and that there is no interaction between the y- and z-planes.

The molecular π -orbitals ψ_j (j = 1, 2, 3) for the y-plane in the cyanate ion were taken as linear combinations of the $2p_y$ atomic orbitals of the carbon, nitrogen, and oxygen atoms which were denoted by $2p_{yC}$, $2p_{yN}$, and $2p_{yO}$, respectively. Using this approximation (LCAO) the following equation was obtained:

$$\psi_j = a_{j1}\,2p_{yN} + a_{j2}\,2p_{yC} + a_{j3}\,2p_{yO}\,, \quad j=1,2,3.$$

Neglecting the overlap integral S_{AB} between two atomic orbitals $2p_A$ and $2p_B$, the energies E of these molecular orbitals were given approximately as the solutions of the secular determinant

$$\begin{vmatrix} \alpha_N - E & \beta_{NC} & 0 \\ \beta_{NC} & \alpha_C - E & \beta_{CO} \\ 0 & \beta_{CO} & \alpha_O - E \end{vmatrix} = 0$$

where α_A is the coulomb integral of A-atom and β_{AB} is the exchange integral between adjacent atomic orbitals $2p_A$ and $2p_B$.

To evaluate the values of E, the following assumptions were made:

$$\alpha_A = \frac{\chi_A}{\chi_C}\alpha \quad (37, p.116)\,,$$

$$\beta_{AB} = \frac{S_{AB}}{S}\beta \quad (41)\,,$$

$$\alpha = 4.1\beta \quad (37, p.616)$$

where χ_A represents the electronegativeity of A atom, S is the overlap integral between atomic orbitals belonging to adjacent carbon atoms in benzene, and α and β are the coulomb and the exchange integrals in the same molecule. The overlap integrals necessary for the determination of the exchange integrals were obtained from a table of values given by Mulliken et al. (28, p. 1265). The

table is a function of two parameters p and t where

$$p = \frac{1}{2}(\mu_A + \mu_B)\frac{R_{AB}}{a_H}$$

and

$$t = \frac{1}{2}\frac{(\mu_A - \mu_B)}{(\mu_A + \mu_B)} .$$

R_{AB} is the bond distance between atom A and atom B, a_H is the Bohr radius for the hydrogen atom, and μ_A is a function related to the effective charge for atom A. A table of Slater μ values is listed by Mulliken et al. (28, p. 1250) for various atoms and ions. μ values were determined for each atom under consideration by extrapolation from the values listed in the table. Extrapolation was necessary in many cases because much of the time in this calculation the formal charge on an atom was not integral. The values listed in the table were only for neutral atoms or ions with unit charge.

Under these conditions, three values of E were evaluated in units of β. Then the values of a_{ij} were calculated for each value of E. The π-electron density of i-atom was then calculated by the equation (42)

$$q_i = 2\sum_j a_{ij}^2$$

where the summation extends over the molecular orbitals which are occupied in the ground state.

From the value of q_i thus obtained it was possible to determine the formal charge Q_i (in electron units) due to electrons in the y-plane of i-atom by subtracting q_i from the number of $2p_y$ electrons that the atom would normally hold in its neutral state. A similar change in charge was contributed by the z-plane.

Having determined the positive or negative formal charge, correction terms for the electronegativity χ_A and the overlap integral S_{AB} were considered. The correction to the electronegativity was made by the method of Pauling (32, p. 64-66). Pauling lists electronegativity values for various atoms with formal charge zero. He indicates that an estimate can be made of the effect of formal charge on the electronegativity values in the following way. The increase in effective nuclear charge acting on the valence electrons for a series of atoms such as C, N, O leads to an increase in electronegativity. The effective nuclear charge is the actual nuclear charge less the screening effects of the electrons. Since the screening effect of one valence electron for another is about 0.4 electron units, the increase in effective nuclear charge from C to N is 1.0 (the increase in actual nuclear charge) less 0.4 (the screening effect due to the additional electron), or 0.6. However, the increase in effective nuclear charge from C to C^+ is 0.4 due to the loss of one electron, hence the loss of its screening effect. Thus the increase in effective charge from C to N is 0.6 electron units, while the

increase in effective charge from C to C^+ is only 0.4. The increase in effective charge due to a unit positive formal charge is two-thirds the amount of increase in effective charge when one moves to the next atom to the right in the periodic table. Since the electronegativity depends upon the effective nuclear charge, a unit positive formal charge increases the electronegativity value for an atom by about two-thirds of the distance to the next atom to the right in the periodic table, and a negative formal charge similarly decreases the electronegativity value.

Corrections for the overlap integral S_{AB} were made by re-evaluating the μ values due to the change in formal charge on the atoms A and B and again referring to the table of Mulliken et al. (28, p. 1250). Thus it was possible to calculate new values of α_A and β_{AB}, using these new values to determine E, q_i and Q_i, and again repeating the procedure until the final results of these quantities were self-consistent.

When a self-consistent electron distribution was finally obtained, the bond orders were calculated in the usual manner according to the equation

$$n_{ij} = 1 + 4 \sum_k a_{ki} a_{kj} , \quad k = 1, 2.$$

From bond length-bond order curves plotted by Anno et al. (1) for CN bonds, from bond order-force constant and force constant-bond

length curves plotted by Jonathan (18) for NO bonds, from the relation (3)

$$R_{CO} = 1.435\left[\frac{2}{3} + \frac{1}{3}\left(\frac{1}{3}\right)^{\frac{p}{2}}\right], \quad p = n-1$$

for CO bonds, or from the relation (17)

$$R_{NN} = \frac{1}{\sqrt{0.263 + 0.193\,n}}$$

for NN bonds, corrections were made for the bond lengths of the structure under consideration from the bond orders previously calculated. Using the new bond lengths the electron distribution was recalculated. This procedure was continued until self-consistency was obtained for both electron distribution and bond length.

Since the program of this procedure written for the ALWAC IIIE computer may be applied to any triatomic molecule or ion where only two bonds are considered, a description will be given for its operation.

Place the "proceed-normal-start" switch in "proceed" or "start" position. Place the data tape in the reader. Set jump 1 to (1) if it is desired to type out the roots to the cubic equation. Clear and type 4f00 to start the routine. As the data tape is being accepted set jump 1 to (0). Set jump 2 to (1) if type-outs of the trial solutions (Newton's Method) to the cubic equation with each iteration are desired. The formal charges on each of the three atoms is typed out

with each major iteration of the routine. When self-consistency has been attained the parameters calculated in the final iteration are typed out along with the bond orders and some of the input data. The output symbols which are not self-explanatory have the following meanings: "R" refers to the bond length between two atoms, " X°'s " refers to the Electronegativity of the neutral atoms, " U°'s " refers to the μ values for the neutral atoms, " U^{*}'s " refers to the values for atoms carrying formal charges obtained in the last iteration, " ρ's " refers to the values calculated from the equation

$$\rho = \frac{1}{2}(\mu_A + \mu_B)\frac{R_{AB}}{a_H}$$

" a's: " refers to the coefficients of E^3, E^2, E, and a constant, respectively, which are obtained upon expansion of the secular determinant, " E's: " refers to the roots of the cubic equation obtained from the expansion of the secular determinant, " a(ji)'s: " refers in the first line to the squares of the coefficients, and in the second line to the coefficients, in the equation

$$\psi_j = a_{j1}2p_{yA} + a_{j2}2p_{yB} + a_{j3}2p_{yC}, \quad j = 1, 2, 3.$$

The last information to be typed out is the question "next molecule?" and input is requested. Set jump 2 to (1) and insert a new data tape. Type a space and the program will recycle.

The data tapes contain the following information: the molecule followed by two carriage returns, S table 1 followed by S table 2, R_1 and R_2, formal charges 1, 2, and 3, neutral electronegativities for atoms 1, 2, and 3, neutral μ_1, μ_2, μ_3, number of p electrons on atoms 1, 2, and 3. Each S table contains 16 S values for p varying at intervals of 0.2 from 6.0 down to 3.0. Table 15 lists the final input data in the same order as it appeared on the data tapes for the six structures treated in this discussion. The final parameters and bond orders are given in Table 16 in the same format as they were typed out by the computer.

From this calculation, the bond orders of the NO bonds in ONO^+ and NNO were 2.41 and 1.83, respectively. Jonathan (18) using the same general method obtained the values of 2.34 and 1.80 for the same structures. The differences have not been accounted for.

Table 15. Input data as it appears on the data tape for the bond order calculation.

NCN

```
.089 .101 .114 .129 .146 .164 .184 .207 .231 .258 .287 .318 .352 .389 .427 .468
.089 .101 .114 .129 .146 .164 .184 .207 .231 .258 .287 .318 .352 .389 .427 .468
1.22 1.22 -1.05452 .10903 -1.05452 3 2.5 3 1.95 1.625 1.95 3 2 3
```

NNN

```
.089 .101 .114 .129 .146 .164 .184 .207 .231 .258 .287 .318 .352 .389 .427 .468
.089 .101 .114 .129 .146 .164 .184 .207 .231 .258 .287 .318 .352 .389 .427 .468
1.178 1.178 -.75708 .51416 -.75708 3 3 3 1.95 1.95 1.95 3 3 3
```

NCO

```
.089 .101 .114 .129 .146 .164 .184 .207 .231 .258 .287 .318 .352 .389 .427 .468
.089 .101 .114 .129 .146 .1635 .1835 .206 .230 .2565 .2855 .3165 .350 .386 .4235 .464
1.173 1.258 -.61279 .30944 -.69665 3 2.5 3.5 1.95 1.625 2.275 3 2 4
```

OCO

```
.089 .101 .114 .129 .146 .1635 .1835 .206 .230 .2565 .2855 .3165 .350 .386 .4235 .464
.089 .101 .114 .129 .146 .1735 .1835 .206 .230 .2565 .2855 .3165 .350 .386 .4235 .464
1.206 1.206 -.54682 1.09364 -.54682 3.5 2 3.5 2.275 1.625 2.275 4 2 4
```

ONO

```
.089 .101 .114 .129 .146 .164 .184 .207 .231 .258 .287 .318 .352 .389 .427 .468
.089 .101 .114 .129 .146 .164 .184 .207 .231 .258 .287 .318 .352 .389 .427 .468
1.150 1.150 -.07322 1.14644 -.07322 3.5 3 3.5 2.275 1.95 2.275 4 3 4
```

NNO

.089 .101 .114 .129 .146 .164 .184 .207 .231 .258 .287 .318 .352 .389 .427 .468
.089 .101 .114 .129 .146 .164 .184 .207 .231 .258 .287 .318 .352 .389 .427 .468
1.118 1.191 -.12069 .71429 -.59360 3 3 3.5 1.95 1.95 2.275 3 3 4

Table 16. Final parameters and bond orders obtained from the molecular orbital calculations.

NCN

-1.05452 .10903 -1.05452

	atom N	atom C	atom N	
formal charges:	-1.05452	.10904	-1.05452	
R =	1.220	1.220		
X^o's:	3.00000	2.50000	3.00000	
U^o's:	1.95000	1.62500	1.95000	
U*'s:	1.76546	1.64408	1.76546	
p's:	3.93082	3.93082		
alphas:	4.34353	4.15960	4.34353	
betas:	1.19089	1.19089		
a's:	1.00000	-12.84666	52.16453	-66.15597
E's:	2.56489	4.34353	5.93825	
$a(1_i)$'s:	.26363	.47274	.26363	
	.51345	.68756	.51345	
$a(2_i)$'s:	.50000	.00000	.50000	
	.70711	.00000	-.70711	
no. of p electrons:	3.00000	2.00000	3.00000	
bond orders:	2.41211	2.41211		

next molecule?

NNN

-.75708 .51416 -.75708

	atom N	atom N	atom N	
formal charges:	-.75708	.51416	-.75708	
R =	1.178	1.178		
X^o's:	3.00000	3.00000	3.00000	
U^o's:	1.95000	1.9500	1.95000	
U*'s:	1.81751	2.03998	1.81751	
p's:	4.29416	4.29416		
alphas:	4.50613	5.20107	4.50613	
betas:	.98115	.98115		
a's:	1.00000	-14.21333	65.25331	-96.93310
E's:	3.42320	4.50613	6.28400	
$a(1_i)$'s:	.18927	.62146	.18927	
	.43505	.78833	.43505	
$a(2_i)$'s:	.5000	.00000	.50000	
	.70711	.00000	-.70711	
no. of p electrons:	3.00000	3.00000	3.00000	
bond orders:	2.37185	2.37185		

next molecule?

NCO

-.61279 .30944 -.69665

	atom N	atom C	atom O	
formal charges:	-.61277	.30944	-.69667	
R =	1.173	1.258		
X^o's:	3.00000	2.50000	3.50000	
U^o's:	1.95000	1.62500	2.27500	
U*'s:	1.84276	1.67915	2.15309	
p's:	3.90396	4.55576		
alphas:	4.58501	4.26916	5.35916	
betas:	1.20755	.84523		
a's:	1.00000	-14.21333	64.85249	-93.81083
E's:	3.02695	5.05291	6.13348	
$a(1_i)$'s:	.21722	.35718	.42560	
	.46606	.59765	.65238	
$a(2_i)$'s:	.43597	.06546	.49857	
	.66028	.25584	-.70609	
no. of p electrons:	3.00000	2.00000	4.00000	
bond orders:	2.78989	1.83698		

next molecule?

OCO

-.54682 1.09364 -.54682

	atom O	atom C	atom O	
formal charges:	-.54682	1.09364	-.54682	
R =	1.206	1.206		
X^o's:	3.50000	2.00000	3.50000	
U^o's:	2.27500	1.62500	2.27500	
U*'s:	2.17931	1.81639	2.17931	
p's:	4.55373	4.55373		
alphas:	5.44107	3.87786	5.44107	
betas:	.84621	.84621		
a's:	1.00000	-14.76000	70.37252	-107.01261
E's:	3.23011	5.44107	6.08882	
$a(1_i)$'s:	.38671	.22659	.38671	
	.62186	.47601	.62186	
$a(2_i)$'s:	.50000	.00000	.50000	
	.70711	.00000	-.70711	
no. of p electrons:	4.00000	2.00000	4.00000	
bond orders:	2.18405	2.18405		

next molecule?

ONO

-.07322 1.14644 -.07322

	atom O	atom N	atom O	
formal charges:	-.07322	1.14644	-.07322	
R =	1.150	1.150		
X^O's:	3.50000	3.00000	3.50000	
U^O's:	2.27500	1.95000	2.27500	
U*'s:	2.26219	2.15063	2.26219	
p's:	4.79558	4.79558		
alphas:	5.69997	5.54672	5.69997	
betas:	.73803	.73803		
a's:	1.00000	-16.94667	94.63263	-174.00182
E's:	4.57681	5.69997	6.66989	
$a(1_i)$'s:	.26830	.46339	.26830	
	.51798	.68073	.51798	
$a(2_i)$'s:	.50000	.00000	.50000	
	.70711	.00000	-.70711	
no. of p electrons:	4.00000	3.00000	4.00000	
bond orders:	2.41042	2.41042		

next molecule?

NNO

-.12069 .71429 -.59360

	atom N	atom N	atom O	
formal charges:	-.12069	.71429	-.59360	
R =	1.118	1.191		
X^O's:	3.00000	3.00000	3.50000	
U^O's:	1.95000	1.95000	2.27500	
U*'s:	1.92888	2.07500	2.17112	
p's:	4.23010	4.77895		
alphas:	4.85402	5.31048	5.41550	
betas:	1.01574	.74568		
a's:	1.00000	-15.58000	79.23525	-131.30989
E's:	3.88391	5.22279	6.47330	
$a(1_i)$'s:	.20815	.52898	.26287	
	.45623	.72731	.51271	
$a(2_i)$'s:	.32203	.04245	.63553	
	.56747	.20602	-.79720	
no. of p electrons:	3.00000	3.00000	4.00000	
bond orders:	2.79493	1.83464		

next molecule?

Program

```
0320 41
  00000000  00000000  00000000  00000000
  00000000  00000000  00000000  00000000
  00000000  00000000  00000000  00000000
  00000000  00000000  00000000  00000000
  00000000  00000000  00000000  00000000
  00000000  00000000  00000000  00000000
  00000000  00000000  00000000  00000000
  00000000  00000000  00000000  00000000
  00000000

0320 4e
  7903f7a2  3000a507  00000000  5b680000
  290ef305  60204825  00000000  00000000
  4907f3g2  30000e00  00000000  00030000
  7907f785  179c7922  00000000  00000000
  7903f7a2  41244924  00000000  00000000
  8372290e  c5228b72  00000000  00000000
  7907a507  814f1100  00000000  00000000
  570ba106  52051680  52051600  52051600
  e179d855

0320 4f
  1308d902  871e8541  87135b03  00100000
  81501100  570c5a20  9d600e00  05100500
  d9011104  9d604844  a1108705  00000000
  00040000  17858371  9d60871f  00000000
  00000000  1319d902  a3105b07  00000000
  00000000  81551116  9d601102  00000000
  00000000  d9011115  00000000  00000000
  001e0000  001a0000  00160000  00120000
  16be8981
```

```
0320 50
 8370871e        9d604848        5b3c9d60        4045e731
 57205b20        179c5730        7921f781        604b4854
 9d604860        5b349d60        179d7925        17035738
 17848d80        484b1709        f7815730        78536054
 85415738        57305b24        4045e729        3000e735
 5b249d60        9d60484e        60483000        3000e642
 48421714        1791871f        e72d4851        4856170f
 57285b2c        57307845        17125730        57388151
 7cd87e80

0320 51
 79214956        c3587856        3000e723        8582130b
 7939613d        49597828        5758485d        81521187
 64561d1c        61563600        17008741        792a4946
 63216056        79570e00        57307851        57387846
 49577956        eb3dc55a        4863178e        0e00eb2b
 61224956        8780787f        5738785d        c44c178f
 79571184        66803000        48661796        5738792b
 63214957        e75a647f        8f828d81        494c8153
 9fd393d9

0320 52
 3000e644        49494140        81551182        00000000
 61484948        e745a125        00000000        0000792a
 171f5738        e7456149        00000000        49465730
 4046e646        49494140        00000000        7843a503
 a5046548        e741a125        00000000        65474947
 4948170c        e7426549        00000000        170f7940
 4142e744        49491102        00000000        49435730
 a125e744        00000000        00000000        7843a504
 b30c99e7

0320 53
 784ca121        e74b3000        3000e72a        61484948
 e64c654c        e740a103        61474947        171a5738
 494c1700        61474947        171d7947        4046e646
 794ca701        414ae74a        0e00eb4c        a5046548
 494c5730        3000e742        c5477940        4948170b
 7843a503        a1036147        49435730        414ae744
 65474947        49475738        7843a504        3000e72e
 1714414b        404ce646        3000e644        30008154
 e04c1674
```

```
0320 54
  e7426548        37444949        81551182        00000000
  4948414b        4140e745        00000000        00000000
  e7453000        a125e745        00000000        00000000
  e72e3000        61494949        00000000        00000000
  e7406548        4140e741        00000000        00000000
  0e00eb4c        a125e742        00000000        00000000
  c5484142        65490e00        00000000        00000000
  e744a125        eb4cc549        00000000        00000000
  80124e02

0320 55
  179b5744        4146e345        119e8d82        78430e00
  17088156        c547614c        87418371        4946c547
  784f0e00        0e00bd47        5720784a        7844494c
  4946c547        4946c547        4864178a        9d1c170b
  7850494c        9f000000        8f838583        79464948
  9d1c1710        871f7945        5721c344        79474949
  79468156        5b229d60        290e4945        57214043
  4147e745        7923f781        15155744        e6294850
  7c602302

0320 56
  67524d8c        c54b794a        794a1112        871f7945
  3000118c        414bab00        51251f1e        5b229d60
  794f0e00        49503800        79536545        7929f785
  119ca500        1d814952        4945119a        7923f781
  49531106        79484149        414ba104        57447945
  00000000        ab00494a        eb507951        48575a43
  00000000        c54b3800        11008155        40436c2d
  4147494a        1d114951        d1031113        00008157
  70fd3876

0320 57
  4d042800        48441785        8d838582        a501644f
  a300e900        118d4142        8758572f        49533000
  7844c444        e7456143        8160118a        e7534952
  30001780        49435744        644f4951        c553497e
  57441794        17161b15        3000111a        c57f7950
  11916c2f        87827956        81551196        41519d60
  4d1c7945        496d7955        e7514950        4954c555
  a5006044        496e8f82        c5517942        00008159
  f2af99f8
```

```
0320 58
  497ac57b        e37a6177        8d95856a        00000000
  417fe77b        9f000000        11400000        00000000
  417ee37b        00000000        00000000        00000000
  49773200        497ac57b        00000000        00000000
  417fe37a        797e617a        00000000        00000000
  0e00a120        0e00bd7f        00000000        00000000
  bd774977        bd7b9f00        00000000        00000000
  3200417e        00000000        00000000        00000000
  04ae3c53

0320 59
  19083000        79544155        c57f7956        3000e65c
  111b815a        9d6d4956        41579d6d        497ec57f
  7944a501        c5577945        4956c557        79504151
  497e3000        a501497e        79544155        9d62485a
  e77e497e        3000e77e        497ec57f        6530665c
  c57f7952        497ec57f        79564157        485e815a
  41539d60        79504151        9d62485c        d9201908
  497ec57f        9d60497e        4144e744        d9101184
  90f0ccff

0320 5a
  795a4961        49658d82        3000e731        784c4865
  795c1114        85815721        110a8157        17038f81
  7927485a        784e4869        a3016449        794d5132
  485e2800        17095721        87611160        1f13815b
  485c111b        7845486c        484f3000        57330000
  49627959        17118f84        e731604c        815b119f
  4963795b        85845721        484c171d        17868741
  4964795d        78436046        87815721        79584960
  bff8c4f8

0320 5b
  0e00a11e        48571798        f7857921        f7848581
  87059d60        57af4057        f7857923        57350000
  a31e4855        e7316134        f7857921        815c1100
  179f8160        48571785        f7857924        00000000
  4054e655        8d848372        f7847925        83708581
  48571710        871f7920        f7857926        81501199
  572f4051        f7847921        f7857927        00000000
  e6526057        f7857922        f7847928        00007846
  79aed4d3
```

0320 5c

78455b36	7929f781	f7811719	1796792a
9d607929	1798792a	792af781	f781792f
f7811700	f781792c	792ef785	f785792d
792af791	f785792d	792df781	f7817928
792bf785	f7817928	7928f784	f7845735
7929f781	f7845735	5735784b	815d1100
57377842	78485b36	5b399d60	00000000
5b389d60	9d607929	7929f781	00000100
2e5b3f9d			

0320 5d

78545b39	7929f781	f7811719	f7817933
9d697929	1798792a	792af781	f7857928
f7811700	f7817931	7932f785	f784573b
792af781	f785792d	7928f784	8582784a
7930f785	f7817928	5737785d	5a409d60
7928f784	f7845735	5b399d60	7929f781
57377856	78515b39	7929f781	178f792a
5b3a9d60	9d607929	1792792a	f781815e
a46cc4d0			

0320 5e

83737923	7925f785	7920f781	f7817922
f7857922	7926f781	57327852	f7845732
f7845732	7922f784	5b349d60	78465b34
81601100	57328584	7920f781	9d607920
9d607920	78435b34	17867921	f781170b
f781170c	9d607920	f7817927	7921f781
7921f781	f7811711	f7857925	7920f781
7924f785	7921f781	f7857926	5732815f
ac4e3e0b			

0320 5f

78555b34	7922f784	f7817922	7930f785
9d607920	57327849	f7845735	7931f783
f7811700	5b339d60	78575b36	7921f781
7921f781	7920f781	9d607920	f1811517
7928f785	17857921	f781170a	1b931113
7929f784	f781792c	7921f781	814e1100
792af785	f785792d	792ef785	00000000
792bf784	f7857926	792ff785	00000000
6f656a3b			

```
0320 60
  85837857        9d074951        7940a501        315e1110
  5b330000        416e7960        8157110e        c558a501
  815e1110        5b529d07        0000138e        67581d13
  00000000        49527962        1102414a        392e9f00
  1117416d        5b549d07        e64fa301        38009f00
  79605b4f        4954572f        65444944        d39b8782
  9d07494f        815b1110        414be64f        11907954
  79625b51        49541195        a3016445        2e00111d
  134e209b

0320 61
  49577924        79576728        00000000        00000000
  3400532f        116c0000        00000000        00000000
  1f617957        00000000        00000000        00000000
  a702664c        00000000        00000000        00000000
  11120000        00000000        00000000        00000000
  00000000        00000000        00000000        00000000
  00000000        00000000        00000000        00000000
  00000000        00000000        00000000        00000000
  df91131f

0320 62
  495ac55b        497ec57f        00000000        00000000
  797e417f        38001dd8        00000000        00000000
  495ec55f        496f797e        00000000        00000000
  795a415b        417fa102        00000000        00000000
  ab00497a        eb7a796f        00000000        00000000
  38001d4c        67734dd9        00000000        00000000
  4973795e        3200a500        00000000        00000000
  415fab00        89959f00        00000000        00000000
  0a57a1dd

0320 70
  00200000        00000000        00010000        80000000
  001c0000        5a000000        00100000        00000000
  00060000        55555555        40000000        80000000
  001e0000        d1eb851f        20000000        00000000
  00030000        16666666        00000000        00000000
  001d0000        f1eb0000        00000000        00000000
  00020000        05999999        00000000        00000000
  011e0500        00666666        00000000        00000000
  f14345dc
```

```
0320 71
  00040000        00030000        011c0400        5a000000
  00000000        00000010        30000000        20000000
  10000000        53df7dd0        001a0000        00160000
  00120000        00060000        000a0000        00020000
  40000000        80000000        00008000        00060000
  02000000        00000000        00000000        00000000
  00000000        00000000        00000000        00000000
  00000000        00000000        00000000        00000000
  d15d01e1

0320 72

  55600000        159c9100        03600000        05600000
  07680000        1f24f114        42018894        4381d900
  53fd1600        58000000        5a000000        53380250
  53b838d0        64000000        53a038d0        53a778d0
  4b4e3464        150ca894        16766564        154e3464
  00000000        00030000        011e0500        00020000
  011c0300        011d0500        01190500        00040000
  011e0500        011a0500        01160500        01120500
  77fa832c

0320 73
  58000000        5a000000        53fd1600        52763464
  15493402        254e18d0        64000000        15493404
  4727e048        1e04a000        1d09c666        4f247900
  17246680        4939a74e        4676f980        45242718
  6909d48c        516d4000        00030000        011c0500
  011e0500        00020000        01190500        00000000
  00000000        00000000        00000000        00000000
  00000000        00000000        00000000        00000000
  8776dcde
```

```
3a00
41 00000000
42 d8ff1db6
43 f2f458fd
44 f76e091c
45 a2c2415e
4e e179d855
4f 16be8981
50 7cd87e80
51 9fd393d9
52 b30c00e7
53 e04c1674
54 80124e02
55 7c602302
56 70fd3876
57 f2af99f8
58 04ae3c53
59 90f0ccff
5a bff8c4f8
5b 79aed4d3
5c 2e5b3f9d
5d a46cc4d0
5e ac4e3e0b
5f 6f656a3b
60 134e209b
61 df91131f
62 0a57a1dd
70 f14345dc
71 d15d01e1
72 77fa832c
73 8776dcde
```

APPENDIX II

Calculation of Coulombic Potential Derivatives in a Sodium Chloride Type Lattice

In a sodium chloride type lattice the electrostatic potential at a point P in a unit cell with a vacancy at the center is given by the equation

$$V_c = -e \sum_{h,k,l}{}' \frac{(-1)^{h+k+l}}{R(h,k,l)}$$

where the prime over the summation symbol means that the term with h = k = l = 0 is omitted from the sum. R(h, k, l) is given by the relation

$$R(h,k,l) = a\left[\left(h - \frac{r}{a}\sin\theta\cos\phi\right)^2 + \left(k - \frac{r}{a}\sin\theta\sin\phi\right)^2 + \left(l - \frac{r}{a}\cos\theta\right)^2\right]^{\frac{1}{2}}$$

The parameter r is the distance between point P and the vacancy point at (0, 0, 0), and a is the equilibrium nearest neighbor distance of the lattice. The angles θ and ϕ are the usual spherical polar coordinate angles in which the z-axis is directed parallel to an edge of the unit cell and passes through the vacancy lattice point.

The first derivative of the potential with respect to r is

$$\frac{\partial V_c}{\partial r} = -ea \sum_{h,k,l}{}' \frac{(-1)^{h+k+l}}{R(h,k,l)^3} \left[\left(h - \frac{r}{a}\sin\theta\cos\phi\right)\sin\theta\cos\phi \right.$$

$$\left. + \left(k - \frac{r}{a}\sin\theta\sin\phi\right)\sin\theta\sin\phi + \left(l - \frac{r}{a}\cos\theta\right)\cos\theta \right]$$

and the second derivative is

$$\frac{\partial^2 V}{\partial r^2} = e \sum_{h,k,l}{}' \frac{(-1)^{h+k+l}}{R(h,k,l)^3} \left\{ 1 \right.$$

$$\frac{-3a^2}{R(h,k,l)^2} \left[\left(h - \frac{r}{a}\sin\theta\cos\phi\right)\sin\theta\cos\phi \right.$$

$$\left. \left. + \left(k - \frac{r}{a}\sin\theta\sin\phi\right)\sin\theta\sin\phi + \left(l - \frac{r}{a}\cos\theta\right)\cos\theta \right]^2 \right\}$$

If point P lies on the body diagonal of the unit cell, then

$\sin\theta = \sqrt{\frac{2}{3}}$, $\cos\phi = \frac{1}{\sqrt{2}}$ and the second derivative simplifies to the expression

$$\frac{\partial^2 V_c}{\partial r^2} = \frac{e}{a^3} \sum_{h,k,l}{}' \frac{(-1)^{h+k+l}}{\left[(h-\tau)^2 + (k-\tau)^2 + (l-\tau)^2\right]^{\frac{3}{2}}} \left\{ 1 \right.$$

$$\left. \frac{-(h+k+l-3\tau)^2}{(h-\tau)^2 + (k-\tau)^2 + (l-\tau)^2} \right\}$$

where $\tau = \frac{r}{a\sqrt{3}}$.

If point P lies on a cell edge which passes through the vacancy lattice point, then $\sin\theta = 1$, $\cos\phi = 1$, so that the first derivative

simplifies to the expression

$$\frac{\partial V_c}{\partial r} = -\frac{e}{a^2} \sum_{h,k,l}{}' \frac{(-1)^{h+k+l}(h-\xi)}{[(h-\xi)^2+k^2+l^2]^{3/2}}$$

and the second derivative simplifies to

$$\frac{\partial^2 V_c}{\partial r^2} = \frac{e}{a^3} \sum_{h,k,l}{}' \frac{(-1)^{h+k+l}}{[(h-\xi)^2+k^2+l^2]^{3/2}} \left\{ 1 - \frac{3(h-\xi)^2}{(h-\xi)^2+k^2+l^2} \right\}$$

where $\xi = \frac{r}{a}$.

Neglecting the coefficient $\frac{e}{a^3}$, the summations for the first derivative along the cell edge and the second derivative both along the body diagonal and along the cell edge have been calculated using an ALWAC IIIE digital computer. Although a list of values for the summation calculated with r or ξ varying at 0.05 intervals is given in Table 17, the program may be used to determine values at much smaller intervals, so a description of its operation will be given.

Store the program in the computer, then clear and type 5e00 for the first derivative taken along the cell edge, or type 5a00 for the second derivative taken along the body diagonal, or type 5c00 for the second derivative taken along the cell edge. The computer will request an input. Type in the value desired for r or ξ between 0

Table 17. Summations for coulombic potential derivatives.

γ or ξ	$\sum'$ 1st deriv. cell edge	$\sum'$ 2nd deriv. body diagonal	$\sum'$ 2nd deriv. cell edge
0.00	0.000	0.000	0.000
0.05	-0.002	-0.212	0.108
0.10	-0.014	-0.817	0.433
0.15	-0.049	-1.693	0.983
0.20	-0.117	-2.639	1.776
0.25	-0.231	-3.375	2.842
0.30	-0.406	-3.595	4.234
0.35	-0.661	-3.067	6.041
0.40	-1.020	-1.679	8.411
0.45	-1.516	0.506	11.592
0.50	-2.199	3.306	15.999
0.55	-3.149	6.518	22.381
0.60	-4.492	10.058	32.104
0.65	-6.458	14.177	47.895
0.70	-9.478	19.887	75.687
0.75	-14.452	30.017	129.895
0.80	-23.560	52.722	252.251
0.85	-43.138	117.774	595.646
0.90	-98.903	388.013	2007.434
0.95	-402.154	3116.064	16264.720

and 1.0 and then type a space. Again the computor will request an input. In this program the summation extends from h = -n, k = -n, l = -n to h = n, k = n, l = n. The value to be typed into the computer is the integer n. This value will then be used to determine over how much of the lattice the summation will be carried. After typing in a value for n, type a space. The computer will start calculating and eventually type out the answer . The program is resetting so that a new value for τ or ξ may be typed in after receiving the result for the previous input data. For values of τ or ξ near 1.0 the computer will overflow before typing out an answer due to the large numerical value of the summation. If n = 1, the calculation requires about 30 seconds; if n = 4, the calculation requires 13 or more minutes. For a value of n = 2, the calculation was accurate out to thousandths, so this value for n was used in calculating the information given in Table 17.

Program

```
0320 5a
  835b871e    492f4933    a310492f    9d265b2f
  57365b2e    57237840    79335b2f    9d359d35
  9d60483c    673a4937    9d354937    9d35612b
  17848705    9d26612f    9d266532    492b5723
  793b2e00    49af7937    4937793d    793b6640
  493d493e    61334933    613e613f    19a87840
  493f2800    1785792f    a11011b8    2e004840
  492b2800    a1109d60    79322e00    17131120
  00111337

0320 5b
  871f5b27    00000000    30009f00    00030000
  792b9d60    00000000    3000e737    05100500
  11807840    00000000    a3109f00    00000000
  61324840    00000000    00010000    00000000
  793d733e    79321103    00010000    00000000
  733f199c    0e00a110    00020000    00000000
  118f0400    e9001122    00000000    00000000
  1f31111e    00000000    00000000    00000000
  08a54870

0320 5c
  835d871e    673a4933    792fa110    613e613f
  57365b2e    49379d26    9d60a310    a11011a5
  9d60483c    492f5736    49af7933    79322e00
  17848705    78400000    5b2f9d35    9d265b2f
  793b2e00    49379d26    49379d26    9d359d35
  493d493e    612f492f    4123c537    9d35612b
  493f2800    00000000    9d266532    492b5723
  492b793d    0000170d    4937793d    793b1120
  41c5030f
```